ELECTRON SPIN RESONANCE OF COLLISION COMPLEXES

BY

JOAQUIN VICTOR MARTINEZ de PINILLOS

A DISSERTATION PRESENTED TO THE GRADUATE COUNCIL OF
THE UNIVERSITY OF FLORIDA IN PARTIAL
FULFILLMENT OF THE REQUIREMENTS FOR THE DEGREE OF
DOCTOR OF PHILOSOPHY

UNIVERSITY OF FLORIDA
1974

TO

JOAQUIN JAVIER

AND

VICTOR IGNACIO

ACKNOWLEDGMENTS

The author wishes to acknowledge Dr. William Weltner, Jr., for his support and encouragement. He also wishes to recognize the special help received from Dr. Weltner's entire research group, primarily from Dr. W. R. M. Graham for his help in running the MAGNSPEC 3 program and his very lucid discussions about ESR; Mr. Clifton H. Durham, Jr., for his help in proofreading and editing the manuscript; and Mr. Warren D. Hewett for very helpful discussions.

A very special word of thanks is due to the author's wife, Carmen, whose help was deeply appreciated, mainly, during the periods of anxiety and depression when her words of reassurance made the outlook a bit brighter. A special recognition is due to the author's mother for all she has done for him and whose help was indispensable during these last few years.

The author also wishes to acknowledge the National Science Foundation (NSF) for support during the period of this research.

TABLE OF CONTENTS

Page

ACKNOWLEDGMENTS iii

ABSTRACT. vii

CHAPTER

I INTRODUCTION 1

Experimental 2

Apparatus 2

References 9

II ESR THEORY 10

Introduction 10
Diatomic Molecules 11
Phenomenological Hamiltonian 13
Hyperfine Tensor 14
g-Tensor 16
Comparison Between $\Delta g_{\perp}$ and the Spin-Doubling Constant 21
Angular Dependence of the Spectrum 22
Molecular Interpretation of ESR Parameters 24
Spin Density Functions 25
Details of the Spectra 30

References 37

III $M^+Cl_2^-$ 39

Introduction 39

Experimental 40

Method of Preparation of the $M^+Cl_2^-$ . . . 40

Observed Spectrum of $M^+Cl_2^-$ 42

$Mg^+Cl_2^-$ 49

$Ca^+Cl_2^-$ 53

$Sr^+Cl_2^-$ 58

$Ba^+Cl_2^-$ 62

TABLE OF CONTENTS (Continued)

CHAPTER Page

III (Continued)

$Li^+Cl_2^-$ 66

Na^+Cl^- 72

$K^+Cl_2^-$ 76

Discussion 80
Linewidths 93
CNDO Calculation 96
Temperature Variation Experiments . . . 97
Optical Experiments 98

M^+Cl^- 99

M and M^+ 100

Summary 103

References 104

IV $M^+F_2^-$ 106

Introduction 106

Experimental 110

Method of Preparation of $M^+F_2^-$ 110

Observed Spectra of $M^+F_2^-$ 111

$K^+F_2^-$ 121

$Ca^+F_2^-$ 125

$Mg^+F_2^-$ 128

$Ba^+F_2^-$ 132

Discussion 132
Linewidths 146
INDO Calculation 149
M^+ Ions 150
Summary 150

References 152

TABLE OF CONTENTS (Continued)

Page

APPENDIX A - PROGRAM TO SIMULATE THE ESR SPECTRUM OF $^2\Sigma$ MOLECULES TO SECOND-ORDER PERTURBATION THEORY 155

APPENDIX B - MATRIX ELEMENTS FOR THE SPIN HAMILTONIAN OF Cl_2^- 189

APPENDIX C - LEAST-SQUARES FIT FOR A LINEAR FUNCTION . 194

APPENDIX D - MATRIX ELEMENTS AND PROGRAM FOR BENT F_2^- NON-COLLINEAR A- AND g-TENSORS 201

APPENDIX E - MATRIX ELEMENTS AND PROGRAM FOR LINEAR F_2^- COLLINEAR A- AND g-TENSORS . . 229

BIOGRAPHICAL SKETCH 258

Abstract of Dissertation Presented to the Graduate Council
of the University of Florida in Partial Fulfillment of the
Requirements for the Degree of Doctor of Philosophy

ELECTRON SPIN RESONANCE OF COLLISION COMPLEXES

By

Joaquin Victor Martinez de Pinillos

August, 1974

Chairman: Professor William Weltner, Jr.
Major Department: Chemistry

Reaction complexes formed when alkali and alkaline-earth atoms are allowed to react with either Cl_2 or F_2 were isolated in argon matrices at 4 K. Ionic complexes are formed where the halogen occurs as essentially X_2^-, which is observable via electron spin resonance (ESR) spectroscopy. The metals used in the case of Cl_2 were Li, Na, K, Mg, Ca, Sr, and Ba; for F_2, Na, K, Cs, Mg, and Ba were used. In all cases, except for Cs, the atoms were produced by heating the metal to a temperature where its vapor pressure was of the order of 10^{-1} torr in a Knudsen cell. Cs metal atoms were prepared by reaction of Cs_2CrO_4 with Si in a Knudsen cell. The complexes produced are too short-lived in the gas phase to be studied by conventional spectroscopic techniques.

The hyperfine interaction observed shows that the intermediate trapped was primarily $M^+X_2^-$. This ion pair is very loosely coupled and the ions can be treated independently of one another. The presence of the metal can be detected, in the cases where it has a magnetic moment, by the broadening

it produces on the X_2^- lines. It also indicates that the electron is in a $^2\Sigma_u$ state with a wavefunction composed mainly of pσ-orbitals with very small s-orbital contribution. The increase in the hyperfine splitting with decreasing ionization potential of the metal indicates that the electron resides mostly on the X_2^- species as expected.

The properties of some of the excited states were studied by the variations observed in the components of the g-tensor. It was found that a low-lying $^2\Pi_u$ state is mixed with the ground state via spin-orbit coupling for the case of Cl_2^- and that this state is inverted (since the observed shift from g_o is positive). On the other hand, it was found that in the case of F_2^- the presence of the metal ion perturbed the system enough to cause a splitting of the linear molecule states and mix in an excited $^2A_1$ state with the resulting $^2B_1$ ground state.

It was interesting that the presence of the M^+ ion was detected when the alkaline-earth metals were used in the Cl_2 but not in the F_2 experiments. This was interpreted as another indication of the degree of interaction between the metal ion and X_2^-. In Cl_2 the interaction was "loose" and allowed for observation of essentially independent ions; in F_2, the coupling was "tighter" and this broadened the M^+ line, making it unobservable.

The presence of the MCl molecules, where M was Mg, Ca, and Sr, was also detected. In the experiments with F_2, only MgF was detected.

CHAPTER I

INTRODUCTION

The technique of electron spin resonance (ESR) has been widely used to study molecules and ions with unpaired electrons. In many instances, the intermediates in some chemical reactions are paramagnetic, which renders them very attractive to the ESR spectroscopist. The major problem he confronts is that many of these intermediates are extremely short-lived and, therefore, their study via conventional methods is, at best, difficult.

With the advent of matrix isolation techniques in which species can be trapped at very low temperatures (usually 4-20 K), these intermediates can now be isolated and studied in a gas-like environment. Some recent studies have been carried out on transition metal ions [1] and of some molecules formed as intermediates in chemical reactions [2,3]. The main advantage of this technique is that the molecular information obtained is gas-like within a few percent. Extensive details and reviews of the matrix isolation technique as applied to atomic and molecular studies have been given by Bass and Broida [4], Jacox and Milligan [5,6] and Weltner [7].

Experimental

Apparatus

The apparatus used to study the reaction intermediates described here will be discussed in this general section. Details of the preparation of different molecules as well as variations from the main structure of the apparatus will be discussed under each specific heading.

The Dewar was adapted from a design of Jen, Foner, Cochran and Bowers [8]. Some of the important features of the apparatus are shown in Figure 1. The sample in the furnace was always placed in a tantalum cell (1" long by 0.25" I.D., 0.025" wall) and firmly attached to two water-cooled electrodes. The electrodes were then connected to a power supply and the cell was heated in a resistance fashion.

The "inert solids" were research grade argon and neon gases (purity 99.999%) obtained from commercial sources and used without further purification. The trapping surface consists of a flat single-crystal sapphire rod (1¼ " long, 1/8" wide, 3/64" thick). The rod is securely embedded in the inner Dewar where it is cooled to approximately 4 K by contact with liquid He. In some cases, the temperature of the rod was monitored by a chromel vs. gold plus 0.07at%-iron thermocouple. This was done when the temperature of the rod was allowed to change in order to anneal the matrix and observe the appearance or disappearance of some features. The thermal

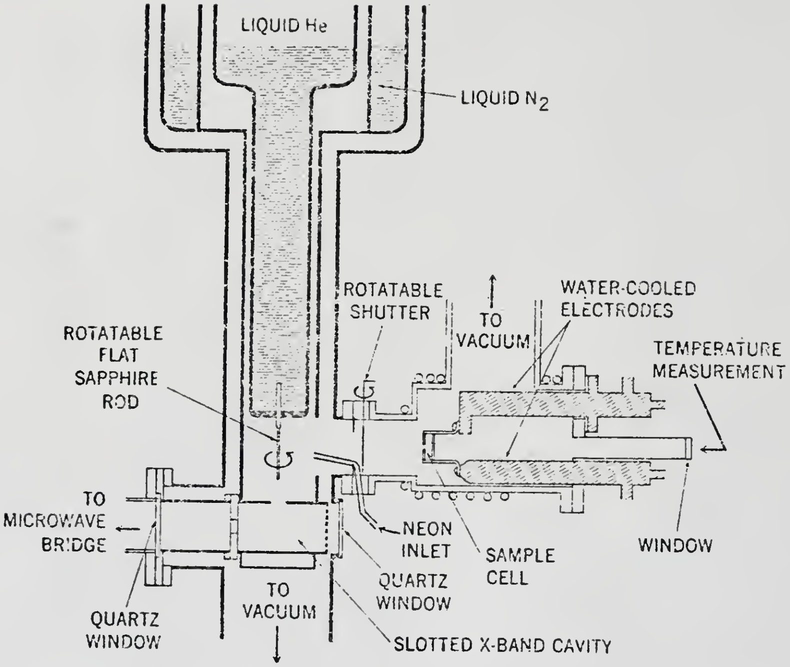

Figure 1. Dewar and Furnace Apparatus

conductivity of single-crystal sapphire is very high so that the rod was an excellent substrate for condensation of the inert gas matrix.

The sapphire rod could be lowered into a microwave cavity by a vacuum-tight bellows assembly located at the top of the Dewar, and it could also be rotated 360° inside or outside the cavity. The front of the cavity is slotted so that photolysis or specialized irradiation can be conducted while scanning the ESR spectrum. The outer Dewar wall is equipped with a quartz window to allow a wide range of photolytic light to be transmitted to the matrix. When needed, for extreme ultraviolet photolysis, LiF could be used for this window.

When the rod is outside the cavity, it is directly in front of the nozzle that carries the gas mixture and in front of the furnace window through which the vaporized metal comes into the reaction chamber. The distance between the Knudsen cell and the sapphire rod is approximately twelve centimeters. The furnace is mounted on a movable table and attached to the Dewar by a double gate valve which allows decoupling of these two systems without breaking the vacuum in either. The Dewar can then be rolled on fixed tracks between the pole faces of the ESR magnet.

The Dewar and the furnace are individually pumped by mechanical and 2" silicone oil diffusion pumps. The pressures obtained before any cryogenic liquids are placed in the Dewar are of the order of 2×10^{-5} torr. When all the traps are filled with liquid nitrogen and the main Dewar filled with liquid helium, the pressure obtained is of the order of 5 x 10^{-8} torr. The pressure in the furnace with its trap filled with liquid nitrogen is of the order of 6 x 10^{-6} torr with the connecting valve to the Dewar closed.

The inert gas was allowed to deposit for 5 minutes on each side of the rod before the gate valve was opened to allow materials vaporized in the furnace to come into the Dewar. While the gas mixture was being deposited, the metal was being warmed up to a temperature at which its vapor pressure was of the order of 10^{-1} torr. The gas was allowed to deposit at a rate of about 0.6 l-atm/hr. This was accomplished by maintaining a pressure of about 3 x 10^{-5} torr in the Dewar as measured by an ion gauge. The co-deposition of the metal and the gas mixture or inert gas, depending on the nature of the experiment, lasted approximately 30 minutes. The rod was turned 180° every five minutes in order to obtain an even surface distribution of matrix material.

To observe ESR spectra of acceptable intensity, a ratio of rare gas molecules to species under study of approximately 1000:1 is required. In the present case, much higher concentration of the X_2 gases was required initially, perhaps because the short half-lives of the intermediates made their trapping very difficult. The concentration ratio was determined by trying different mixtures until sufficiently intense ESR signals were obtained.

The instrument used to record the spectrum was the Varian V-4500 Electron Spin Resonance Spectrometer employing superheterodyne detection. The magnetic field was measured with an NMR fluxmeter, whose frequency was determined with a Beckman 6121 counter. The X-band microwave cavity frequency was determined with a high Q wavemeter.

When annealing was considered necessary, the Dewar was changed to one in which the amount of liquid helium in contact with the rod could be varied. This consisted of a copper cylinder connected to the main reservoir and to the outside via another tube. The latter was fitted with a needle value (see Figure 2). The liquid helium in the main reservoir would be forced down by pressure and cooled the rod to 4 K. When an increase in temperature was desired, the flow of liquid helium into the lower copper chamber could be either reduced or completely stopped by closing the needle valve. This allowed the temperature to rise while being monitored by the chromel-gold thermocouple. When the desired level was achieved, the needle valve was opened and the flow of liquid helium brought the temperature down to 4 K again. The major disadvantage encountered with the variable-temperature Dewar was that the evaporation rate of the liquid helium was much larger than for the fixed temperature one. This made its utilization on a permanent basis impractical when the matrix was to be studied for a long period. Long studies could only be achieved by refilling the

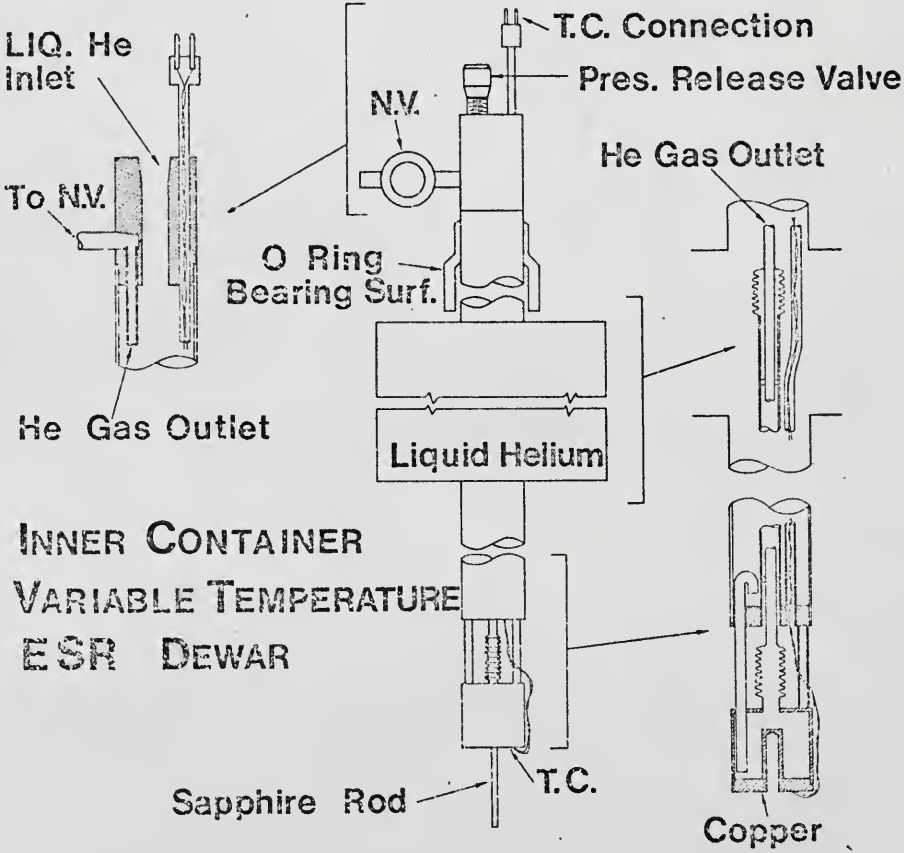

Figure 2. Variable Temperature Dewar

Dewar with liquid helium, which was difficult when neon matrices were used because they are very unstable and any small perturbation can cause them to evaporate.

The annealing process was used when the presence of different sites in the matrix was suspected or when the progress of the reaction was to be followed over a temperature range. Sites tend to obscure some features of the ESR spectrum and in order to understand all the details, their removal may become mandatory.

When the matrix was warmed in order to follow the reaction, an expected observation was the disappearance of some of the spectral features and the appearance of others. In most of the systems studied, annealing had to be done very carefully since the reactions involved were extremely exothermic and, occasionally, the matrix was lost since the heat generated vaporized the inert gas solid, destroying the vacuum and vaporizing the liquid helium in the reservoir.

References

[1] Ozin, G. A., and Vander Voet, A., Acc. Chem. Res., 6, 313 (1973).

[2] Noble, P. N., and Pimentel, G. C., J. Chem. Phys., 49, 3165 (1968).

[3] Milligan, D. E., and Jacox, M. E., J. Chem. Phys., 53, 2034 (1968).

[4] Bass, A. M., and Broida, H. P., Formation and Trapping of Free Radicals, Academic Press, New York (1960).

[5] Jacox, M. E., and Milligan, D. E., Appl. Opt., 3, 873 (1964).

[6] Milligan, D. E., and Jacox, M. E., MTP International Review of Science, University Park Press (1972), Vol. 3, p. 1.

[7] Weltner, W., Advances in High Temperature Chemistry, Academic Press, New York (1970), Vol. 2, p. 85.

[8] Jen, C. K., Foner, S. N., Cochran, E. L., and Bowers, V. A., Phys. Rev., 112, 1169 (1958).

CHAPTER II

ESR THEORY

Introduction

The systems of interest in this work consist of $^2\Sigma$ molecules in all cases; therefore, the description of the theory will be restricted to these types of molecules.

A $^2\Sigma$ molecule consists of a linear molecule with an unpaired electron and no angular momentum. When these molecules are placed in a magnetic field, the degenerate spin levels are split and a transition between them can be induced. The energy difference between these levels is approximately equal to $g_c\beta_oH = h\nu_o$, where g_o is the free electron g-factor (2.0023), β_o is the Bohr magneton (9.2732×10^{-21} erg/G), H is the magnetic field, h is Planck's constant (6.6256×10^{-27} erg sec) and ν_o is the frequency of the transition inducing radiation. It is then expected that an absorption line at a given H value for the ν_o of the instrument will occur at the position of the g-value for the molecule under study. In the present case, an X-band instrument with $\nu_o \simeq 9400$ MHz was used.

The Hamiltonian describing the interaction under study was introduced by Dirac [1].

It can be shown (see McWeeny [2] and McWeeny and Sutcliffe [3]) that Dirac's Hamiltonian can be broken down into a sum of terms representing the different interactions present in a molecule placed in a magnetic field.

Diatomic Molecules

The Hamiltonian $\mathcal{H}$ for a diatomic molecule with one unpaired electron in an external magnetic field is given by

$$\mathcal{H} = \mathcal{H}_F + \mathcal{H}_{LS} + \mathcal{H}_Z + \mathcal{H}_{hf}$$

where

$\mathcal{H}_F$ = Hamiltonian of the free (non-rotating in this case) molecule in the absence of spin-orbit coupling and an external magnetic field.

$\mathcal{H}_{LS}$ = Hamiltonian for the coupling of spin and orbital angular momenta of the electrons.

$\mathcal{H}_Z$ = Zeeman energy arising from the interaction between the electron spin, orbital and nuclear-spin magnetic moments and an externally applied magnetic field.

$\mathcal{H}_{hf}$ = Hyperfine interaction arising from the electron-spin magnetic moment interacting with any nuclear moment present in the molecule.

The nuclear Zeeman term $(\underset{\sim}{H}\cdot\underset{\sim}{I})$ and other types of interactions will be neglected here since, in general, they are very small, and in the cases of interest here, they are particularly small.

Since $\mathcal{H}_F$ is much larger than any of the other terms, $\mathcal{H}_{LS}$, $\mathcal{H}_Z$ and $\mathcal{H}_{hf}$ can be treated as perturbations. The different perturbing terms are given by (for a detailed discussion of these terms, see McWeeny [2], McWeeny and Sutcliffe [3], and Hameka [4]).

$$\mathcal{H}_{LS} = \xi\underset{\sim}{L}\cdot\underset{\sim}{S} \tag{1a}$$

$$\mathcal{H}_Z = \beta_o\underset{\sim}{H}\cdot(\underset{\sim}{L} + g_o\underset{\sim}{S}) \tag{1b}$$

$$\mathcal{H}_{hf} = g_n\beta_n g\ \beta_o\left[\frac{\underset{\sim}{L}\cdot\underset{\sim}{I}}{r^3} + \frac{3(\underset{\sim}{S}\cdot\underset{\sim}{r})(\underset{\sim}{r}\cdot\underset{\sim}{I})}{r^5} - \frac{\underset{\sim}{S}\cdot\underset{\sim}{I}}{r^3} + \frac{8\pi}{3}\underset{\sim}{S}\cdot\underset{\sim}{I}\delta(r)\right] \tag{1c}$$

where $\underset{\sim}{L}$, $\underset{\sim}{S}$, and $\underset{\sim}{I}$ are the orbital, electron-spin and nuclear-spin angular momentum operators, $\underset{\sim}{H}$ is the magnetic field, β_o and β_n are the Bohr and nuclear magnetons, respectively, g and g_n are the electronic and nuclear g-factors, respectively. ξ is the molecular spin-orbit coupling constant.

$\mathcal{H}_{hf}$, the hyperfine Hamiltonian of Eq. (1c), consists of three parts. The first term in square brackets involves the interaction between the magnetic field produced by the orbital momentum and the nuclear moment. This term will necessarily be zero for a $^2\Sigma$ molecule since $L = 0$, except for any small orbital angular momentum entering through the $\underset{\sim}{L}\cdot\underset{\sim}{S}$ interaction. The next two terms are related to the interaction of two magnetic dipoles, the spin of the electron and the nuclear magnetic dipole. The third part of $\mathcal{H}_{hf}$ is the isotropic Fermi or contact term and depends on the electron spin density at the nucleus since the Dirac δ-function indicates that its value is zero unless $r = 0$. Within a simple linear combination of atomic orbitals (LCAO) treatment it can be seen that this term is a measure of the amount of s-character of the wavefunction for the odd electron.

Phenomenological Hamiltonian

The spin Hamiltonian can be represented in a phenomenological manner by

$$\mathcal{H}_{spin} = \beta_o\underset{\sim}{H}\cdot\underset{\sim}{g}\cdot\underset{\sim}{S} + \underset{\sim}{I}\cdot\underset{\sim}{A}\cdot\underset{\sim}{S} \tag{2}$$

as has been shown in several texts (e.g., see McWeeny [2]). In this expression, $\underset{\sim}{g}$ and $\underset{\sim}{A}$ are second-order tensors, where all the interactions that may affect the Zeeman and hyperfine terms, respectively, are presented in a compact form.

For a diatomic molecule, it can easily be seen that these tensors can be written as

$$\underset{\sim}{A} = \begin{pmatrix} A_x & 0 & 0 \\ 0 & A_y & 0 \\ 0 & 0 & A_z \end{pmatrix} \qquad \underset{\sim}{g} = \begin{pmatrix} g_x & 0 & 0 \\ 0 & g_y & 0 \\ 0 & 0 & g_z \end{pmatrix}$$

where the off-diagonal elements can be made equal to zero by a suitable rotation of the axes (see the discussion on each tensor below). If the z-axis is taken as parallel to the magnetic field, A_z and g_z will then be called $A_\parallel$ and $g_\parallel$ respectively, while the x and y axes are perpendicular to the parallel axis and therefore A_x and A_y and g_x and g_y will be called $A_\perp$ and $g_\perp$, respectively. For a linear molecule, g_x and g_y will be equal, as will be A_x and A_y, since the two directions are equivalent.

Hyperfine Tensor

As was seen in Eq. (1c), the hyperfine tensor $\underset{\sim}{A}$ will comprise two types of interactions, one due to the amount of s-character of the wavefunction (the Fermi contact term) and one due to the non-s-character of the wavefunction (the middle two terms). Calling these two types of interaction A_{iso} for the one dependent on the s-character and A_{dip} for the one dependent on the non-s-character of the wavefunction, Eq. (1c) can then be written

$$\mathcal{H}_{hf} = \left[A_{iso} + A_{dip}\right] \underset{\sim}{S}\cdot\underset{\sim}{I} \tag{3}$$

where $A_{iso} = \frac{8\pi}{3} g_n\beta_n g\ \beta_o \langle\delta(r)\rangle = \frac{8\pi}{3} g_n\beta_n g_o\beta_o |\psi(o)|^2$

and $A_{dip} = g_n\beta_n g\ \beta_o \left\langle\frac{3\cos^2\theta-1}{2r^3}\right\rangle.$

The brackets indicate the average of the expressed operator over the wave function ψ. In tensor form, Eq. (3) can then be written

$$\mathcal{H}_{hf} = \underset{\sim}{I}\cdot(A_{iso}\,\underset{\sim}{1} + \underset{\sim}{T})\cdot\underset{\sim}{S} \tag{4}$$

where T and A_{dip} are related in a manner to be discussed. Equating the hyperfine tensor in Eq. (2) with the one in Eq. (4) it is found that

$$\begin{pmatrix} A_\perp & 0 & 0 \\ 0 & A_\perp & 0 \\ 0 & 0 & A_\parallel \end{pmatrix} = \begin{pmatrix} A_{iso} & 0 & 0 \\ 0 & A_{iso} & 0 \\ 0 & 0 & A_{iso} \end{pmatrix} + \begin{pmatrix} T_x & 0 & 0 \\ 0 & T_y & 0 \\ 0 & 0 & T_z \end{pmatrix} .$$

T can be shown to be (see Wertz and Bolton [5])

$$T \simeq -g\,\beta_o g_n \beta_n \begin{pmatrix} \left\langle \frac{r^2-3x^2}{r^5} \right\rangle & 0 & 0 \\ 0 & \left\langle \frac{r^2-3y^2}{r^5} \right\rangle & 0 \\ 0 & 0 & \left\langle \frac{r^2-3z^2}{r^5} \right\rangle \end{pmatrix}$$

and, therefore, it is a traceless tensor. It has been assumed that the off-diagonal elements are small and therefore have been equated to zero. From this fact, it can then be seen that

$$A_{iso} = (A_\parallel + 2A_\perp)/3 \; . \tag{5}$$

The relationship between T and A_{dip} can be seen, for some special cases. Referring to Eq. (3), it can also be written

$$\mathcal{H}_{hf_{iso}} + \mathcal{H}_{hf_{dip}} = \left[A_{iso} + A_{dip}\right] \underset{\sim}{S}\cdot\underset{\sim}{I} \; .$$

Therefore,

$$\mathcal{H}_{hf_{dip}} = \left(A_{dip}\right) \underset{\sim}{S} \cdot \underset{\sim}{I}. \tag{6}$$

Since both $\underset{\sim}{S}$ and $\underset{\sim}{I}$ are quantized along $\underset{\sim}{H}$, taken as the direction of the z-axis, the x and y components of $\underset{\sim}{S}$ and $\underset{\sim}{I}$ may be neglected in Eq. (6). With the substitution $z = r\cos\theta$, and for the special case of a p orbital centered on the interacting nucleus, it can be seen (Wertz and Bolton [5]) that

$$A_{dip} = g\ \beta_o g_n \beta_n \left\langle \frac{3\cos^2\theta - 1}{2r^3} \right\rangle = \frac{A_{\parallel} - A_{\perp}}{3}. \tag{7}$$

(For more details see Frosch and Foley [6]).

g-Tensor

Let us assume that the solution to $\mathcal{H}_F$ gave us a wavefunction for the ground state of our molecule $|0\rangle$ and a series of excited states $|n\rangle$. If $\mathcal{H}_{LS}$ is now applied as a perturbation, to first order we get

$$\psi_\Sigma = |0\rangle + \sum_n \frac{\langle n|\xi\ \underset{\sim}{L}\cdot\underset{\sim}{S}|0\rangle}{E_n - E_0} |n\rangle$$

where $\mathcal{H}_{LS}$ was defined in Eq. (1a). (This is for a nonrotating molecule.) If the spin is taken into consideration, and in view of the fact that only one unpaired spin is present, we can write two different wave functions

$$|+\rangle = |0\alpha\rangle - \sum_n \frac{\langle n|\xi\, \underset{\sim}{L}\cdot\underset{\sim}{S}|\ 0\alpha\rangle}{E_n - E_0}|n\rangle$$

and (8)

$$|-\rangle = |0\beta\rangle - \sum_n \frac{\langle n|\xi\, \underset{\sim}{L}\cdot\underset{\sim}{S}|\ 0\beta\rangle}{E_n - E_0}|n\rangle$$

where α and β refer to spin up or down as usual. This is the so-called Kramer doublet representing degenerate wavefunctions, which will, however, have different energies in a magnetic field (see Carrington and McLachlan [7]).

Now, $\underset{\sim}{L}\cdot\underset{\sim}{S}$ can be written as

$$\underset{\sim}{L}\cdot\underset{\sim}{S} = L_xS_x + L_yS_y + L_zS_z = L_zS_z + \tfrac{1}{2}(L^+S^- + L^-S^+)$$

where L^+ and S^+ are the raising operators and L^- and S^- are the lowering operators defined by

$$L^{\pm} = L_x \pm i\, L_y$$

and

$$S^{\pm} = S_x \pm i\, S_y .$$

Since $\underset{\sim}{S}$ acts only on the spin part of the wavefunction it can be seen that

$$S_z|\alpha\rangle = \tfrac{1}{2}|\alpha\rangle \quad , \quad S_z|\beta\rangle = -\tfrac{1}{2}|\beta\rangle$$

$$S^+|\beta\rangle = |\alpha\rangle \quad , \quad S^+|\alpha\rangle = 0$$

$$S^-|\beta\rangle = 0 \quad , \quad S^-|\alpha\rangle = |\beta\rangle .$$

Therefore, the non-zero spin integrals are

$$\langle\alpha|\ S^+|\beta\rangle = \langle\beta|\ S^-|\alpha\rangle = 1$$

$$\langle\alpha|\ S_z|\alpha\rangle = \tfrac{1}{2},\ \langle\beta|S_z|\beta\rangle = -\tfrac{1}{2}$$

and for a molecule where $|0\rangle$ is a Σ state,

$$\langle 0| L_z |0\rangle = \langle n| L_z| 0\rangle = \langle 0| L_z| n\rangle = 0.$$

Then Eq. (8) becomes

$$|+\rangle = |0\alpha\rangle - \tfrac{1}{2}\sum_n \frac{\langle n| \xi L^+ |0\rangle}{E_n - E_0} |n\beta\rangle$$

$$|-\rangle = |0\beta\rangle - \tfrac{1}{2}\sum_n \frac{\langle n| \xi L^- |0\rangle}{E_n - E_0} |n\alpha\rangle .$$

The Zeeman term of the phenomenological Hamiltonian (Eq. (2)) was given by

$$\mathcal{H}_Z = \beta \underset{\sim}{H}\cdot\underset{\sim}{g}\cdot\underset{\sim}{S}$$

$$\mathcal{H}_Z = \beta \underset{\sim}{H}\cdot\begin{pmatrix} g_\perp & 0 & 0 \\ 0 & g_\perp & 0 \\ 0 & 0 & g_\parallel \end{pmatrix}\cdot S$$

but, from Eq. (1b), the Zeeman term is

$$\mathcal{H}'_Z = \beta \underset{\sim}{H}\cdot(\underset{\sim}{L} + g_o \underset{\sim}{S})$$

where the prime is introduced to differentiate it from the phenomenological one.

From these equations, assuming that the magnetic field is acting in the x-direction (if it acts in the y-direction a similar result is obtained), it can be seen that

$$\mathcal{H}_Z = \beta_o H(g_\perp S_x + g_{xy} S_y + g_{zy} S_z) = \beta_o H g_\perp S_x$$

since all the off-diagonal elements of the g-tensor can be made equal to zero. But, from $\mathcal{H}'_Z$, we get the following matrix

$$\beta_o H \begin{pmatrix} 0 & \langle -|L_x + g_o S_x|+\rangle \\ \langle +|L_x + g_o S_x|-\rangle & 0 \end{pmatrix}$$

while from the phenomenological Hamiltonian we get

$$\begin{array}{cc} & \begin{array}{cc} |+\rangle & |-\rangle \end{array} \\ \begin{array}{c} \langle +| \\ \langle -| \end{array} & \begin{pmatrix} 0 & \frac{1}{2}g_\perp \beta_o H \\ \frac{1}{2}g_\perp \beta_o H & 0 \end{pmatrix} \end{array} .$$

Solving these two systems, we obtain

$$g_\perp = \langle +|L_x + g_o S_x|-\rangle + \langle -|L_x + g_o S_x|+\rangle .$$

If we let $L_x + g_o S_x = \frac{1}{2}\{L^+ + L^- + g_o(S^+ + S^-)\}$

substituting the values of $|+\rangle$ and $|-\rangle$ and carrying out the operations involving S^+ and S^-, we obtain

$$\langle +|L_x + g_o S_x|-\rangle = \frac{1}{2}\left\{ g_o - \frac{1}{2}\sum_n \frac{\langle n|\xi L^-|0\rangle}{E_n - E_0}\left[\langle 0|L^+|n\rangle + \langle 0|L^-|n\rangle\right] - \frac{1}{2}\sum_n \frac{\langle n|\xi L^-|n\rangle}{E_n - E_0}\left[\langle n|L^+|0\rangle + \langle n|L^-|0\rangle\right]\right\}$$

where the terms proportional to $\xi^2/(E_n - E_0)^2$ have been neglected. If L^+ and L^- are replaced by their L_x and L_y counterparts, we obtain

$$\langle + | L_x + g_o S_x | - \rangle = \tfrac{1}{2} \left\{ g_o - \sum_n \frac{\langle n | \xi L_x | 0 \rangle}{E_n - E_0} \langle 0 | L_x | n \rangle + \sum_n \frac{\langle 0 | \xi L_x | n \rangle}{E_n - E_0} \langle n | L_x | 0 \rangle \right\}$$

and similarly for $\langle - | L_x + g_o S_x | + \rangle$. Therefore,

$$g_\perp = g_o - 2 \sum_n \frac{\langle n | \xi L_x | 0 \rangle \langle 0 | L_x | n \rangle}{E_n - E_0} . \tag{9a}$$

For $g_\parallel$ a similar treatment can be carried out and

$$g_\parallel = g_o - 2 \sum_n \frac{\langle n | \xi L_z | 0 \rangle \langle 0 | L_z | n \rangle}{E_n - E_o} \tag{9b}$$

but (for a Σ molecule) this reduces to

$$g_\parallel = g_o .$$

Thus, any changes on $g_\parallel$ can only be attributed to matrix effects to this order of approximation.

Comparison Between $\Delta g_\perp$ and the Spin-Doubling Constant

It has just been shown, Eq. (9a), that $\Delta g_\perp$ is given by

$$\Delta g_\perp = g_\perp - g_o = -2 \sum_n \frac{\langle n|\xi L_x|0\rangle \langle 0|L_x|n}{E_n - E_0} . \qquad (10)$$

On the other hand, $^2\Sigma$ molecules exhibit a splitting of their rotational levels given by $\gamma(K+\frac{1}{2})$, where γ is very small compared with the rotational constant, B, and K is the rotational quantum number. γ is called the spin-doubling constant and has been shown by Van Vleck [8] to be given by

$$\gamma = 4 \sum_n \langle 0|\xi L_x|n\rangle \langle n|BL_x|0\rangle/(E_n-E_0)$$

where $|n\rangle$ includes all excited $^2\Pi$ states, x is an axis perpendicular to the symmetry axis, ξ is the spin-orbit operator and B is the rotational operator $h^2/(8\Pi^2 \mu r^2)$. If B is assumed to be constant, it can be taken out of the integral and γ reduces to

$$\gamma = 4B \sum_n \langle 0|\xi L_x|n\rangle \langle n|L_x|0\rangle/(E_n-E_0) . \qquad (11)$$

Then, from Eqs. (10) and (11), we obtain

$$\gamma = -2B \Delta g_\perp$$

for a molecule in a $^2\Sigma$ state. This relation was derived by Knight and Weltner [9].

Angular Dependence of the Spectrum

So far we have not discussed the behavior of the spectrum when the angle between the molecular axis and the magnetic field varies. The Hamiltonian for a linear molecule can be written

$$\mathcal{H} = g_{\parallel} \beta_o H_z \hat{S}_z + g_{\perp} \beta_o (H_x \hat{S}_x + H_y \hat{S}_y) + A_{\parallel} I_z \hat{S}_z + A_{\perp} (\hat{I}_x \hat{S}_x + I_y \hat{S}_y) \qquad (12)$$

by simply expanding Eq. (2) and substituting the values of $\underset{\sim}{g}$ and $\underset{\sim}{A}$ for a linear molecule. The problem then consists of finding a relationship between these quantities and the angle between the magnetic field and the molecular axis.

Let us consider the Zeeman term first. It is desirable to write this term in the form

$$\mathcal{H}_Z = g\beta_o H\hat{S}_{z'},$$

where x', y' and z' are a new set of axes and z' is parallel to H. Let x, y and z be the coordinate axes of the molecule, where z is along the molecular axis. For a linear molecule the direction of H can be taken as the polar axis and θ the angle between z and H (or z'). The y axis can be arbitrarily chosen as perpendicular to H so that y = y' and therefore $H_y = 0$. Since $H_x = H \sin\theta$ and $H_z = H \cos\theta$,

$$\mathcal{H}_Z = \beta_o \left[g_{\parallel} \cos\theta\, \hat{S}_z + g_{\perp} \sin\theta\, \hat{S}_x\right] H.$$

If new direction cosines are chosen such that

$$l_z = (g_{\parallel} \cos \theta)/g \quad \text{and} \quad l_x = (g_{\perp} \sin \theta)/g$$

where $g^2 = g_{\parallel}^2 \cos^2\theta + g_{\perp}^2 \sin^2\theta$, (13a)

we get

$$\mathcal{H}_Z = g\beta_o H S_{z'} \tag{13b}$$

where

$$\begin{aligned} S_{z'} &= l_z S_z + l_x S_x \\ S_{x'} &= -l_x S_z + l_z S_x \\ S_{y'} &= S_y \ . \end{aligned} \tag{14}$$

For the hyperfine term, a similar transformation can be used. If Eq. (14) is inverted and new direction cosines are chosen for the nuclear coordinate system relative to the electronic coordinate such that

$$\begin{aligned} l_z^n &= (A_{\parallel} g_{\parallel} \cos \theta)/Kg \\ l_x^n &= (A_{\perp} g_{\perp} \sin \theta)/Kg \end{aligned}$$

where $K^2g^2 = A_{\parallel}^2 g_{\parallel}^2 \cos^2\theta + A_{\perp}^2 g_{\perp}^2 \sin^2\theta$, then Eq. (12) becomes

$$\begin{aligned} \mathcal{H} = g\beta_o H S_z{}' &+ K I_{z'} S_{z'} + (A_{\parallel} A_{\perp}/K) I_{x'} S_{x'} \\ &+ \frac{(A_{\perp}^2 - A_{\parallel}^2)}{K} g_{\parallel} g_{\perp} \sin \theta \cos \theta \, I_{z'} S_{x'} \\ &+ A_{\perp} I_{y'} S_{y'} . \end{aligned} \tag{15}$$

If we now introduce the raising and lowering operators $S^{\pm} = S_x \pm iS_y$ and $I^{\pm} = I_x \pm iI_y$, the Hamiltonian (Eq. (15)) becomes

$$\mathcal{H} = g\beta_o BS_z + KS_zI_z + \frac{A_\perp^2 - A_\parallel^2}{K} \cdot \frac{g_\parallel g_\perp}{g} \cdot \cos\theta \sin\theta \left(\frac{S^+ + S^-}{2}\right) I_z$$

$$+ \left(\frac{A_\parallel A_\perp}{4K} - \frac{A_\perp}{4}\right)\left(S^+I^+ + S^-I^-\right) + \left(\frac{A_\parallel A_\perp}{4K} + \frac{A_\perp}{4}\right)\left(S^+I^- + S^-I^+\right) \ . \quad (16)$$

When a matrix is written using this Hamiltonian, the eigenvalues, as well as the corresponding eigenvectors, can be found. This can be a laborious exercise; however, in most cases, a second-order perturbation solution suffices.

The allowed transitions are observed when $\Delta M = -1$ and $\Delta m = 0$, where $M = S, S-1, \ldots, -S$ and $m = I, I-1, \ldots, -I$. The second-order solution gives (see Abragam and Bleaney [10]),

$$h\nu = g\beta_o H + Km + \frac{A_\perp^2}{4g\beta_o H_o}\left(\frac{A_\parallel^2 + K^2}{K^2}\right)\left[I(I+1) - m^2\right]$$

$$+ \frac{1}{2g\beta_o H_o}\left(\frac{A_\parallel^2 - A_\perp^2}{K^2}\right)\left(\frac{g_\parallel g_\perp}{g^2}\right)^2 \sin^2\theta \cos^2\theta \, m^2 \quad (17)$$

for a $^2\Sigma$ molecule, where $H_o = (h\nu)/(g\beta_o)$.

Molecular Interpretation of ESR Parameters

In Eq. (3), it was shown that the observed ESR parameters $A_\parallel$ and $A_\perp$ can be related to fundamental molecular parameters in terms of A_{iso} and A_{dip}. If we now write the molecular wavefunction ψ as a linear combination of atomic orbitals, we get

$$\psi = C_1\phi_s + C_2\phi_{non-s}$$

where ϕ_s and ϕ_{non-s} are the atomic orbitals representing an s-type orbital and the non-s character is collected under

ϕ_{non-s}. In most cases these latter orbitals refer predominantly to the p-character, but since mixtures of d-functions are conceivable, particularly for the Cl case, it will be left as non-s. If it is assumed that this wavefunction is normalized and that the cross terms are small, integration and evaluation yields

$$|\psi(0)|^2 = C_1^2|\phi(0)_s|^2.$$

It can be seen that A_{iso} for the molecule is proportional to the term on the left, while $|\phi(0)|^2$ is approximately proportional to A'_{iso} for the atom. Therefore

$$C_1^2 \approx \frac{A_{iso}}{A'_{iso}} . \tag{18}$$

Similarly,

$$C_2^2 \approx \frac{A_{dip}}{A'_{dip}}$$

where A'_{dip} is the value of the anisotropic hyperfine splitting constant for the atom (see Ayscough [11]).

Spin Density Functions

In chemistry, one is usually interested in orbital wavefunctions; i.e., electrons are allocated to orbitals A,B,...,R,..., with spin factor α or β, and antisymmetrical functions are formed from them in accordance with the Pauli principle (Slater determinants). Each orbital with its spin factor is a spin-orbital (Aα, Aβ), and any specification of spin orbitals for all the electrons concerned is a spin-orbital configuration associated with one Slater determinant.

An orbital is a function of position in space (position vector $\underset{\sim}{r}$) and its value squared at $\underset{\sim}{r}$, $|A(\underset{\sim}{r})|^2 = |A^*(\underset{\sim}{r})\cdot A(\underset{\sim}{r})|$, indicates the probability of finding the electron there. Space and spin variables $(\underset{\sim}{r},s)$ will be denoted collectively by $\underset{\sim}{x}$ and the spin-orbital $\tilde{\phi}_A(\underset{\sim}{x}) = A(\underset{\sim}{r})\alpha(s)$ describes an electron in orbital A with spin $+\frac{1}{2}$. The probability of finding the electron in volume element $d\underset{\sim}{r}$ and with spin between s and s+ds, is given by a density function $\rho(\underset{\sim}{x})$ such that

$$\text{Probability of finding the electron in } d\underset{\sim}{x} = \rho(\underset{\sim}{x})d\underset{\sim}{x}$$

$$= |\phi_A(\underset{\sim}{x})|^2 \; d\underset{\sim}{x}$$

$$= |A(\underset{\sim}{r})|^2|\alpha(s)|^2 \; d\underset{\sim}{r} \; ds$$

and is zero unless s is in the vicinity of $+\frac{1}{2}$ since this is a "plus-spin" electron.

If the position is of particular interest at a given time regardless of spin, a sum over all possible spins can be carried out, and then the probability of the electron being found in dr can be written as

$$P(\underset{\sim}{r})d\underset{\sim}{r} = \left(\int \rho(\underset{\sim}{x}) \; ds\right) \; d\underset{\sim}{r} = |A(\underset{\sim}{r})|^2 \; d\underset{\sim}{r}$$

just as if the electron had no spin and was simply put into orbital A.

For a many-electron system, the wavefunction can be written as

$$\psi(\underset{\sim}{x}_1,\underset{\sim}{x}_2,\ldots,\underset{\sim}{x}_N)$$

and has the interpretation

$$\psi(\underset{\sim}{x}_1,\underset{\sim}{x}_2,\ldots,\underset{\sim}{x}_N)\ \psi^*(\underset{\sim}{x}_1,\underset{\sim}{x}_2,\ldots,\underset{\sim}{x}_N)d\underset{\sim}{x}_1 d\underset{\sim}{x}_2,\ldots,d\underset{\sim}{x}_N =$$

Probability of electron 1 in $d\underset{\sim}{x}_1$,2 simultaneously in $d\underset{\sim}{x}_2,\ldots$.

The probability of 1 in $d\underset{\sim}{x}_1$ and the other electrons anywhere is thus

$$d\underset{\sim}{x}_1 \int \psi(\underset{\sim}{x}_1,\underset{\sim}{x}_2,\ldots,\underset{\sim}{x}_N)\ \psi^*(\underset{\sim}{x}_1,\underset{\sim}{x}_2,\ldots,\underset{\sim}{x}_N)\ d\underset{\sim}{x}_2,d\underset{\sim}{x}_3,\ldots,d\underset{\sim}{x}_N$$

and the probability of finding any of the N electrons in dx_1 is N times this. This is now written as $\rho_1(\underset{\sim}{x}_1)$, defined as

$$\rho_1(\underset{\sim}{x}_1) = N\,d\underset{\sim}{x}_1\int\psi(\underset{\sim}{x}_1,\underset{\sim}{x}_2,\ldots,\underset{\sim}{x}_N)\ \psi^*(\underset{\sim}{x}_1,\underset{\sim}{x}_2,\ldots,\underset{\sim}{x}_N)\ d\underset{\sim}{x}_2,d\underset{\sim}{x}_3,\ldots,d\underset{\sim}{x}_N$$

It should be noted that this statement implies a slight change in the interpretation of $\underset{\sim}{x}_1$ as an argument in the density function; it no longer denotes exclusively the variables of particle 1 but rather a point of configuration space at which any particle may be found (with equal probability due to indistinguishability). Thus, $\rho_1(\underset{\sim}{x}_1)d\underset{\sim}{x}_1$ is the probability of finding any electron (1,2,...,N) in volume element $d\underset{\sim}{x}_1$ at $\underset{\sim}{x}_1$.

As in the case of one electron, the probability of finding an electron in a volume element $d\underset{\sim}{r}_1$ in ordinary threedimensional space with any spin can be found by

$$P_1(\underset{\sim}{r}_1) = \int \rho_1(\underset{\sim}{x}_1)\, ds_1 .$$

If this integral is to be carried over the electrons with spin α and over those with spin β separately, we can write

$$P_1(\underset{\sim}{r}_1) = P_1^{\alpha}(\underset{\sim}{r}_1) + P_1^{\beta}(\underset{\sim}{r}_1)$$

where the superscript indicates over which spin the summation is taken. Now, let us define a spin-density function by

$$Q_s(\underset{\sim}{r}_1) = \tfrac{1}{2}(P_1^{\alpha}(\underset{\sim}{r}_1) - P_1^{\beta}(\underset{\sim}{r}_1))$$

since this measures the resultant z-component of spin (excess of up-spin over down-spin density multiplied by the spin magnitude $\frac{1}{2}$).

Let us introduce a slightly different notation. Let $\rho_1(\underset{\sim}{x}_1) = \rho_1(\underset{\sim}{x}_1, \underset{\sim}{x}_1')$. This change is introduced so that when dealing with operators we can write the expectation value of the one-electron operator F as

$$\begin{aligned}\langle F\rangle &= \int \psi^*(\underset{\sim}{x}_1)\, F\psi(\underset{\sim}{x}_1)\, d\underset{\sim}{x}_1 = \int F\psi(\underset{\sim}{x}_1)\, \psi^*(\underset{\sim}{x}_1)\, d\underset{\sim}{x}_1 \\ &= \int F\rho_1(\underset{\sim}{x}_1, \underset{\sim}{x}_1')\, d\underset{\sim}{x}_1\end{aligned}$$

since the order of the factors does not matter. The expectation value is obtained simply by averaging $F = F(\underset{\sim}{x}_1)$ over the electron density $\rho_1(\underset{\sim}{x}_1)$. In order to avoid confusion, the density matrix is written as $\rho_1(\underset{\sim}{x}_1, \underset{\sim}{x}_1')$ to indicate that the operator acts on x_1 first, then x_1' is made equal to x_1 and the integral is taken. Therefore, this is simply a clarification, or change in notation.

Applying this to the case of the S_z operator, we have

$$\langle S_z \rangle = \int S_z(1)\ \rho_1(x_1,x_1')\ dx_1$$

$$= \int S_z(1)\ P_1^{\alpha\alpha}(r_1,r_1')\alpha(S_1)\alpha^*(S_1)$$

$$+ P_1^{\beta\beta}(r_1,r_1')\beta(S_1)\beta^*(S_1)\quad dx_1$$

and carrying out the summation over spins after operating with $S_z(1)$ we get

$$\langle S_z \rangle = \int Q_s(r_1)\ dr_1 = M\ .$$

Therefore, Q_s could be normalized. So, the function

$$D_s(\underset{\sim}{r}_1) = M^{-1}\ Q_s(\underset{\sim}{r}_1)$$

is the normalized spin-density function.

It can be proved that

$$A_{iso} = \frac{8\Pi}{3}\ g\ \beta_o g_n\ {}_nD_s(\underset{\sim}{R}_n) \tag{19a}$$

and

$$A_{dip} = 3g\ \beta_o g_n \beta_n \int (x_n y_n/r_n^5) D_s(\underset{\sim}{r})\ d\underset{\sim}{r} \tag{19b}$$

where $\underset{\sim}{R}_n$ is the radial distance to nucleus n, usually represented as $D_s(0)$, and $\underset{\sim}{r}_n$ is the distance of the field point $(\underset{\sim}{r})$ from nucleus n and has Cartesian coordinates x_n, y_n, and z_n (see McWeeny [3] and McWeeny and Sutcliffe [4]).

It can be seen then, that the magnetic parameters provide a direct relationship to the density matrix. Therefore, A_{iso} gives a probe into the nature of the density matrix at each nucleus and A_{dip} measures the magnetic dipole-dipole interaction in a distribution of spins of density $D_s(r_1)$.

Details of the Spectra

It has been shown (see Eq. (13a)) that the angular dependence of the g-factor can be written as

$$g^2 = g_{\parallel}^2 \cos^2\theta + g_{\perp}^2 \sin^2\theta$$

where θ was the angle between the molecular axis and the magnetic field. Then, as far as the Zeeman term is concerned, two absorptions will be observed, one at the field position corresponding to $g_{\parallel}$ and another one at the field position corresponding to $g_{\perp}$. Let us call these corresponding field positions $H_{\parallel}^o$ and $H_{\perp}^o$, respectively, and define them by

$$H_{\parallel}^o = \frac{h\nu_o}{g_{\parallel}\beta_o} \qquad \text{and} \qquad H_{\perp}^o = \frac{h\nu_o}{g_{\perp}\beta_o} \; .$$

It is assumed that the molecules are randomly oriented in the matrix, but rigidly held by it. Under these conditions, the spectrum will be independent of the angle the magnetic field makes with the sample. Experimentally, the random orientation of the molecules may be established by rotating the sample with respect to the magnetic field and recording the spectrum. If no changes are detected, the molecules are assumed to be randomly oriented. The spectrum expected for randomly oriented molecules was first analyzed by Bleaney [12,13] and by Sands [14]. Later treatments can be found in the literature [15-26].

If a sample contains N_o randomly oriented molecules, the number of them within an increment of angle $d\theta$, where θ is the angle measured from the field direction, is given by

$$dN = \frac{N_o}{2} \sin\theta \, d\theta \ . \tag{20}$$

Therefore, dN is proportional to the area of the surface of a sphere included within $d\theta$. The factor ½ is introduced since it is only necessarry to include a hemisphere.

The intensity of the ESR absorption is proportional to the number dN of molecules between θ and $\theta + d\theta$, if it is assumed that the transition probability is independent of orientation.

The field position at which a transition will be observed can be written as

$$H = \frac{h\nu_o}{\beta_o} (g_{\parallel}^2 \cos^2\theta + g_{\perp}^2 \sin^2\theta)^{-\frac{1}{2}} \tag{21}$$

where the angular dependence of the g-factor has been introduced. Differentiating Eq. (21) and letting $H_o = h\nu_o/g'\beta$, and $g' = (g_{\parallel} + 2g_{\perp})/3$, it is found that

$$\sin\theta \, d\theta = - \frac{g'^2 H_o^2}{H^3} \left\{ (g_{\parallel}^2 - g_{\perp}^2)(g'H_o/H)^2 - g_{\perp}^2 \right\}^{-\frac{1}{2}} dH \ . \tag{22}$$

The intensity of absorption in range of magnetic field dH is proportional to

$$|dN/dH| = |dN/d\theta| \cdot |d\theta/dH| .$$

Manipulation of Eqs. (20) and (22) and solving Eq. (21) for $\theta = 0°$ and for $\theta = 90°$ yields

$$|dN/dH| = N_o g_\parallel^3/2g'H_o(g_\parallel^2 - g_\perp^2) \quad \text{at} \quad \theta = 0°$$

and that

$$dN/dH = \infty \text{ at } \theta = 90° .$$

Therefore, if the natural width of the line is considered, the extreme points of the absorption become rounded and in Figure 3a a plot of this absorption versus the field intensity for the case of $g_\parallel > g_\perp$ is shown. When the first derivative of this curve is obtained, Figure 3b results under the same conditions. The line that occurs at $\theta = 0°$ is called a parallel line and the one that occurs at $\theta = 90°$ is called a perpendicular line.

In almost every molecule that is studied, at least one nucleus possessing a magnetic moment is encountered. Hyperfine (Hf) interaction can occur and each line will be split into $2I + 1$ lines (where I is the nuclear spin), if only one nucleus of spin I is present. In Figure 3c the spectrum obtained when the molecule has one unpaired electron and a nucleus with $I = \frac{1}{2}$ has been plotted. It is further assumed that $g_\parallel \approx g_\perp$ and that $A_\parallel > A_\perp$. The distance between the two

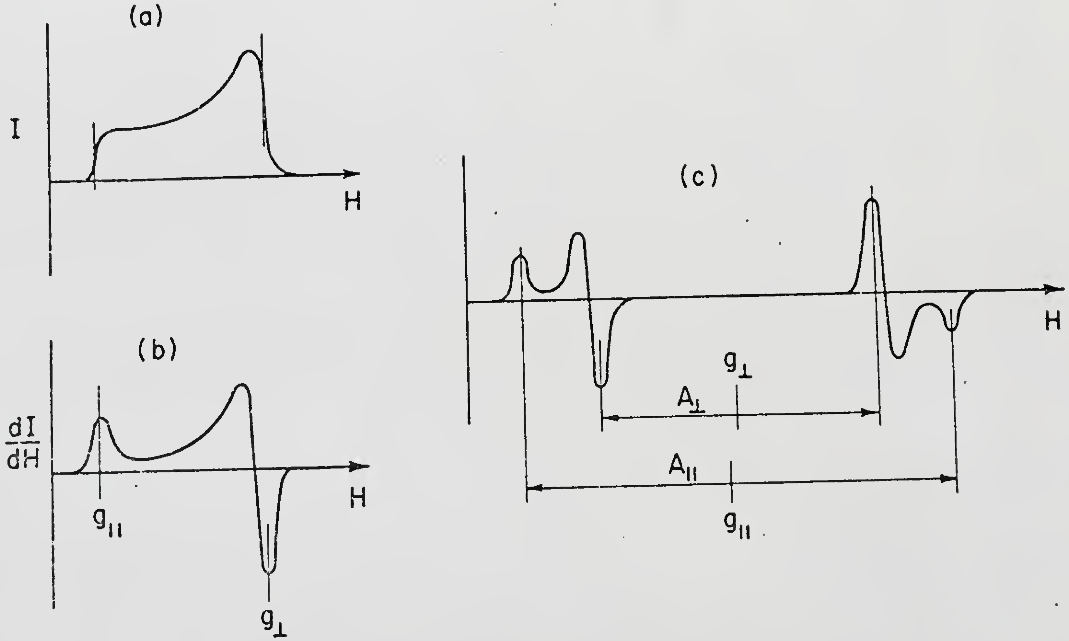

Figure 3. Powder Pattern

parallel lines is called $A_{\parallel}$ and the distance between the two perpendicular lines is called $A_{\perp}$.

The spin Hamiltonian for an axially symmetric molecule, including Hf interaction, was given in Eq. (12). In it, the nuclear Zeeman term ($\underset{\sim}{I} \cdot \underset{\sim}{H}$ type) has been omitted since it is usually small. The nuclear quadrupole interaction has also been omitted for the same reason. To first-order perturbation theory, the field position at which absorption will occur is given by (Eq. (17))

$$H = \frac{h\nu_o}{g\beta_o} - \frac{K}{g\beta_o} m_I \tag{23}$$

where all symbols have been already defined.

The absorption intensity $|dN/dH|$ can be written

$$\left|\frac{dN}{dH}\right| = \frac{N_o}{2}\left\{\frac{2\cos\theta}{g^2}\left[\frac{(g_{\parallel}^2 - g_{\perp}^2)g'H_o}{2g} + \frac{m_I}{\beta_o}\left(\frac{g_{\parallel}^2 A_{\parallel}^2 - g_{\perp}^2 A_{\perp}^2}{2K} - \frac{K(g_{\parallel}^2 - g_{\perp}^2)}{g^2}\right)\right]\right\}^{-1} . \tag{24}$$

The solution to Eq. (24) is much more complicated than that for Eq. (21), since there is no explicit form for sin θ, so that $|dN/dH|$ cannot be written as a function of only the magnetic parameters. One must solve Eq. (23) and (24) for a series of values of θ to obtain the resonant fields and intensities as a function of orientation. For the cases $\theta = 0°$ and $\theta = 90°$, we have

$$H = (g'H_o/g_\parallel) - (m_I A_\parallel/g_\parallel \beta_o) \qquad \text{at} \quad \theta = 0°$$

and

$$H = (g'H_o/g_\perp) - (m_I A_\perp/g_\perp \beta_o) \qquad \text{at} \quad \theta = 90°;$$

therefore, $|dN/dH|$ goes to ∞ as $\theta \rightarrow 90°$ (see Low [27]).

It is then concluded that the absorption pattern will consist of $2I + 1$ superimposed patterns of the type in Figure 1a. Therefore, we get $2I + 1$ parallel lines and $2I + 1$ perpendicular lines.

When several nuclei in the molecule possess magnetic moments, each nucleus will split the line into $2I_i + 1$ lines, where I_i is the nuclear spin of the i^{th} nucleus. In Figure 4a, this is illustrated for a molecule containing two magnetic nuclei; the first one has $I_1 = 3/2$ and the second one has $I_2 = \frac{1}{2}$. It is further assumed that the hyperfine splitting produced by the first nucleus is larger than that produced by the second one. Each one of these absorption lines gives rise to one parallel and one perpendicular component as depicted in Figure 4b. In this case, it is assumed that $A_\parallel > A_\perp$ and that $g_\parallel \approx g_\perp$. In Figure 4c, the first derivative spectrum obtained when this kind of a system is simulated is recorded. The values used for the simulation were $g_\parallel = g_\perp = 2.0023$, $A^1_\parallel = 40.0$ G, $A^1_\perp = 20.0$ G, $A^2_\parallel = 10.0$ G, and $A^2_\perp = 5.0$ G.

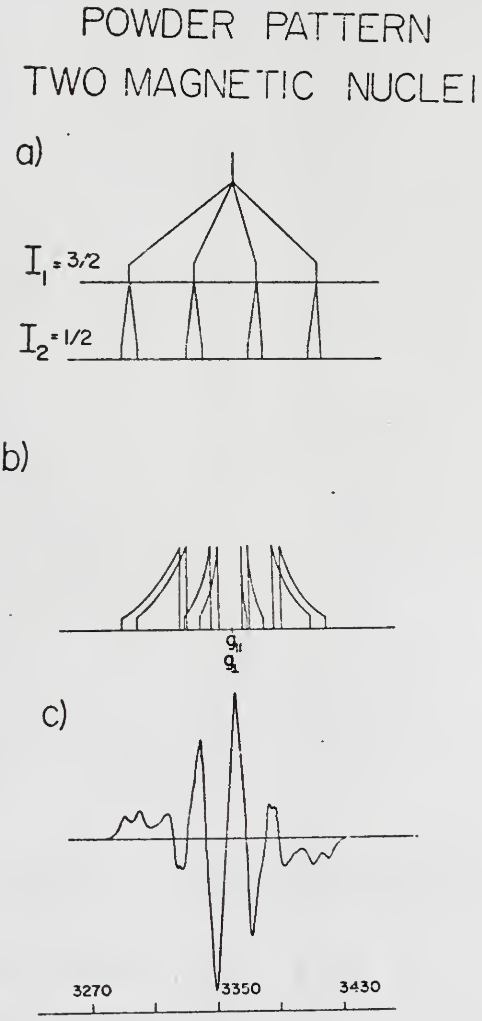

Figure 4. Powder Pattern

References

[1] Dirac, P. A. M., Proc. Roy. Soc. (London) Ser. A 117. 610 (1928).

[2] McWeeny, R., Spins in Chemistry, Academic Press, New York (1970).

[3] McWeeny, R., and Sutcliffe, B. T., Methods of Molecular Quantum Mechanics, Academic Press, New York (1969).

[4] Hameka, H. F., Advanced Quantum Chemistry, Addison and Wesley, Massachusetts (1965).

[5] Wertz, J. E., and Bolton, J. R., Electron Spin Resonance, McGraw-Hill, New York (1972).

[6] Frosch, R. A., and Foley, H. M., Phys. Rev. 88, 1337 (1952).

[7] Carrington, A., and McLachlan, A. D., Introduction to Magnetic Resonance, Harper & Row, New York (1967).

[8] Van Vleck, J. H., Phys. Rev., 33, 467 (1929).

[9] Knight, L. B., and Weltner, Jr., W., J. Chem. Phys., 53, 4111 (1970).

[10] Abragam, A., and Bleaney, B., Electron Paramagnetic Resonance of Transition Ions, Clarendon, Osford (1970).

[11] Ayscough, P. B., Electron Spin Resonance in Chemistry, Methuen, London (1967).

[12] Bleaney, B., Proc. Phys. Soc. (London), A63, 407 (1950).

[13] Bleaney, B., Phil. Mag., 42, 441 (1951).

[14] Sands, R. H., Phys. Rev., 99, 1222 (1955).

[15] Searl, J. W., Smith, R. C., and Wyard, S. J., Proc. Phys. Soc., 74, 491 (1959).

[16] Bleaney, B., Proc. Phys. Soc., A75, 621 (1960).

[17] Roberts, E. M., and Koski, W. S., J. Am. Chem. Soc., 82 (1960).

[18] O'Reilly, D. E., J. Chem. Phys., 29, 1188 (1958).

[19] Kneubuhl, F. K., J. Chem. Phys., 33, 1074 (1960).

[20] Neiman, R., and Kivelson, D., J. Chem. Phys., 35, 156 (1961).

[21] Ibers, J. A., and Swalen, J. D., Phys. Rev., 127, 1914 (1962).

[22] Gersmann, H. R. and Swalen, J. D., J. Chem. Phys., 36, 3221 (1962).

[23] Swalen, J. D., and Gladney, H. M., IBM J. Res. and Develop., 8, 515 (1964).

[24] Johnston, T. S., and Hecht, H. G., J. Mol. Spectr., 17, 98 (1965).

[25] Malley, M. M., . Mol. Spectr., 17, 210 (1965).

[26] Kasai, P. H., Whipple, E. B., and Weltner, Jr., W., J. Chem. Phys., 44, 2581 (1966).

[27] Low, W., Paramagnetic Resonance in Solids, Academic Press, New York (1960).

CHAPTER III

$M^+Cl_2^-$

Introduction

The Cl_2^- molecule ion has received very intense study in the last few years. Since Castner and Kanzig [1] discussed the nature of the V_k color centers in crystalline solids, this species has been investigated in several environments. The V_k center is a trapped electronic hole between two Cl^- ions in alkali halide crystals. It is formed upon the irradiation of these crystals.

This molecule has been postulated as a possible intermediate in the general reaction $M + Cl_2 \rightarrow MCl + Cl$. This intermediate must be very short-lived, since the molecular beam data fail to show its presence. This reaction apparently proceeds via the spectator stripping model [2], implying that the metal atom collides with the Cl_2 molecule and that the reaction product, MCl, proceeds with very little angular variation from the original path. The data indicate that the reaction cross section is very large. Some luminescence experiments [3,4] detected a short-lived intermediate formed when an electron leaves the metal atom and goes on the Cl_2 molecule forming the $M^+Cl_2^-$ specie.

The study of the $M^+Cl_2^-$ specie was decided via the ESR method since the ground state of Cl_2^- is $^2\Sigma$, which makes them observable trapped in matrices at 4 K. Cl_2^- has been studied trapped in other matrices [5,6]. It has also been studied in different types of irradiated crystals [7-13].

Experimental

Method of Preparation of the $M^+Cl_2^-$

A problem in the production of the $M^+Cl_2^-$ species is the trapping of a large enough amount in order to obtain a sufficiently intense signal. Several mole ratios of Cl_2 to argon were tried: 1:1000, 1:200, 1:100 and 1:20. The 1:20 produced the most intense ESR signal, although this is a higher concentration than is usually used in matrix isolation studies.

The metals were deposited at different temperatures, and measured with a Chromel-Alumel thermocouple attached to the Knudsen cell. It was found that the best temperatures were those that provided a metal vapor pressure of the order of 10^{-1} torr (see Table I). The temperature was recorded by using a Leeds and Northrup potentiometer, with a cold junction immersed in an ice-water bath.

The matrices formed were all opaque, greenish-yellow in color and icy in appearance. When either too large a concentration of the metal or too low a concentration of Cl_2

TABLE I

METALS, SOURCES AND TEMPERATURES USED

Metal	Source and Purity	T (K) to Obtain a Vapor Pressure of About 10^{-1} Torr
Mg	J. T. Baker (99.9%)	782
Ca	Fisher (99.9%)	962
Sr	Alpha Inorganics (99.9%)	900
Ba	Alpha Inorganics (99.999%)	984
Li	MC & B (99.9%)	900
Na	J. T. Baker (99.9%)	630
K	Mallickrodt (99.9%)	540

is present in the matrix, the color was red to orange, which is the typical color that the alkali and alkaline-earth metals exhibit when isolated in inert gases by themselves.

The Cl_2 used was obtained from research grade (99.9%) chlorine provided by Air Products Company without further purification. The gas mixture was prepared in a glass vacuum line that was evacuated to pressures of the order of 2×10^{-7}, as read on an ion gauge. Cl_2 was allowed to enter the bulb until a pressure of 36 torr was achieved. Then, Ar was passed into the bulb until the pressure was 760 torr. The metals were obtained from commercial sources with purity as specified in Table I.

All these experiments were done in argon since several trials in neon were unsuccessful. This appears to be due to the fact that quenching in a neon matrix is slower than that in an argon matrix, since its solidification point is considerably lower (24 K) than that of argon (84 K).

Observed Spectrum of $M^+Cl_2^-$

The observed spectra correspond to the Cl_2^- ion. Figures 7, 9, 11, 13, 15, 17, and 19 show the spectra recorded when Mg, Ca, Sr, Ba, Li, Na, and K, respectively, were used as electron donors. In all cases the parallel features of the Cl_2^- ion could be observed, consisting of seven lines for the $^{35}Cl\text{-}^{35}Cl^-$, sixteen lines for the $^{35}Cl\text{-}^{37}Cl^-$, and seven lines for the $^{37}Cl\text{-}^{37}Cl^-$

(see Fig. 5). These lines should have intensities proportional to their relative abundances, i.e.,

$$\begin{array}{ll}
{}^{35}\mathrm{Cl}{}^{35}\mathrm{Cl} & 3/4 \times 3/4 = 9/16 \\
\begin{array}{l} {}^{35}\mathrm{Cl}{}^{37}\mathrm{Cl} \\ {}^{37}\mathrm{Cl}{}^{35}\mathrm{Cl} \end{array} & \left.\begin{array}{l} 3/4 \times 1/4 = 3/16 \\ 1/4 \times 3/4 = 3/16 \end{array}\right\} 6/16 \\
{}^{37}\mathrm{Cl}{}^{37}\mathrm{Cl} & 1/4 \times 1/4 = 1/16 \; .
\end{array}$$

This is observed in the spectra, although some of the ${}^{37}\mathrm{Cl}{}^{37}\mathrm{Cl}$ signals are very weak at certain points.

Each Cl nucleus has a spin of 3/2 and therefore splits the signal into $2(3/2) + 1 = 4$ lines. In the homonuclear cases some of them overlap, increasing their intensities, but in the heteronuclear case they do not. This yields a total of seven lines in an intensity ratio of 1:2:3:4:3:2:1 for the homonuclear case and sixteen equally intense lines for the heteronuclear case. In Figure 1, the different parallel lines for these molecules are identified with a bar whose height is proportional to the relative intensity and abundance of the given species. The perpendicular lines could not be individually identified since they overlap to a great extent.

The values of $A_{\parallel}$ for the different molecules are larger than the corresponding values for $A_{\perp}$. The ratio of the corresponding A values for the two isotopes is in very close agreement with the ratio of their magnetic moments ${}^{35}\mu/{}^{37}\mu = 1.201$, as expected. Values of $A_{\parallel}$ and $A_{\perp}$ for each molecule studied are given in Table II.

ESR SPECTRUM OF Cl_2^- ION

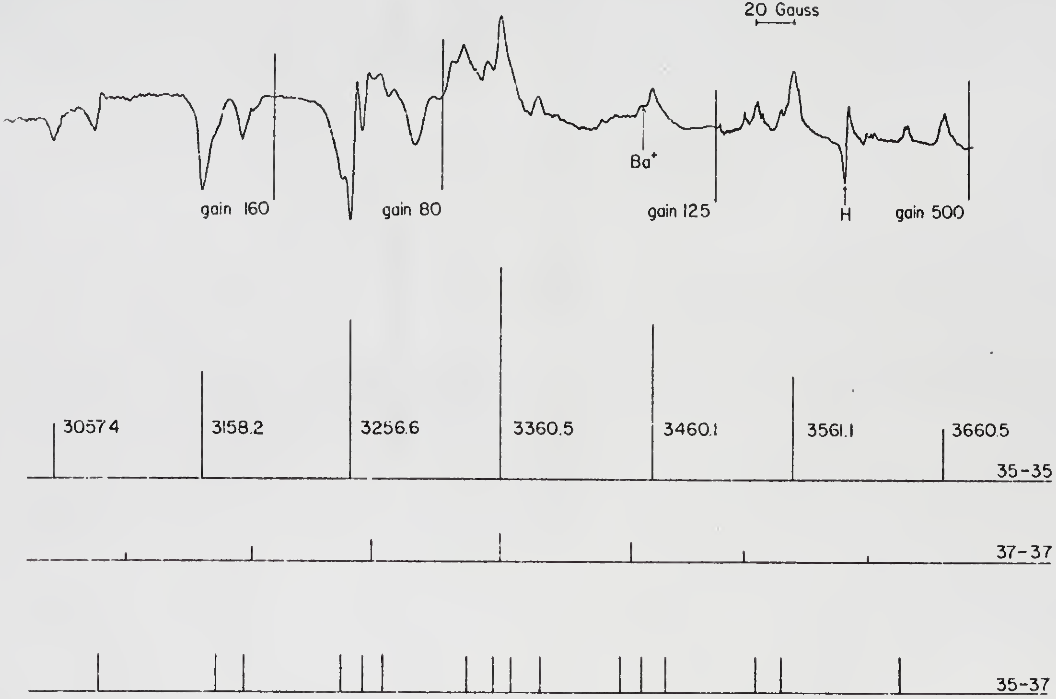

Figure 5

TABLE II

MAGNETIC PARAMETERS FOR Cl_2^-

	$A_{\parallel}$ (G)		$A_{\perp}$ (G)				Schoemaker's (14)				
Metal	^{35}Cl	^{37}Cl	^{35}Cl	^{37}Cl	$g_{\parallel}$	$g_{\perp}$	$A_{\parallel}$(G)	$A_{\perp}$(G)	g_x	g_y	g_z
Mg	95.4	78.8	7.5	6.2	2.0030	2.0342					
Ca	98.8	83.8	7.8	6.2	2.0020	2.0353					
Sr	99.4	84.6	7.9	6.5	2.0030	2.0364					
Ba	100.7	84.8	8.0	6.7	2.0020	2.0393					
Li	99.4	83.9	7.9	6.6	2.0004	2.0367	95.54	6.23	2.0012	2.0432	2.0569
Na	100.7	84.3	8.0	6.6	2.0006	2.0371	98.71	9.04	2.0013	2.0424	2.0492
K	102.5	85.6	8.1	6.8	2.0009	2.0370	101.31	121.3	2.0015	2.0445	2.0424

Experimental $A_{\parallel}$ parameters within ± 1.0 G, $A_{\perp}$ within ± 2.06G, and g values within ± 0.001.

In all of these cases, the values of $A_\perp$ and of $g_\perp$ had to be determined through computer simulation of the spectrum (see Appendix A). $A_\perp$ is small and $g_\perp$ is located close to where a parallel line for the 35-35 case is located. In the same region there are one 37-37 and two 35-37 parallel lines. To add to the complexity, it should be realized that all the perpendicular lines for all three molecules reside within the same region of the spectrum.

The procedure used to determine the value of $A_\perp$ and $g_\perp$ consisted of feeding to a computer the values of $A_\parallel$, $A_\perp$, $g_\parallel$, $g_\perp$, the spectrometer frequency, and the estimated linewidth. By careful comparison of the simulated spectra with the exprmentally obtained one, a final value for the $A_\perp$ and $g_\perp$ parameters could be obtained. In Figure 6, the chosen spectrum for the $Ba^+Cl_2^-$ case, as a typical example, is displayed compared with other small variations in the parameters in order to indicate the sensitivity of this method to the different parameters and their variations. The parameters used for Figure 2a are those listed in Table II for $Ba^+Cl_2^-$. Figure 2b is drawn by using the same parameters except that g was changed to a value of 2.0420 rather than 2.0393. Figure 2c shows the results of changing the $A_\perp$ values from 8.0 G and 6.7 G to 10.0 G and 8.0 G for the 35 and 37 nuclei, respectively. Figure 2d shows the result of changing the linewidth from 4.0 G to 8.0 G.

The sensitivity of the spectrum in this region to the different parameters allowed the determination of their experimental values to the accuracy stated in Table II.

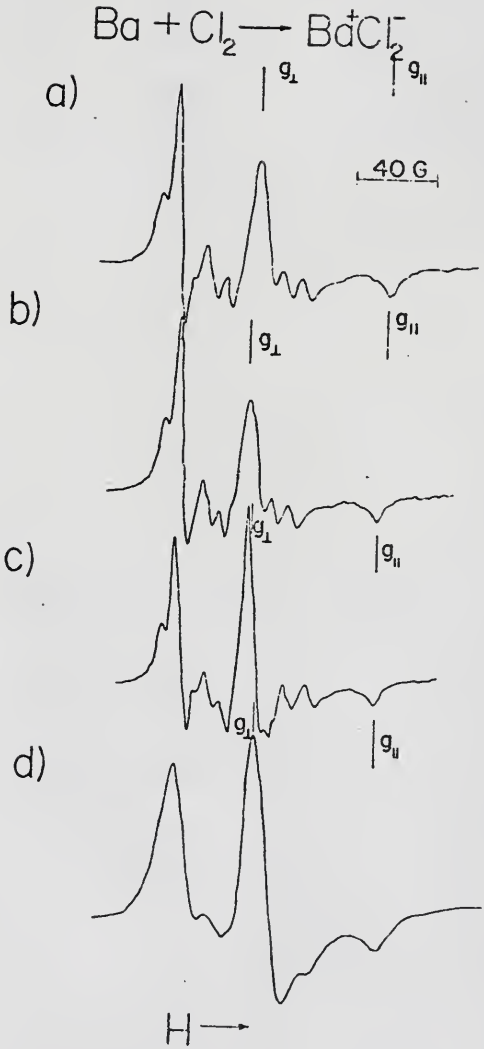

Figure 6

In all of these experiments there was no way to determine the sign of the A values since they all enter the mathematical formulation as the square root of the square of the given value. Therefore, they will all be reported as the absolute value throughout this paper.

No angular variation was detected when the rod was turned to different positions with respect to the applied magnetic field. This is taken as evidence that there is a completely random distribution of the species under study in the matrix.

No variation of the spectra was encountered when the metal was deposited at different rates. It is assumed, then, that all the spectra were essentially recorded at infinite dilution as far as these experiments can distinguish. This may appear as a rather strong assumption since a mole ratio of Cl_2 to Ar of 1:20 was used. However, it should be realized that although the initial concentration of Cl_2 is high the actual amount of trapped $M^+Cl_2^-$ may be small.

In the spectra in which the alkaline-earth metals were used as electron donors, the presence of the corresponding MCl specie could be tentatively assigned, except in the case of BaCl. The perpendicular lines of these molecules occur close to $g_o = 2.0023$. Parallel lines were not assigned since they are small and appear to be covered by the Cl_2^- signals.

In all the alkaline-earth spectra, the presence of the M^+ ion could be observed at $g_o = 2.0023$. In the Mg case, even the lines corresponding to $^{25}Mg^+$ (abundance 10.13%) could be observed.

$Mg^+Cl_2^-$

In Figure 7, the spectrum obtained when Mg atoms were deposited with the Cl_2 and Ar mixture is shown. The salient features observed are those of the Cl_2^- ion.

The values of $A_\parallel$ and of $g_\parallel$ were obtained directly from the spectrum by measuring the separation of the parallel lines. Since $A_\perp$ is small, the second-order correction (see Low [15]) is of the order of 0.05 G, and therefore will not affect the accuracy of $A_\parallel$ and $g_\parallel$ within the accuracy of the experimentally measurable value. In Table III a list of the parallel line positions, both as observed and as calculated, is included using the previously determined parallel parameters. The perpendicular parameters were obtained by computer simulation. The assigned values for this molecule are: $A_\parallel = 95.4 \pm 1.0$ G, $A_\perp = 7.5 \pm 2.0$ G, for the ^{35}Cl nucleus and $A_\parallel = 78.8 \pm 1.0$ G, $A_\perp = 6.2 \pm 2.0$ G for the ^{37}Cl nucleus; $g_\parallel = 2.0030 \pm 0.001$, $g_\perp = 2.0342 \pm 0.001$.

In Figure 8, a comparison between the computer simulated spectrum (Fig. 8a) and the experimentally determined one (Fig. 8b) in the region around $g_\parallel$ and $g_\perp$ is plotted.

It is believed that the MgCl spectrum is also observed in this system. In Table XVIII the $A_\perp$ value for this molecule is listed. The parallel lines could not be identified since they probably lie under some of the Cl_2^- lines.

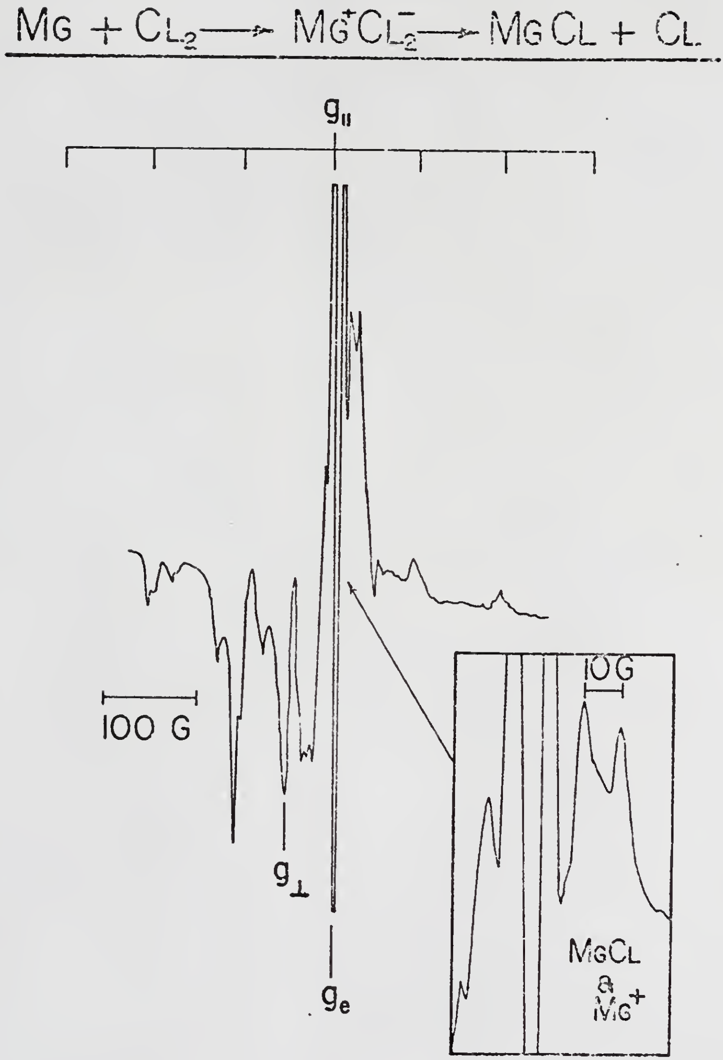

$Mg + Cl_2 \rightarrow Mg^+Cl_2^- \rightarrow MgCl + Cl$

Figure 7

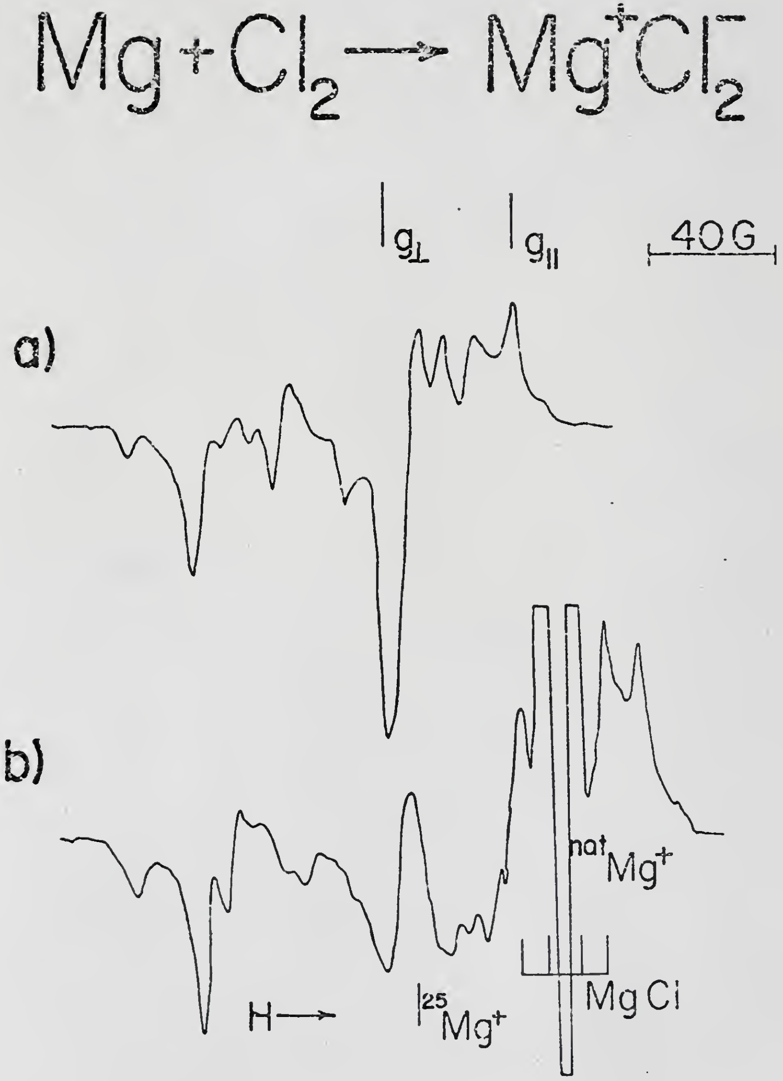
$Mg + Cl_2 \longrightarrow Mg^+Cl_2^-$
$g_\perp$
$g_\parallel$
40G
a)
b)
$^{nat}Mg^+$
MgCl
$^{25}Mg^+$
H→

Figure 8

TABLE III

PARALLEL LINE POSITIONS FOR THE $Mg^+Cl_2^-$

		$^{35}Cl^{35}Cl$		$^{37}Cl^{37}Cl$		$^{35}Cl^{37}Cl$	
m_I	m_I	exp.	calc.	exp.	calc.	exp.	calc.
3/2	3/2	3066.9	3066.4	3116.1	3116.0	3092.5	3091.1
3/2	1/2	3161.7	3161.7	3194.8	3194.8	3169.9	3169.9
1/2	3/2					3185.9	3186.5
3/2	-1/2	3256.0	3257.0*	*	3273.6	3249.0	3248.7
1/2	1/2					3262.6*	3265.3
-1/2	3/2					3281.3	3281.9
3/2	-3/2	3352.4	3352.4	3352.4	3352.4	*	3329.5
1/2	-1/2					*	3344.1
-1/2	1/2					*	3360.7
-3/2	3/2					3377.7	3377.3
1/2	-3/2	3447.4	3447.4	3431.6	3431.2	3422.1	3422.9
-1/2	-1/2					3439.1	3439.5
-3/2	1/2					3455.9	3456.1
-1/2	-3/2	3542.5	3543.1	3510.9	3510.0	**	3518.3
-3/2	-1/2					3534.9	3534.1
-3/2	-3/2	3638.8	3638.5	*	3588.8	3612.7	3613.7

* Denotes heavy overlap of lines.

** Denotes the fact that the line is weak, therefore difficult to evaluate.

} Denotes overlap in homonuclear molecules.

All values in G.

The analysis of this spectrum also shows evidence of the presence of the Mg^+ ion. This ion is believed to accompany the formation of Cl_2^-, forming an ion pair system (see discussion). The $^{nat}Mg^+$ signal appears at 3364.6 ± 0.5 G which yields a g-value of 1.9940. The lines for $^{25}Mg^+$ (10.13%) natural abundance, I = 5/2) were also observed. In this case, it is assumed that $A_{iso} \approx A_{\parallel} \approx A_{\perp}$ and therefore $A_{dip} = 0.0$ (for a treatment of these parameters see the discussion). The A_{iso} value for this ion is found to be 130.3 G. This value compares favorably with the one obtained by Brom and Weltner [16] for MgOH.

The values of the line positions as observed experimentally and those calculated (see Low [15, p. 60 ff]) are listed in Table IV.

$Ca^+Cl_2^-$

In Figure 9, the spectrum obtained when Ca atoms were deposited simultaneously with the Cl_2 and Ar mixture is shown. The salient features of it are those of the Cl_2^- ion. The values of $A_{\parallel}$ and $g_{\parallel}$ were directly obtained from the spectrum by measuring the difference between the parallel lines as in the case of $Mg^+Cl_2^-$. The values of $A_{\perp}$ and of $g_{\perp}$, however, had to be obtained by computer simulation. In Figure 10, the computer simulated spectrum (Fig. 10a) is compared with the experimentally observed one (Fig. 10b) for the region close to $g_{\parallel}$ and $g_{\perp}$.

TABLE IV

$^{25}Mg^+$ Lines

m_I	Experimental (G)	Calculated (G)
5/2	3059.5	3059.4
3/2	3187.8	3188.9
1/2	3318.8	3318.8
-1/2	3447.8	3447.8
-3/2	3566.2	3577.2
-5/2	*	3706.6

* Indicates the line is too weak to be measured correctly.

$$\mathrm{Ca} + \mathrm{Cl_2} \longrightarrow \mathrm{Ca^+Cl_2^-} \longrightarrow \mathrm{CaCl} + \mathrm{Cl}$$

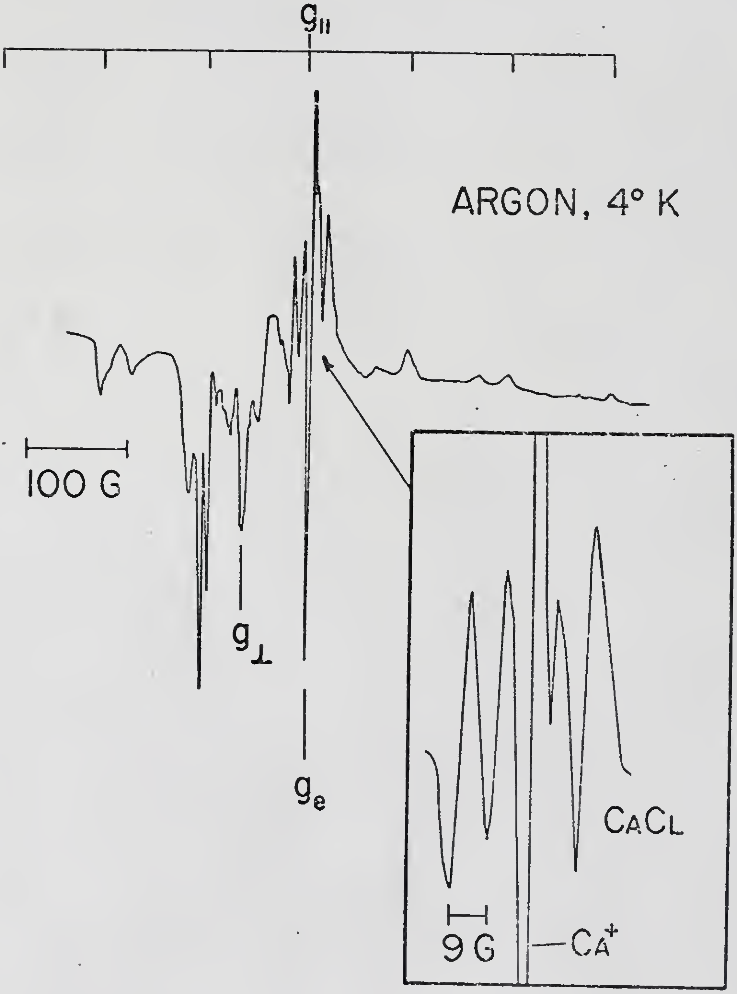

Figure 9

$$Ca + Cl_2 \longrightarrow Ca^+Cl_2^-$$

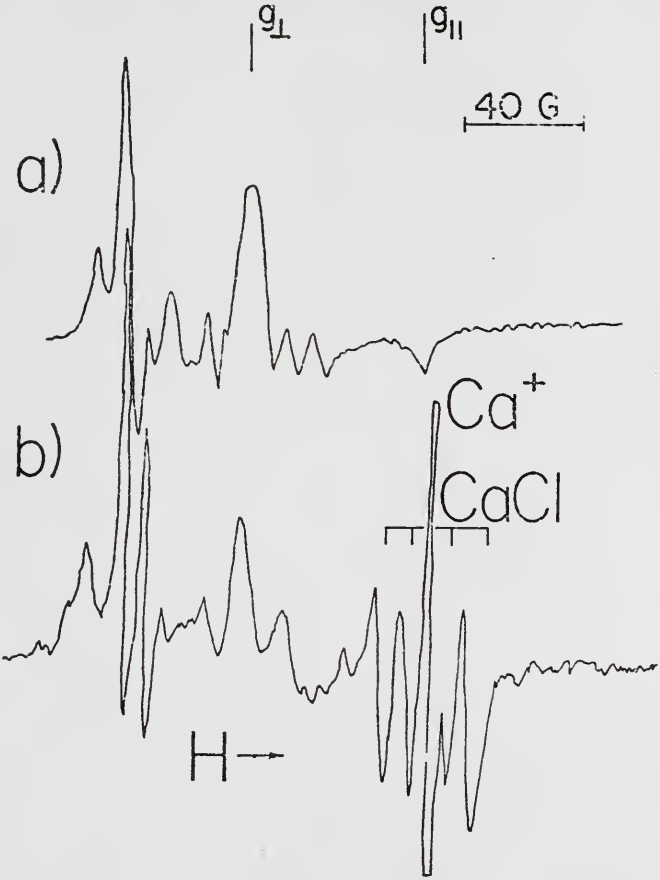

Figure 10

TABLE V

PARALLEL LINE POSITIONS FOR THE $Ca^+Cl_2^-$

		$^{35}Cl^{35}Cl$		$^{37}Cl^{37}Cl$		$^{35}Cl^{37}Cl$	
m_I	m_I	exp.	calc.	exp.	calc.	exp.	calc.
3/2	3/2	3057.5	3057.1	3103.7	3102.3	3079.4	3079.8
3/2	1/2	3155.8	3155.8	3187.0	3186.1	3163.6	3163.6
1/2	3/2					3179.2	3178.6
3/2	-1/2	3253.4	3254.5*	*	3269.9	*	3247.4
1/2	1/2					*	3262.4
-1/2	3/2					*	3277.4
3/2	-3/2	3353.7	3353.7	3353.7	3353.7	3330.3	3331.2
1/2	-1/2					*	3346.2
-1/2	1/2					*	3361.2
-3/2	3/2					*	3376.2
1/2	-3/2	3451.8	3452.1	3437.5	3437.5	**	3430.0
-1/2	-1/2					3447.0	3445.0
-3/2	1/2					3459.1	3460.0
-1/2	-3/2	3550.8	3551.1	3521.5	3521.3	3525.3	3528.8
-3/2	-1/2					3544.6	3543.8
-3/2	-3/2	3650.0	3649.9	3606.7	3605.1	**	36.27.6

* Denotes heavy overlap.

** Denotes the fact that the line is weak, therefore difficult to evaluate.

} Denotes overlap in homonuclear molecules.

All values in G.

In Table V, the field positions of the parallel lines as observed and as calculated are listed. The magnetic parameters used are: $A_{\parallel} = 98.8 \pm 1.0$ G, $A_{\perp} = 7.8 \pm 2.0$ G for the 35 nucleus, $A_{\parallel} = 83.8 \pm 1.0$ G, $A_{\perp} = 6.2 \pm 2.0$ G for the 37 nucleus; $g_{\parallel} = 2.0020 \pm 0.001$ and $g_{\perp} = 2.0353 \pm 0.001$.

It is believed that the presence of the CaCl molecule can be positively identified. In Table XVIII, the $A_{\perp}$ value for it is listed. As in the case of MgCl, only the perpendicular lines are observed.

Ca^+ is also observed in this spectrum at 3364.6 G for a g-value of 1.9957. $^{43}Ca^+$ ($I = 7/2$) is only present to the extent of 0.145% so that no Hf splittings due to interaction with the metal nucleus could be observed.

$Sr^+Cl_2^-$

In Figure 11, the spectrum observed when Sr atoms were deposited with the Cl_2 and Ar mixture is reproduced. The salient features are again those of the Cl_2^- ion. The values of $A_{\parallel}$ and of $g_{\parallel}$ were directly obtained from the line positions as before. The values of $A_{\perp}$ and of $g_{\perp}$ had to be obtained by computer simulation. In Figure 12a, the computer simulated spectrum is compared with the experimentally observed one (Fig. 12b) for the region close to $g_{\parallel}$ and to $g_{\perp}$.

In Table VI, the field positions of the parallel lines as observed and as calculated are listed. The magnetic parameters used are: $A_{\parallel} = 99.4 \pm 1.0$ G, $A_{\perp} = 7.8 \pm 2.0$ G

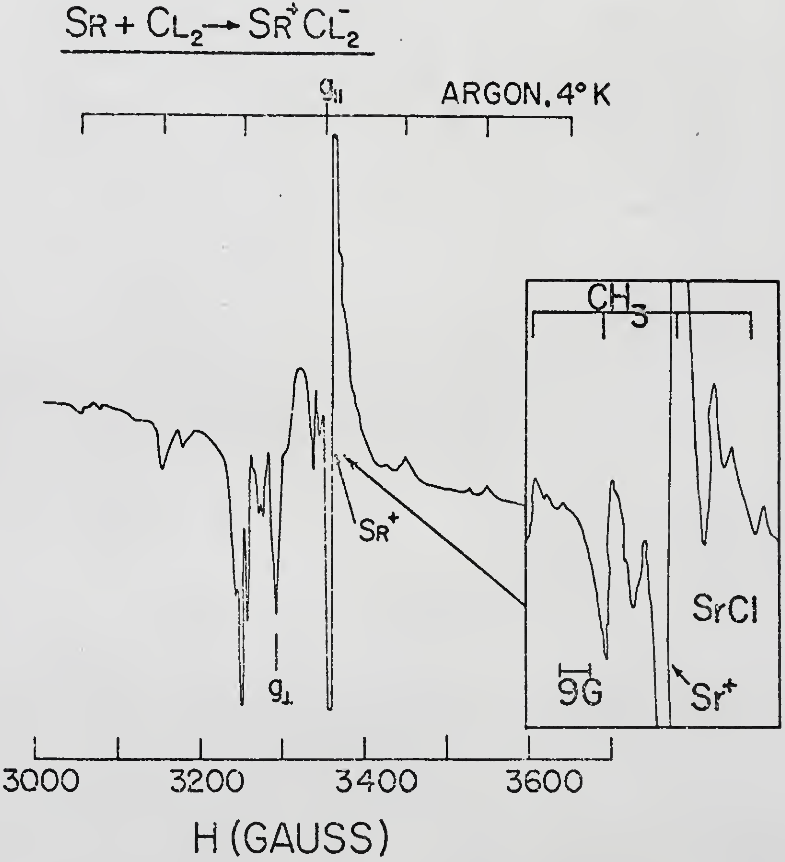
SR + CL2 → SR+CL2-
ARGON, 4° K
g∥
g⊥
SR+
CH3
9G
SrCl
Sr+
3000
3200
3400
3600
H (GAUSS)

Figure 11

$$Sr + Cl_2 \longrightarrow Sr^+Cl_2^-$$

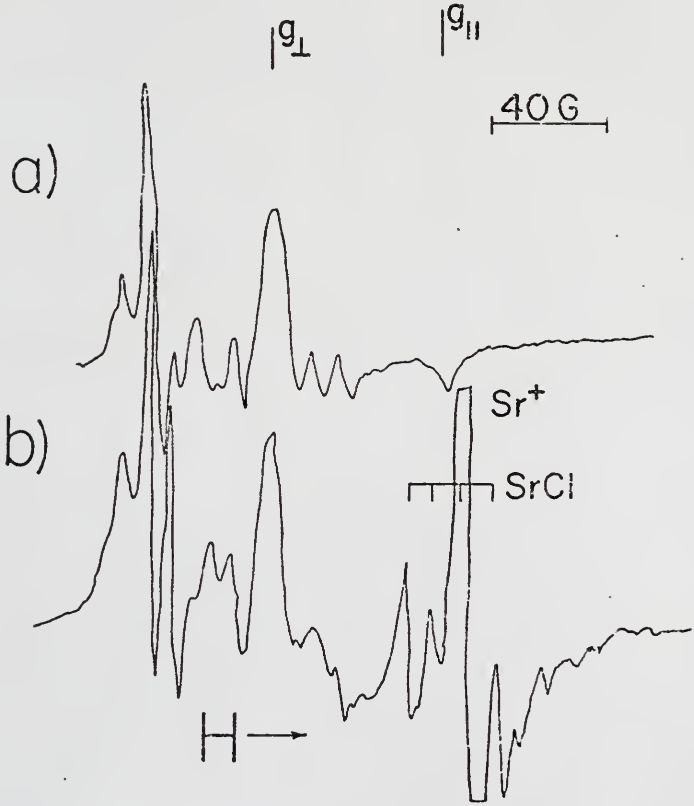

Figure 12

TABLE VI

PARALLEL LINE POSITIONS FOR THE $Sr^+Cl_2^-$

		$^{35}Cl^{35}Cl$		$^{37}Cl^{37}Cl$		$^{35}Cl^{37}Cl$	
m_I	m_I	exp.	calc.	exp.	calc.	exp.	calc.
3/2	3/2	3054.0	4053.6	*	3097.8	3075.2	3075.6
3/2	1/2	3153.3	3152.9	3182.9	3182.4	3160.2	3160.2
1/2	3/2					3176.7	3175.0
3/2	-1/2	3250.6	3252.3*	*	3267.0	*	3244.8
1/2	1/2					*	3259.6
-1/2	3/2					*	3274.4
3/2	-3/2	3351.6	3351.6	3351.6	3351.6	3330.4	3329.4
1/2	-1/2					3344.4	3344.2
-1/2	1/2					3359.1	3359.0
-3/2	3/2					3373.8	3373.8
1/2	-3/2	3451.5	3451.0	3436.7	3436.2	3429.4	3428.8
-1/2	-1/2					3443.0	3443.6
-3/2	1/2					3458.5	3458.4
-1/2	-3/2	3551.1	3550.3	3519.2	3520.8	3527.7	3528.2
-3/2	-1/2					3542.2	3543.0
=3/2	-3/2	3649.7	3649.7	*	3605.4	3627.4	3627.6

* Denotes heavy overlap.

} Denotes overlap in homonuclear molecules.

All values in G.

for the 35 nucleus and $A_{\parallel} = 84.6 \pm 1.0$ G, $A_{\perp} = 6.5 \pm 2.0$ G for the 37 nucleus; $g_{\parallel} = 2.0030 \pm 0.001$ and $g_{\perp} = 2.0364 \pm 0.001$.

It is believed that the presence of the SrCl molecule can be detected. In Table XVIII the $A_{\perp}$ value for it is listed. As in the case of MgCl, only the perpendicular lines are observed.

Sr^+ is detected at a field position of 3359.1 G for a g-value of 1.9991. $^{87}Sr^+$ $(I = 9/2)$ is only present to the extent of 7.02% and no Hf splittings due to the interaction with the metal nucleus could be observed.

$Ba^+Cl_2^-$

In Figure 13, the spectrum recorded when Ba atoms were allowed to react with the Cl_2 and Ar mixture is shown. In it, again, the salient features are those of the Cl_2^- ion. The magnetic parameters were obtained as in the previous cases; the parallel parameters by direct measurement of the line positions, and the perpendicular parameters by computer simulation. In Figure 14, the computer simulated spectrum (Fig. 14a) is compared with the experimentally obtained one (Fig. 14b) for the region close to $g_{\parallel}$ and $g_{\perp}$.

In Table VII, the field positions of the parallel lines as observed and as calculated are listed. The magnetic parameters used are: $A_{\parallel} = 100.7 \pm 1.0$ G, $A_{\perp} = 8.0 \pm 2.0$ G for the 35 nucleus, $A_{\parallel} = 84.8 \pm 1.0$ G, $A_{\perp} = 6.7 \pm 2.0$ G for the 37 nucleus: $g_{\parallel} = 2.0020 \pm 0.001$ and $g_{\perp} = 2.0393 \pm 0.001$.

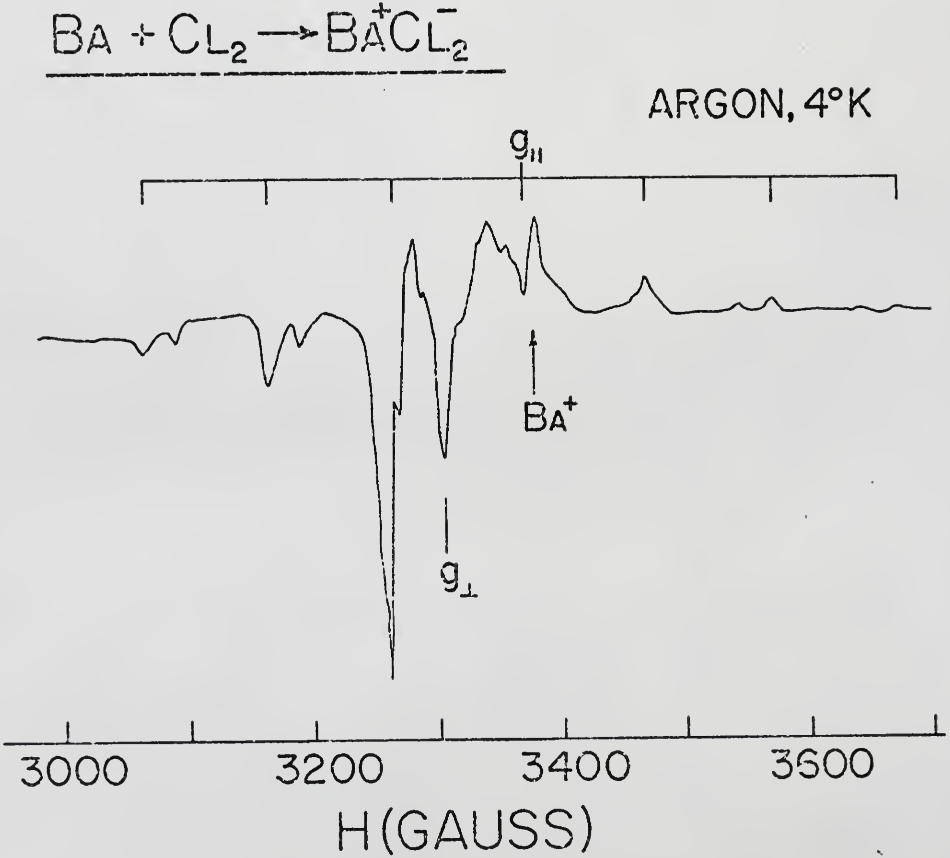
$Ba + Cl_2 \longrightarrow Ba^+Cl_2^-$
ARGON, 4°K
$g_{\parallel}$
Ba^+
$g_{\perp}$
3000
3200
3400
3600
H(GAUSS)

Figure 13

$Ba + Cl_2 \longrightarrow Ba^+Cl_2^-$

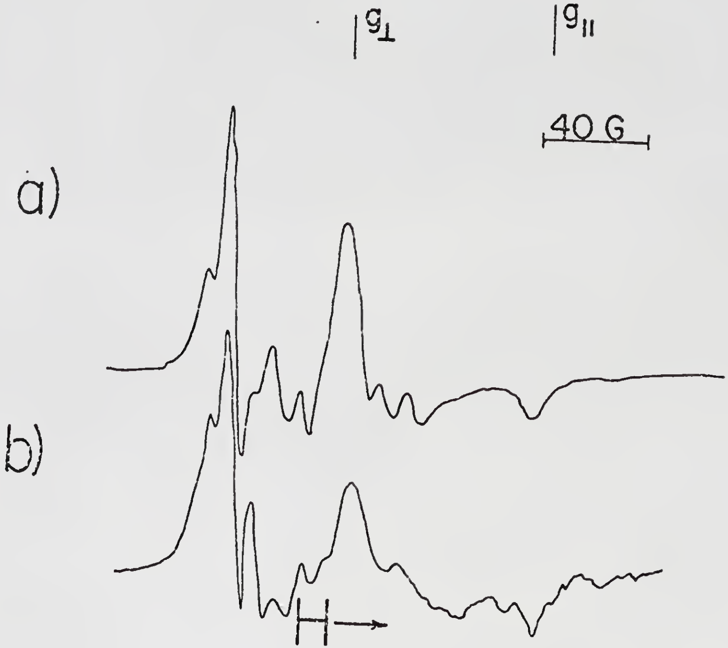

Figure 14

TABLE VII

PARALLEL LINE POSITIONS FOR THE $Ba^+Cl_2^-$

		$^{35}Cl^{35}Cl$		$^{37}Cl^{37}Cl$		$^{35}Cl^{37}Cl$	
m_I	m_I	exp.	calc.	exp.	calc.	exp.	calc.
3/2	3/2	3057.4	3057.4	3107.3	3107.3	3084.1	3083.5
3/2	1/2	3158.2	3158.1	3192.1	3195.5	3167.7	3167.5
1/2	3/2					3184.3	3184.2
3/2	-1/2	3256.6	3258.8*	*	3275.5	*	3251.5
1/2	1/2					*	3268.2
-1/2	3/2					*	3284.9
3/2	-3/2	3360.5	3359.5	3360.5	3359.5	*	3335.5
1/2	-1/2					3351.3	3352.2
-1/2	1/2					3367.4	3368.9
-3/2	3/2					3384.0	3384.4
1/2	-3/2	3460.1	3460.2	3444.0	3443.5	3436.8	3436.2
-1/2	-1/2					3452.4	3452.9
-3/2	1/2					3468.9	3469.2
-1/2	-3/2	3560.4	3560.9	3528.0	3527.5	3536.7	3536.9
-3/2	-1/2					3552.9	3553.6
-3/2	-3/2	3661.9	3661.6	3612.1	3611.5	3637.0	3637.6

* Denotes heavy overlap.

} Denotes overlap in homonuclear molecules.

All values in G.

The presence of the BaCl molecule is not detected in this case.

Ba^+ is detected at a field position of 3360.5 G for a g-value of 2.0020. $^{137}Ba^+$ (I = 3/2) is only present to the extent of 11.32% and no Hf splittings due to the interaction with the metal nucleus could be observed.

The $Ba^+Cl_2^-$ case was also run in the variable-temperature Dewar in order to observe, if possible, whether BaCl would form as the temperature was being increased. When the temperature was raised to about 15 K, a sudden change in the spectrum was detected. The Ba^+ line increased significantly, while the Cl_2^- pattern decreased a small amount. No lines that could be attributed to BaCl appeared.

$Li^+Cl_2^-$

In Figure 15, the spectrum obtained when Li atoms were deposited with the Cl_2 and Ar mixture is shown. In it, again, the salient features are those of the Cl_2^- ion. The magnetic parameters for this species were determined as before, the parallel ones by direct measurement of the line positions and the perpendicular ones by computer simulation. It is interesting to notice that this is the only case in which the alkali metals were used in which the unreacted atoms appear in the spectrum. The ^7Li lines are indicated in

Figure 15. It appears that since Li has the highest ionization potential of the alkaline metals, the reaction is not as efficient.

In Table VIII the field positions of the parallel lines as observed and as calculated are listed. The magnetic parameters used are: $A_{\parallel} = 99.4 \pm 1.0$ G, $A_{\perp} = 7.9 \pm 2.0$ G for the 35 nucleus, $A_{\parallel} = 83.9 \pm 1.0$ G, $A_{\perp} = 6.6 \pm 2.0$ G for the 37 nucleus; $g_{\parallel} = 2.0004 \pm 0.001$ and $g_{\perp} = 2.0328 \pm 0.001$.

In Figure 16, the computed spectrum (Fig. 16a) is compared with the experimentally obtained one (Fig. 16b) for the area close to $g_{\parallel}$ and $g_{\perp}$.

No lines corresponding to either Li^+ or to LiCl are observed or expected in this spectrum since they have ^1S and $^1\Sigma$ ground states, respectively.

In this spectrum, the presence of HCO and CH_3 is detected in fairly large amounts. This is probably due to the fact that Li is kept under a generous amount of petroleum jelly. It was thoroughly washed in benzene before introduction into the furnace, but in spite of this, it is believed that some hydrocarbons stay with it, producing the radicals HCO and CH_3 due to either thermal decomposition or reaction with the Cl_2.

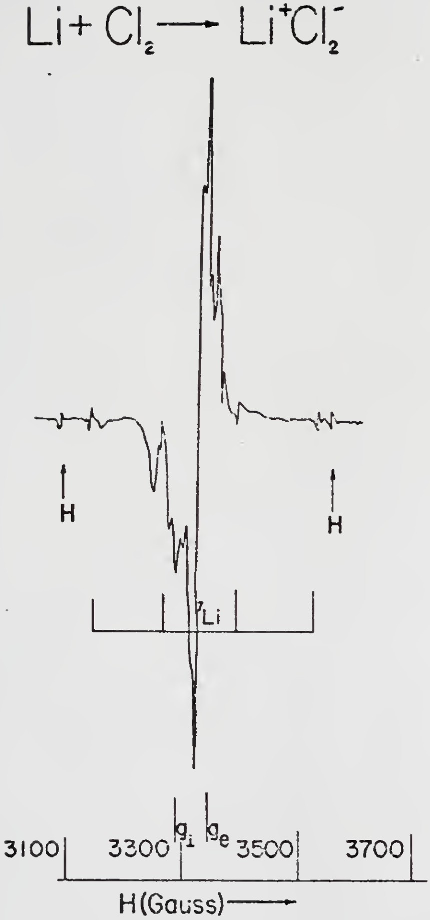

Figure 15

$Li + Cl_2 \rightarrow Li^+Cl_2^-$

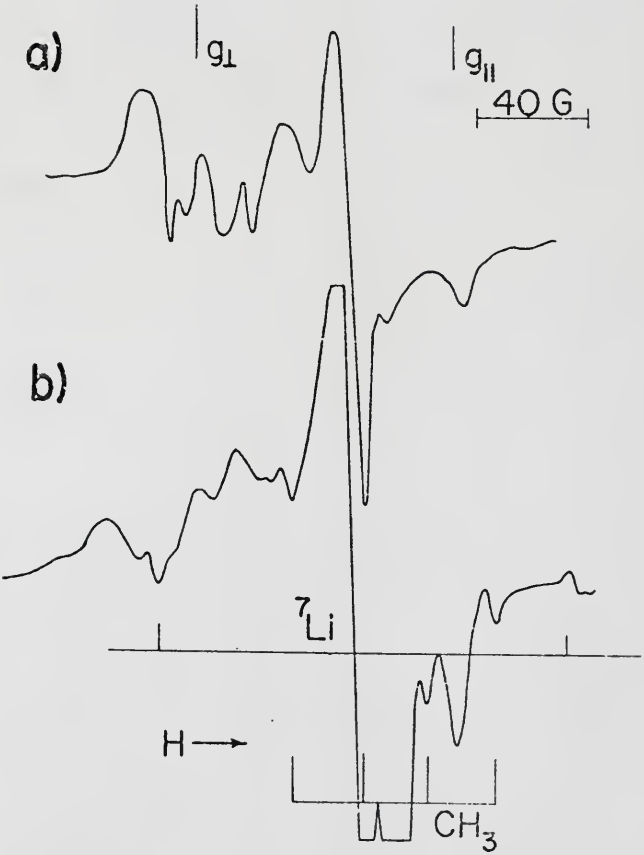

Figure 16

TABLE VIII

PARALLEL LINE POSITIONS FOR THE $Li^+Cl_2^-$

		$^{35}Cl^{35}Cl$		$^{37}Cl^{37}Cl$		$^{35}Cl^{37}Cl$	
m_I	m_I	exp.	calc.	exp.	calc.	exp.	calc.
3/2	3/2	3053.0	3052.2	**	3098.7	*	3075.4
3/2	1/2	3151.6	3151.6	3182.4	3182.5	3159.5	3159.3
1/2	3/2					3174.8	3174.8
3/2	-1/2	3251.8*	3250.9	*	3266.4	*	3243.2
1/2	1/2					*	3258.7
-1/2	3/2					*	3274.2
3/2	-3/2	*	3350.3	*	3350.3	*	3327.1
1/2	-1/2					*	3342.6
-1/2	1/2					*	3358.0
-3/2	3/2					*	3373.5
1/2	-3/2	3449.7	3449.7	3433.9	3434.2	3426.6	3426.4
-1/2	-1/2					3442.1	3441.9
-3/2	1/2					3457.3	3457.4
-1/2	-3/2	***	3549.0	3517.7	3518.1	3525.0	3525.8
-3/2	01/2					3451.5	3541.3
-3/2	-3/2	3648.0	3648.4	3601.9	3601.9	3524.9	3625.2

*Denotes heavy overlap.

**Denotes weak lines.

***Denotes overlap with the ^{7}Li lines.

}Denotes overlap in homonuclear molecules.

All values in G.

In Table IX, the value of the parallel and the perpendicular lines for ^{7}Li $(I = 3/2)$ are listed. The magnetic parameters determined for this atom are $A_{\parallel} = 149.5 \pm 1.0$ G, $A_{\perp} = 141.2 \pm 1.0$ G, $g_{\parallel} = 2.0008 \pm 0.001$ and $g_{\perp} = 2.0011 \pm 0.001$, which compare favorably with the values of $A = 143.4$ G and $g = 2.0023$ determined by Jen, Bowers, Cochran and Foner [17].

TABLE IX

PARALLEL AND PERPENDICULAR LINES FOR ^{7}Li ATOMS IN ARGON

m_I	Parallel Lines		Perpendicular Lines	
	exp.	calc.	exp.	calc.
3/2	3120.9	3120.9	3132.6	3132.6
1/2	*	3264.5	*	3267.4
-1/2	3414.6	3414.0	3408.6	3407.1
-3/2	3569.4	3569.4	3556.0	3555.5

* Indicates that the line could not be measured accurately due to overlap.

Note: All line positions are estimated to be correct to ±0.5 G.

$Na^+Cl_2^-$

In Figure 17, the spectrum obtained when Na atoms were deposited with the Cl_2 and Ar mixture is shown. The salient features of it are those of the Cl_2^- ion. The magnetic parameters for this species were obtained as in the previous cases, the parameters by actual measurement of the line positions and the perpendicular parameters by computer simulation. In Figure 18, the computed spectrum (Fig. 18a) is compared with the experimentally obtained one (Fig. 18b), for the area close to $g_\parallel$ and $g_\perp$.

In Table X, the parallel line positions, both calculated and experimental, are listed. The magnetic parameters used are: $A_\parallel = 100.7 \pm 1.0$ G, $A_\perp = 8.0 \pm 2.0$ G for the 35 nucleus, $A_\parallel = 83.4 \pm 1.0$ G, $A_\perp = 6.5 \pm 2.0$ G for the 37 nucleus; $g_\parallel = 2.006 \pm 0.001$ and $g_\perp = 2.0371 \pm 0.001$.

As in all the other alkali metals, neither the metal ion nor the monochloride is observable via ESR.

No Na lines were observed in this spectrum, indicating that Na has essentially reacted completely.

HCO and CH_3 are present in this case, as they were in the $Li^+Cl_2^-$ case. Again, Na is kept under kerosene and, in spite of being washed with benzene, it is believed that it will generate the radicals upon thermal decomposition or reaction with Cl_2.

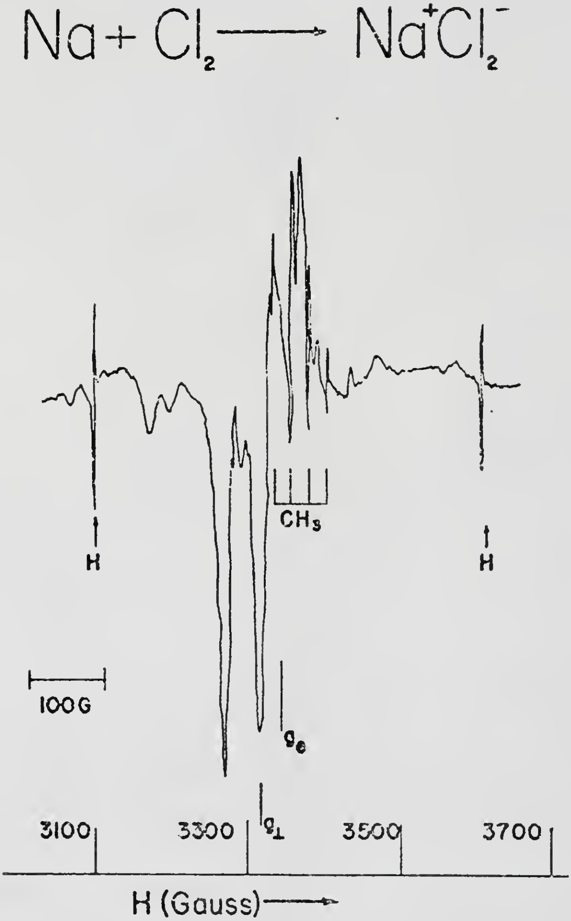
$Na + Cl_2 \longrightarrow Na^+Cl_2^-$
H
CH$_3$
H
100G
g$_\parallel$
g$_\perp$
3100
3300
3500
3700
H (Gauss)

Figure 17

$Na + Cl_2 \longrightarrow Na^+Cl_2^-$

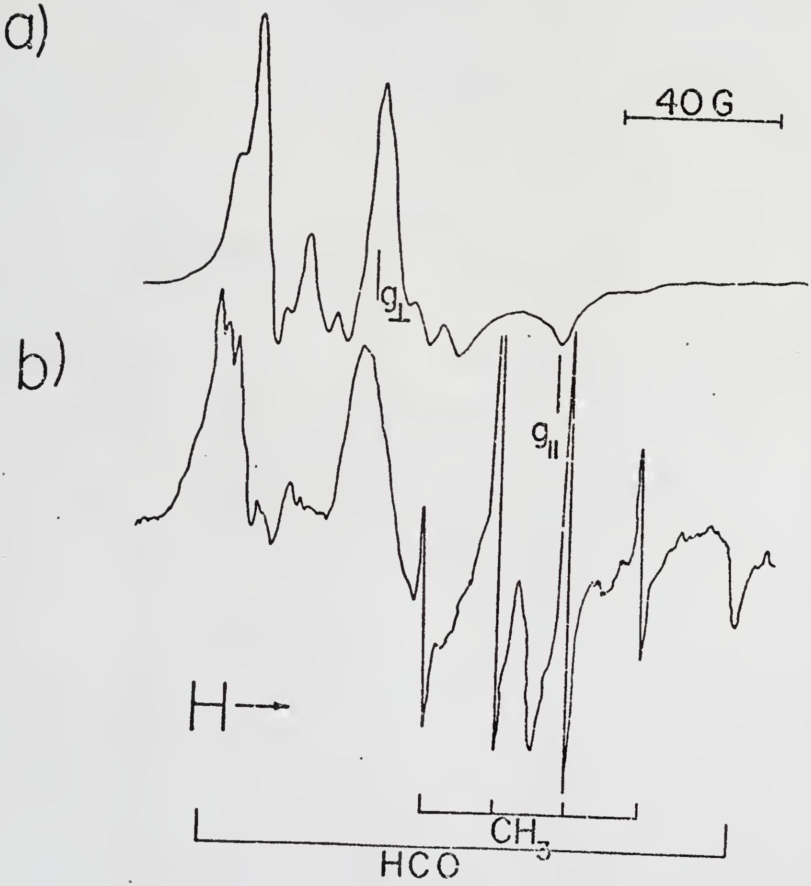

Figure 18

TABLE X

PARALLEL LINE POSITIONS FOR THE $Na^+Cl_2^-$

		$^{35}Cl^{35}Cl$		$^{37}Cl^{37}Cl$		$^{35}Cl^{37}Cl$	
m_I	m_I	exp.	calc.	exp.	calc.	exp.	calc.
3/2	3/2	3054.1	3053.7	3101.7	3102.9	**	3078.3
3/2	1/2	3154.1	3154.4	3187.2	3187.2	3162.9	3162.6
1/2	3/2					3180.1	3179.0
3/2	-1/2	3256.3	3255.1*	*	3271.5	*	3246.9
1/2	1/2					3279.1	3279.7
-1/2	3/2					*	3331.2
3/2	-3/2	3355.8	3355.8	3355.8	3355.8	*	3347.6
1/2	-1/2					*	3364.0
-1/2	1/2					3379.6	3380.4
-3/2	3/2					*	3431.9
1/2	-3/2	3456.7	3456.5	3440.1	3440.1	3449.0	3448.3
-1/2	-1/2					3465.0	3464.7
-3/2	1/2					3465.0	3464.7
-1/2	-3/2	3556.1	3557.2	**	3524.4	3533.2	3532.6
-3/2	-1/2					3550.8	3549.0
-3/2	-3/2	3657.3	3657.9	**	3608.7	*	3633.3

* Denotes heavy overlap.

** Denotes very weak lines.

} Denotes overlap for homonuclear molecules.

All values in G.

$K^+Cl_2^-$

In Figure 19, the spectrum obtained when K atoms are deposited with the Cl_2 and Ar mixture is shown. The salient features are those of the Cl_2^- ion. The magnetic parameters for this specie were obtained in the same fashion as before, parallel parameters by direct measurement of the line positions and the perpendicular ones by computer simulation. In Figure 20, the computed spectrum (Fig. 20a) is compared with the experimentally obtained one (Fig. 20b) for the region close to $g_\parallel$ and $g_\perp$.

In Table XI, the parallel line positions as obtained both from calculation and experiment are listed. The parameters used are: $A_\parallel = 102.5 \pm 1.0$ G, $A_\perp = 8.1 \pm 2.0$ G for the 35 nucleus, $A_\parallel = 85.6 \pm 1.0$ G, $A_\perp = 6.8 \pm 2.0$ G for the 37 nucleus; $g_\parallel = 2.0009 \pm 0.001$ and $g_\perp = 2.0370 \pm 0.001$.

As in all other alkali metals, neither the metal ion nor the monochloride is observable via ESR since they are ^1S and $^1\Sigma$, respectively.

No K lines were observed in this spectrum, indicating that K has essentially reacted completely.

HCO and CH_3 are again present in this spectrum. K is kept under kerosene and, although it was thoroughly washed with benzene before insertion in the furnace, it is believed that the kerosene generated the radicals by either thermal decomposition or reaction with Cl_2.

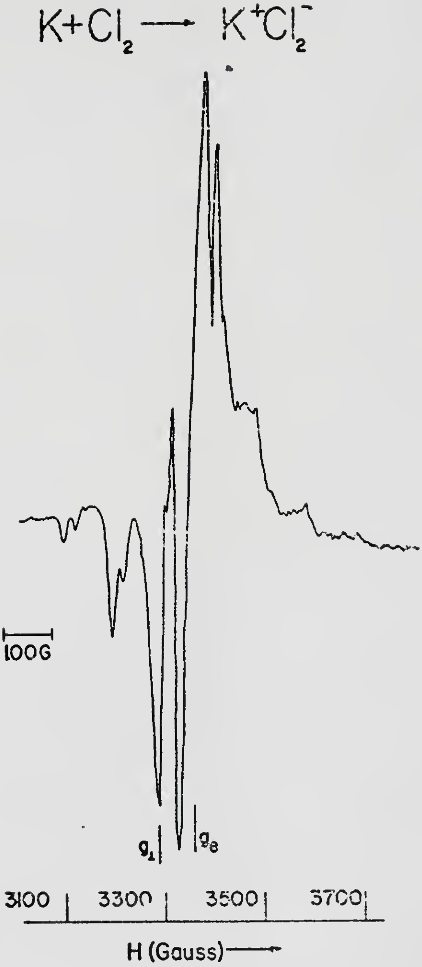

Figure 19

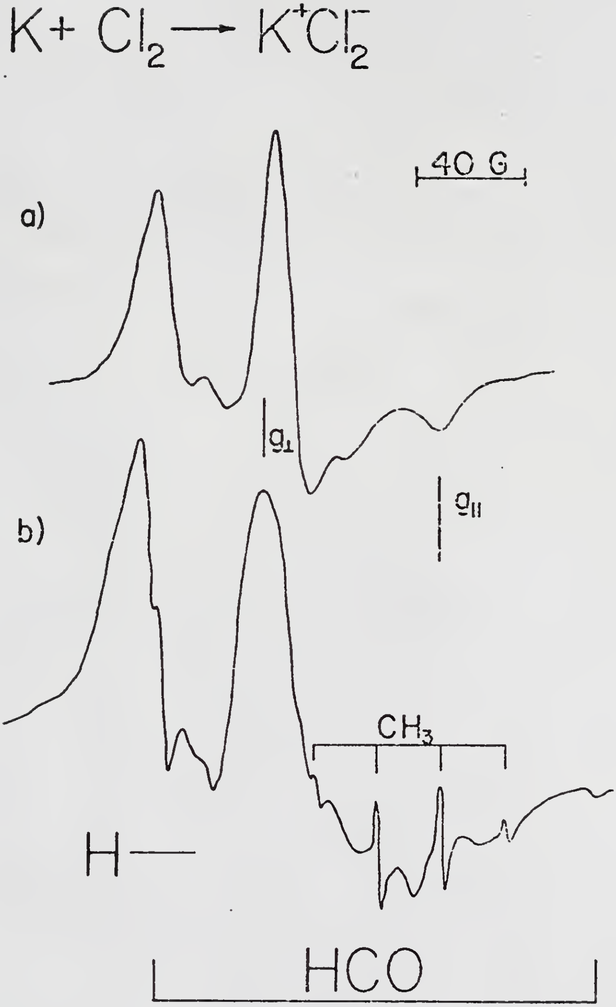

Figure 20

TABLE XI

PARALLEL LINE POSITION FOR THE $K^+Cl_2^-$

		$^{35}Cl^{35}Cl$		$^{37}Cl^{37}Cl$		$^{35}Cl^{37}Cl$	
m_I	m_I	exp.	calc.	exp.	calc.	exp.	calc.
3/2	3/2	3048.4	3047.7	3100.9	3098.5	3074.0	3073.1
3/2	1/2	3150.0	3150.2	3186.4	3184.1	3158.5	3158.7
1/2	3/2					3174.7	3175.6
3/2	-1/2	3251.5	3252.7*	3269.4	3269.6	*	3244.3
1/2	1/2					*	3261.2
-3/2	1/2					*	3278.1
3/2	-3/2	3355.2	3355.2	3355.2	3355.2	*	3329.8
1/2	-1/2					*	3346.8
-1/2	1/2					*	3363.7
-3/2	3/2					3379.7	3380.6
1/2	-3/2	3458.3	3457.7	3441.0	3440.8	3432.8	3432.3
-1/2	-1/2					3450.1	3449.3
-3/2	1/2					3465.9	3466.2
-1/2	-3/2	3559.6	3560.2	3524.8	3526.4	3534.5	3534.9
-3/2	-1/2					3551.9	3551.8
-3/2	-3/2	3663.4	3662.8	3614.6	3612.0	3637.0	3637.4

* Denotes heavy overlap.

} Denotes overlap for homonuclear molecules.

All values in G.

Discussion

In the following discussion of the obtained spectra, the main assumption made is that the experimental results can be explained by treating the complex as two loosely bound entities, M^+ and Cl_2^-, and that they can be treated independently of one another.

1. Hyperfine Tensor

The spin Hamiltonian used to describe the behavior of a molecule in a magnetic field can be written (Eq. (16))

$$\mathcal{H} = g\beta_o HS_z + KS_zI_z + Y(S^+ + S^-)I_z + X^-(S^+I^+ + S^-I^-)$$
$$+ X^+(S^+I^- + S^-I^+)$$

where

$$X^\pm = \frac{A_\| A_\perp}{4K} \pm \frac{A_\perp}{4} \qquad \text{and} \qquad Y = \frac{A_\perp^2 - A_\|^2}{2K}\,\frac{g_\| g_\perp}{g} \cos\theta \sin\theta .$$

In Appendix B, the matrix elements and the Hamiltonian matrix are derived for basis eigenvectors of the type $|S,M\rangle|I,m\rangle$ where S,M,I, and m have their usual meaning. The diagonal elements of the largest magnitude involve terms of the type $F \pm 3K$, where $F = gH/2g_o$; and the off-diagonal terms are dependent upon $X^\pm$ and Y. For the values we are interested in, the off-diagonal elements are very small, e.g., in the case of $Mg^+Cl_2^-$, for a typical field of about 3000.0 G, F = 1500.5 G for the parallel lines, while $X^+ = 3.8$, $X^- = 0$, and $Y = 0$; for the perpendicular lines, F = 1515.7 G, while $X^+ = 25.7$ g, $X^- = 22.0$ G and $Y = 0$.

These two particular orientations were chosen since they are the ones of greatest interest here; in any event, all other orientations will give values lying between these two extemes. Therefore, a second-order perturbation theory solution can be used in this case. This is given by Eq. (17) as

$$h\nu = g\beta_o H + Km + \frac{A_\perp^2}{4g\beta_o H_o} \; \frac{A^2 + K^2}{K^2} \; [I(I+1) - m^2]$$

for the parallel and perpendicular positions since in this case, either sin θ or cos θ equals zero, making the last term of Eq. (17) equal to zero.

From the values of $A_\parallel$ and $A_\perp$ thus determined, the values of A_{iso} and of A_{dip} can be obtained from Eqs. (3 & 7) by

$$A_{iso} = (A_\parallel + 2A_\perp)/3 \quad \text{and} \quad A_{dip} = (A_\parallel - A_\perp)/3 \; .$$

A_{iso} is correlated with the Fermi contact term. It measures the spin density at the nucleus. A_{dip}, on the other hand, is a measure of the anisotropy of the ion. It is usually correlated with the amount of p-character of the wavefunction describing the system. The values obtained for A_{iso} and A_{dip} from the experimentally determined hyperfine splittings are listed in Table XIV for all the different complexes studied.

As will be seen, the value of A_{dip} is relatively large in all cases and substantiates the idea that the electron goes into an orbital with distinctive p-character. This is to be expected if the electronic configuration of the Cl_2^- ion is

TABLE XIV

MAGNETIC PARAMETERS FOR Cl_2^-

Metal	^{35}Cl		^{37}Cl	
	A_{iso}(MHz)*	A_{dip}(MHz)**	A_{iso}(MHz)*	A_{dip}(MHz)**
Mg	104.0	82.8	85.9	68.4
Ca	107.6	85.5	91.2	72.5
Sr	108.9	86.5	92.2	73.7
Ba	110.3	87.6	92.7	70.9
Li	108.9	86.5	91.8	73.1
Na	110.3	87.6	91.3	72.6
K	112.2	89.3	93.8	74.5

*All these values are within ± 4.0 MHz.

**All these values are within ± 2.0 MHz.

$$(\sigma_g 35)^2(\sigma_u 35)^2(\sigma_g 3p)^2(\Pi_u 3p)^4(\Pi_g 3p)^4(\sigma_u 3p)^1,$$

in agreement with past work [14].

The values of A_{iso} and A_{dip} can be correlated with fundamental properties of the molecule via the Dirac equation, as discussed in detail in Chapter II. As was shown there (Eqs. (3 & 7))

$$A_{iso} = \frac{8\Pi}{3} \; g \; \beta_o g_n \beta_n |\psi_{(o)}|^2$$

and

$$A_{dip} = g \; \beta_o g_n \beta_n \left\langle \frac{3 \cos^2\theta - 1}{2r^3} \right\rangle .$$

The values of $|\psi_{(o)}|^2$ and $\left\langle \frac{3 \cos^2\theta - 1}{2r^3} \right\rangle$ derived from the values of A_{iso} and A_{dip} found in Table XIV are listed in Table XV.

If the wavefunction ψ for the Cl_2^- ion is assumed to be expandable by an LCAO in terms of the atomic orbitals ϕ of the Cl atoms, it can be seen that

$$\psi = C_1\phi_s^{(1)} + C_2\phi_{non-s}^{(1)} + C_3\phi_s^{(2)} + C_4\phi_{non-s}^{(3)}$$

where the superscripts identify the atomic center involved and the subscripts identify the character of the atomic orbital. The Cs are the weighting coefficients. If the two Cl atoms are identical, then $C_1 = C_3$ and $C_2 = C_4$. If the wavefunction is normalized, $\sum_i C_i^2 = 1$ and the cross terms, C_iC_j $(i \neq j)$, are small. It can be seen, following the

TABLE XV

MOLECULAR PARAMETERS FOR Cl_2^-

Metal	^{35}Cl		^{37}Cl	
	$\lvert\Psi_{(o)}\rvert^2$ (a.u.) *	$\left\langle \frac{3\cos^2\theta-1}{2r^3} \right\rangle$ (a.u.)	$\lvert\Psi_{(o)}\rvert^2$ (a.u.) **	$\left\langle \frac{3\cos^2\theta-1}{2r^3} \right\rangle$ (a.u.)
Mg	0.2372	1.583	0.2354	1.570
Ca	0.2456	1.635	0.2499	1.664
Sr	0.2485	1.654	0.2526	1.692
Ba	0.2517	1.675	0.2540	1.624
Li	0.2485	1.654	0.2515	1.678
Na	0.2517	1.675	0.2502	1.667
K	0.2561	1.707	0.2570	1.710

*All these values are within ± 0.008.

**All these values are within ± 0.04.

procedure outlined in Eq. (18) that

$$C_1^2 = C_3^2 = \frac{A_{iso}}{A_{iso}^{atom}} \quad \text{and} \quad C_2^2 = C_4^2 = \frac{A_{dip}}{A_{dip}^{atom}} .$$

The values of these coefficients were obtained utilizing the atomic values given by Ayscough [17] and are tabulated in Table XVI. From the nature of the wavefunction, its coefficients can be interpreted as the percent character of its given parts. It is easy to see, then, that the wavefunction consists of very small (the order of 2%) s-character and a larger contribution (the order of 48%) for the p-character for each Cl atom.

If the amount of s- and non-s-character is plotted against the ionization potential for the donor metal, two straight lines are obtained. This indicates that as the ionization potential of the metal decreases, the amount of electronic density lying on the Cl_2 increases. This indicates that an ion-pair, $M^+Cl_2^-$, is formed; although its presence is felt only to a small degree, the metal does influence the spin density and bonding of the halogen anion. In Figure 21, the spin density both for s- and non-s-character is plotted against the ionization potential of the metal. It should be noted that the scale used for the spin-density axis for the s-character in Figure 21 is larger than for non-s-character in order to show the small variations.

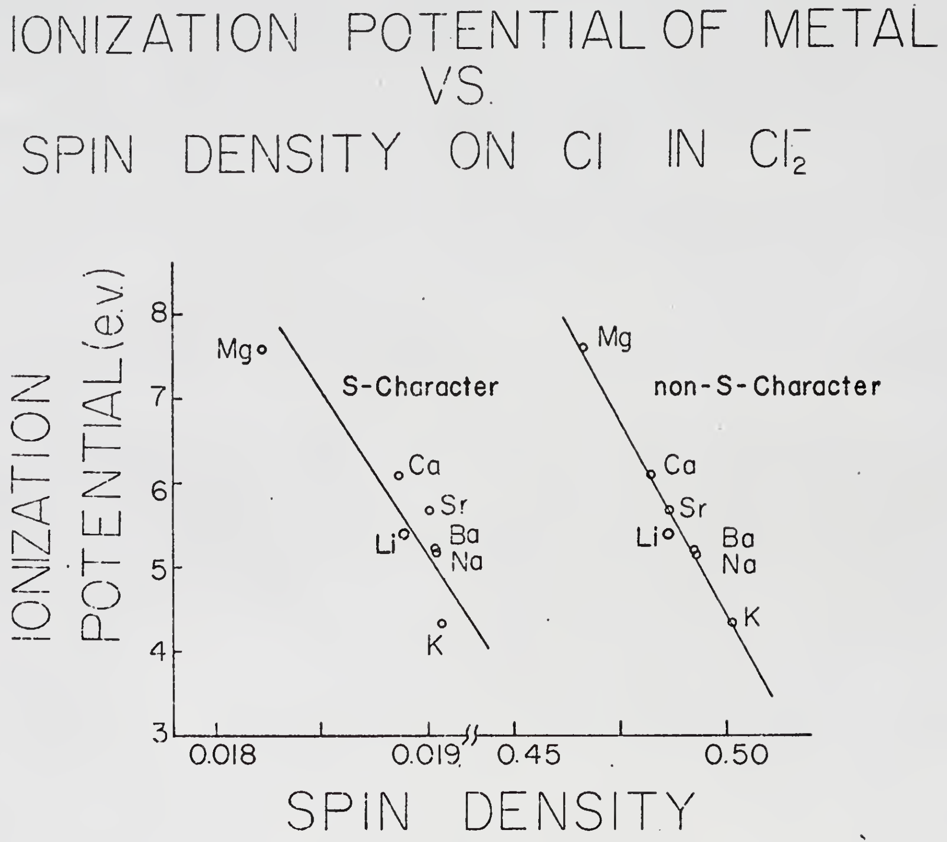
IONIZATION POTENTIAL OF METAL
VS.
SPIN DENSITY ON Cl IN Cl_2^-
IONIZATION POTENTIAL (e.v.)
8
7
6
5
4
3
0.018
0.019
0.45
0.50
SPIN DENSITY
S-Character
non-S-Character
Mg
Ca
Sr
Li
Ba
Na
K

Figure 21

TABLE XVI

MO-WAVE FUNCTION COEFFICIENTS FOR Cl_2^-

Metal	Ionization Potential (eV)	C_1^2 *	C_2^2 **
Mg	7.61	0.0182	0.467
Ca	6.09	0.0189	0.483
Sr	5.67	0.0190	0.486
Ba	5.19	0.0193	0.492
Li	5.36	0.0190	0.486
Na	5.12	0.0193	0.492
K	4.32	0.0196	0.501

(All these values are per Cl atom).

Atomic values used (Ayscough [18]).

A_{iso}^{atom} = 5650 MHz.

A_{dip}^{atom} = 176 MHz.

*All these values are within ± 0.0007.

**All these values are within ± 0.01.

The lines going through the experimental points can be determined by a least-square linear fitting program. This program is listed in Appendix C. The lines obtained were,

$$\text{s-character} \quad Y = -2.4 \times 10^{2}\ X + 2.4 \times 10^{-1}$$

$$\text{non-s-character} \quad Y = -8.4\ X + 5.2 \times 10^{-1}$$

where Y is the ionization potential in eV of the metal atom and X is the corresponding s- or non-s-spin density in atomic units.

2. g-Tensor

The deviations from $g_o = 2.0023$ in the g-values for the molecules studied can be accounted for by mixing of $^2\Pi$ states with the $^2\Sigma$ ground state. As was discussed in the derivation of Eq.(9a & b), this mixing of excited states enters the wavefunction via spin-orbit coupling. The changes in $g_\perp$ were shown to be, according to second-order perturbation theory (for a general treatment, see Stone [19])

$$g_\perp - g_o = -2 \sum_n \frac{\langle n | \xi\ L_x | 0 \rangle \ \langle 0 | L_x | n \rangle}{E_n - E_0} .$$

On the other hand, the mixing of excited states affects $g_\parallel$ only in higher order so that the changes in $g_\parallel$ are believed to be due to matrix effects. If it is assumed that the matrix effects will be the same for both $g_\parallel$ and $g_\perp$, then it might be more meaningful to study $g_\perp - g_\parallel$ rather than $g_\perp - g_o$, but since the value of $\Delta g_\parallel$ is very small the conventional way of treating the problem will be used here.

The experimentally determined values of both $g_{\parallel}$ and $g_{\perp}$ are listed in Table II. In Table XVII, the values for $\Delta g_{\parallel}$ and $\Delta g_{\perp}$ are listed. It can be seen there that the derivations from g_o of $g_{\parallel}$ are indeed very small. On the other hand, the deviations from g_o of $g_{\perp}$ are approximately two orders of magnitude larger and indicate that there are some low-lying $^2\Pi$ states mixed with the ground state. It can also be seen in Table XVII that as the atom becomes larger within a given group of the Periodic Table, the mixing of the excited states increases. This is very apparent, primarily in the alkaline-earth metals. In the alkali metals, on the contrary, the changes are fairly constant.

In Gilbert and Wahl's [20] calculation, they found two $^2\Pi$ excited states. The lowest one, $^2\Pi g$, lies about 2 eV above the $^2\Sigma_u$ ground state, a higher one, $^2\Pi_u$, lies about 3.5 eV above the ground state. These two $^2\Pi$ states are assumed to have the MO configuration

$$^2\Pi_u\text{:}\ (\sigma_g 3s)^2(\sigma_u 3s)^2(\sigma_g 3p)^2(\Pi_u 3p)^3(\Pi_g 3p)^4(\sigma_u 3p)^2$$

$$^2\Pi_g\text{:}\ (\sigma_g 3s)^2(\sigma_u 3s)^2(\sigma_g 3p)^2(\Pi_u 3p)^4(\Pi_g 3p)^3(\sigma_u 3p)^2\ .$$

(See Slichter [21].) As has been discussed by Herzberg [22], in order to have coupling between states, the parity must be the same; i.e., since the ground state of the Cl_2^- molecule-ion is $^2\Sigma_u$, it can only mix with the $^2\Pi_u$ excited state.

The sign of $\Delta g_{\perp}$ can be correlated with the nature of the mixed $^2\Pi$ state as shown by Knight and Weltner [23].

TABLE XVII

SPIN-DOUBLING CONSTANT AND Δg FOR Cl_2^-

Metal	$\Delta g_{\parallel}$*	$\Delta g_{\perp}$*	γ (cm^{-1})**
Mg	0.0007	0.0319	-0.0087
Ca	-0.0003	0.0330	-0.0090
Sr	0.0007	0.0341	-0.0093
Ba	-0.0003	0.0370	-0.0101
Li	-0.0019	0.0344	-0.0094
Na	-0.0017	0.0348	-0.0095
K	-0.0014	0.0347	-0.0094

$B = 0.136\ cm^{-1}$.

*All these values are within ± 0.001.

**All these values are within ± 0.0005.

If the excited state is regular, the value of $\Delta g_\perp$ will be negative, whereas if the excited state is inverted, it will be positive. In the present case, since all the values of $\Delta g_\perp$ are positive, it is concluded that the state that is mixed with the ground state is inverted. Both excited states described previously are inverted, but, for symmetry considerations, it is concluded that the $^2\Pi_u$ is the one that contributes most to the mixing. This is in agreement with Schoemaker [14] and Slichter's [21] study of the g-tensor for the V_k center, and also with Castner and Kanzig's [1] experimental results.

As far as the effects encountered in moving down a given group in the Periodic Table, it can be seen that the effect is most noticeable in the alkaline-earth metals. The alkali metals have an ns^0 configuration, while the alkaline-earth ones have an ns^1 configuration after losing one electron. If the effect encountered in the g-tensor were to be ascribed to changes in size of the monovalent ion as one moves down the Periodic Table, the alkali metals should display an effect similar to the one found for the alkaline-earth metals. This is not observed and it is believed that the differences in $\Delta g_\perp$ are due to the presence of the outermost, supposedly very loose, electron in the alkaline-earth ones. This electron will interact with Cl_2^- to a greater extent as the ionic radius for the metal increases, causing a larger perturbation on its ground state.

The values of both $g_{\parallel}$ and of $g_{\perp}$ are in good agreement, as stated before, with those determined experimentally by Castner and Kanzig [1] and those theoretically calculated by Schoemaker [14] for Cl_2^- in the crystal. This is interpreted to mean that the field exerts very little or a similar effect on the molecule-ion in both the crystal and the matrix.

Within the LCAO-MO approximation, Knight and Weltner [23] showed that the deviations from g_o of $g_{\perp}$ can be related to the spin-doubling constant γ (see Eq. (11)) by

$$\gamma = 4 \sum_n \left[\langle 0 | \xi \, L_x | n \rangle \, \langle n | BL_x | 0 \rangle / (E_n - E_0) \right] = -2B\Delta g_{\perp}$$

where B is the rotational constant and ξ is the spin-orbit operator for the molecule. Using the value of B = 0.136 cm^{-1} calculated by Gilbert and Wahl [20], values for γ were calculated and are included in Table XVII. This is a measure of the value expected for a free-rotating Cl_2^- ion in the gas phase, if it is assumed that the metal donor contributes a negligible amount. It can be seen that γ does not change its value to a large extent with the different metals. Therefore, it is assumed that the value of γ for a free rotating Cl_2^- in the gas phase, is of the order of $-0.009 \ cm^{-1}$.

Linewidths

The linewidths of the observed spectra are listed in Table XVIII. All linewidths were measured at half-height for the 1/2-1/2 parallel transition of the $^{35}Cl^{35}Cl^-$ specie. It can be seen that those metals whose most abundant isotopes have no magnetic moment have linewidths which are relatively narrow. On the other hand, for those that have nuclear magnetic moments, the linewidths are larger. A graph in which magnetic moment is plotted against linewidths is presented in Figure 22 for the alkali metal complexes.

The interpretation given to the increase of the linewidths is that the metal associated with the Cl_2^- ion, possessing a magnetic moment of its own, will cause further hyperfine splitting of the Cl_2^- lines. These splittings, however, will not be large, since, as has been mentioned previously, the complex is extremely ionic and little interaction exists between the metal ion and the Cl_2^- ion. Therefore, this unresolved splitting will only broaden the observed ESR lines. This has been previously observed in the ESR spectra of ion-pairs (see Szwarc [24]). This evidence enhances the idea that we are dealing with a loosely bound ion-pair system composed of a metal ion and the Cl_2^- molecule-ion.

TABLE XVIII

LINEWIDTHS AND MAGNETIC MOMENTS FOR METAL DONORS IN Cl_2^-

Metal	Linewidths (G)*	Magnetic Moment (magnetons)
Mg	4.99	0.00
Ca	4.98	0.00
Sr	4.98	0.00
Ba	4.98	0.00
Li	17.7	3.256
Na	16.7	2.216
K	14.7	0.391

* All linewidths were measured at half-height for the 1/2-1/2 parallel transition of the $^{35}Cl^{35}Cl^-$.

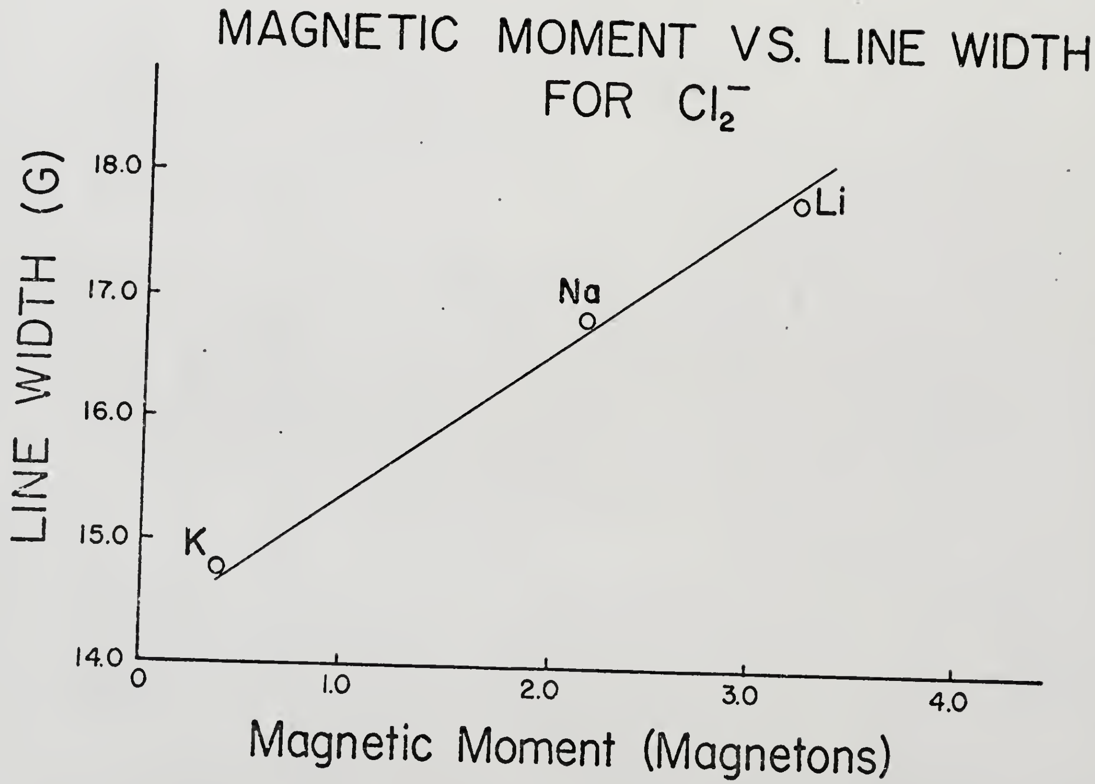
MAGNETIC MOMENT VS. LINE WIDTH
FOR Cl_2^-
LINE WIDTH (G)
18.0
17.0
16.0
15.0
14.0
0
1.0
2.0
3.0
4.0
Magnetic Moment (Magnetons)
K
Na
Li

Figure 22

CNDO Calculation

In order to better understand the nature of the different terms obtained from the ESR spectra, as well as to test the suitability of the model, a CNDO calculation was carried out. The internuclear distance was varied until a minimum in the total energy was obtained. From the terms in the spin-density matrix, the values of the fundamental ESR parameters, A_{iso} and A_{dip}, were calculated and compared with the experimentally obtained ones. INDO has been used previously in this same way with a moderate amount of success by Knight, Brom, and Weltner [25].

The value obtained for the equilibrium internuclear distance at the lowest total energy was 2.238 A°. The value obtained by Gilbert and Wähl [20] was 2.65 A°. This is largely to be expected since CNDO tends to give smaller distances than more accurate calculations or experimental evidence [26].

The value obtained for $|\psi_{(o)}|^2$ was 0.0192. The smallest value obtained for this parameter experimentally was for the case of $Mg^+Cl_2^-$ in which it was 0.2373. The value calculated for $\left\langle \frac{3\cos^2\theta-1}{2r^3} \right\rangle$ using the spin-density matrix generated by CNDO and Beveridge and McIver's [27] method was 0.4796, as compared with 1.5831 in the $Mg^+Cl_2^-$ case. In order to compare other values, refer to Table XV.

The poor agreement found was to be expected since CNDO neglects many terms and approximates others that contribute substantially to the ESR parameters.

Temperature Variation Experiments

Several experiments in which Ba and Na were used as the electron donors were run by using a variable-temperature Dewar. After the initial spectrum was recorded and the presence of Cl_2^- was positively identified, the temperature was raised to approximately 30 K in about 5 K intervals. After the desired temperature was reached, liquid helium was allowed to again come in contact with the rod, lowering the temperature to 4 K and quenching the possible reactions that were occurring. The spectrum was recorded after every trial.

When the temperature was about 15 K, a sudden and large change was observed in the spectrum, accompanied with a large evolution of heat as observed by the amount of liquid helium escaping from the Dewar. In the case of Ba, after cooling back to 4 K, a large increase in the intensity of the Ba^+ line was detected. This was accompanied with a steady reduction of the Cl_2^- signal. The increase in the Ba^+ signal can be explained by the disappearance of different trapping sites that may broaden the line and obscure the presence of the metal ion.

In the case of Na, no radical change was noticed even after passing the 15 K point. A small and steady disappearance of the Cl_2^- spectrum took place until, at about 30 K, it became unrecognizable. This was also observed in the Ba case.

The lack of appearance of any BaCl lines can be attributed to a high activation energy so that only diffusion through the matrix to form clusters occurs or that, at these temperatures, the reaction that takes place leads to the formation of $BaCl_2$ rather than BaCl + Cl.

Optical Experiments

In conjunction with the ESR spectra of the different species, optical spectra were often also taken. A search was conducted from 190 nm to 1200 nm. No bands were observed that could be assigned to the $M^+Cl_2^-$.

Delbecq, Smaller and Yuster [28] and Delbecq, Hayes and Yuster [29] have reported the optical spectrum of Cl_2^- in crystals. They found it consisted of two bands, one at 365 nm and the other one at 750 nm.

Negative data are difficult to evaluate; however, this result is in agreement with Gilbert and Wahl's [20] calculation. They found that all the excited states for the Cl_2^- molecule-ion were repulsive and will, therefore, lead to a continuous absorption. The observed optical spectra in the crystals can be understood if it is realized that the crystal field will tend to induce at least a small minimum in the excited states, leading to weakly attractive ones and producing line spectra rather than a continuous one. It is believed that the concentration is large enough since Howard and Andrews [30] were able to observe resonance Raman spectra this way.

M^+Cl^-

In the reaction between the metal atoms and Cl_2, the formation of the monochlorides of the metals is possible. Those of the Alkaline-earth metals are expected to have $^2\Sigma$ ground states and therefore be observable via ESR. The monochlorides of the alkali metals are all $^1\Sigma$ and not observable in ESR spectra.

The monochlorides of the alkaline-earth metals were tentatively identified in Mg, Ca and Sr but not in Ba. Since the molecular beam work [2] does not allow us to make any definite statements about the stability of the $M^+Cl_2^-$ complex, all we can suggest is a tentative explanation on the basis of the expected lifetimes of the complex.

The stability of the electron-jump complex, $M^+Cl_2^-$, would be expected to be inversely proportional to the atomic number of the metal. The light elements should form a less stable complex than the heavier ones. This idea is substantiated more strongly if it is realized that the ionization potential of the metals decrease in the same direction, therefore, making the electron-jump process more likely. It is, therefore, expected that Mg, Ca and Sr complexes would be shorter-lived than the Ba one. Furthermore, the chemistry of Mg, Ca and Sr is closely related, as observed by Lin, Mims and Herm [2], but that of Ba is not. This might be due to mixing of some d-orbitals into the wavefunction of the Ba. The difference in the behavior of the Ba + Cl_2 system could then be accounted for by this anomaly in the expected behavior of Ba.

The values of $A_\perp$ for Cl in these molecules can be found in Table XIX. Parallel lines were not observed in these experiments; therefore, no definite statement can be made about them.

TABLE XIX

APPROXIMATE MAGNETIC PARAMETERS
FOR M^+Cl^-

Metal	$A_\perp$ for Cl (G)
Mg	10.
Ca	10.
Sr	10.

M and M^+

In the spectra recorded when some of the metals were used as electron donors, the presence of the monovalent ion for the alkaline-earth atoms and that of ^7Li atoms was detected.

In the Mg case, a line at $g = 1.9940 \pm 0.001$ has been identified with Mg^+. Lines due to $^{25}Mg^+$ (10.13% natural abundance, $I = 5/2$) are also observed. In the case of $^{24}Mg^+$, only one line is found since it has no nuclear magnetic moment. For $^{25}Mg^+$ (magnetic moment = -0.85470 nuclear magnetons), six lines are identified, separated by a distance of 130.3 ± 1.0 G. Since no parallel lines are observed, and the ion has its unpaired electron in the 3s state, the value of A_{iso} is assumed to be close to this number (363.7 MHz). From it, the value of $|\psi_{(o)}|^2$ is found to be 1.329 a.u., which is in approximate agreement with the one found by Brom and Weltner [16] in $^{25}MgOH$, 1.114 a.u. Unfortunately, no gas-phase data for $^{25}Mg^+$ exist that could be used to compare with this result. The value of $|\psi_{(o)}|^2$ indicates that there is more spin density on the $^{25}Mg^+$ in $^{25}Mg^+Cl_2^-$ than in $^{25}MgOH$, which is the trend to be followed since the OH is expected to be more electronegative than Cl_2.

The other alkaline-earth ions appear as single lines since no magnetic moment is present in their isotopes with sufficiently high natural abundances. The only exception is ^{137}Ba (natural abundance 11.32%) for which no lines could be found. In ^{137}BaF, the A-value for the ^{137}Ba nucleus was found to be of the order of 857 G according to Knight, Easley and Weltner [31]. The values for the g-factors for these ions can be found in Table XX. The fact that the g-factors increase toward the $g_o = 2.0023$ with increasing atomic number value can be interpreted as a movement toward a more "free" electron since the atomic number is increasing and the atomic radius is also increasing, causing a smaller mixing of the higher ^2P states into the ^2S ground state function.

TABLE XX

g-FACTORS FOR THE M^+ IONS

Metal	g
Mg^+	1.9940
Mg^+	1.9940
Ca^+	1.0078
Sr^+	1.9985
Ba^+	2.0059

In the Li experiments, lines attributable to ^7Li (92.6% abundance) are found. Although all the alkali metals are ^2S and therefore observable via ESR, only the ^7Li was observed when the Ar:Cl ratio was 1:20.

This can be understood on the basis of the ionization potential of these metals. Li has the largest one; therefore, it would be the one that will require more energy for the reaction to occur, making it less efficient.

An A_{iso} value of 403 MHz was found, in good agreement with the work by Jen, Bowers, Cochran and Foner [19]. From it, a value for $|\psi_{(o)}|^2$ equal to 0.232 is calculated

Summary

The ESR spectrum of the trapped intermediate in the reaction between some alkali- and alkaline-earth metals and Cl_2 has been observed at 4 K. The observed spectra imply that an ion pair, $M^+Cl_2^-$, is formed in which the two species retain, to a large extent, their individual identity. The variation of the magnetic parameters of the Cl_2^- ion with the ionization potential of the metal donor was studied.

The dependence of linewidths on the magnetic moment of the donor metal was analyzed in terms of the broadening of the Cl_2^- lines due to the hyperfine interaction in these metals.

The g-tensor was analyzed in terms of mixing of excited $^2\Pi$ states with the $^2\Sigma$ ground state.

The lack of observed optical spectra is tentatively interpreted in terms of the repulsiveness of the excited states according to theoretical studies.

References

[1] Castner, T. B., and Kanzig, W., J. Phys. Chem. Solids, 3, 178 (1957).

[2] Lin, S., Mims, C. A., and Herm, R. R., J. Chem Phys., 58, 327 (1973).

[3] Jonah, C. D., and Zare, R. N., Chem. Phys., Letters, 9, 65 (1971).

[4] Ham, D. O., and Chang, H. W., Chem. Phys., Letters, 24, 579 (1974).

[5] Bennett, J. E., Mile, B., and Ward, B., J. Chem. Phys., 49, 5556 (1968).

[6] Symons, M. C. R., J. Chem. Soc., 570 (1963).

[7] Catton, R. C., and Symons, M. C. R., J. Chem. Soc., 446 (1969).

[8] Fayet, J., Thieblemont, B., and Pariset, C., Comptes Rendu, 268, 177 (1969).

[9] Feldmann, T., and Treinin, A., J. Chem. Phys., 74, 1352 (1963).

[10] Arai, S., Kira, A., and Inamura, M., J. Phys. Chem., 74, 2102 (1970).

[11] Box, H. C., Budzinski, E. E., and Freund, H. G., J. Chem. Phys., 50, 2880 (1969).

[12] Coope, J. A. R., Gardner, C. L., McDowell, C. A., and Pelman, A. I., Mol. Phys., 21, 1043 (1971).

[13] Wilkins, J. W., and Gabriel, J. R., Phys. Rev., 132 1950 (1963).

[14] Schoemaker, D., Phys. Rev., B, 7, 786 (1973).

[15] Low, W., Paramagnetic Resonance in Solids, Academic Press, New York (1960).

[16] Brom, J. M., and Weltner, W., Jr., J. Chem. Phys., 58, 5322 (1973).

[17] Jen, C. K., Bowers, V. A., Cochran, E. L., and Foner, S. N., Phys. Rev., 126, 1749 (1963).

[18] Ayscough, P. D., Electron Spin Resonance in Chemistry, Methuen & Co., London (1967).

[19] Stone, A. J., Proc. Roy. Soc., A271, 424 (1963).

[20] Gilbert, T. I. and Wahl, A. C., J. Chem. Phys., 55, 5247 (1971).

[21] Slichter, C. P., Principles of Magnetic Resonance, Harper & Row, New York (1963).

[22] Herzberg, G., Molecular Spectra and Molecular Structure I, Spectra of Diatomic Molecules, Van Nostrand-Reinhold, New York (1950).

[23] Knight, L. B. and Weltner, W., Jr., J. Chem. Phys., 53, 4111 (1970).

[24] Szwarc, M., Ions and Ion Pairs in Organic Reactions, Wiley and Sons, New York (1972).

[25] Knight, L. B., Brom, J. M., and Weltner, W., Jr., J. Chem. Phys., 56, 1152 (1972).

[26] Pople, J. A., and Beveridge, D. L., Approximate Molecular Orbital Theory, McGraw-Hill, New York (1970).

[27] Beveridge, D. L., and McIver, J. W., J. Chem. Phys., 54, 4681 (1971).

[28] Delbecq, C. J., Smaller, B., and Yuster, P. H., Phys. Rev., 111, 1235 (1958).

[29] Delbecq, C. J., Hayes, W., and Yuster, P. H., Phys. Rev., 121, 1043 (1961).

[30] Howard, W. F., Jr., and Andrews, L., J. Am. Chem. Soc., 95, 2056 (1973).

[31] Knight, L. B., Easley, W. C., and Weltner, W., Jr., J. Chem. Phys., 54, 322 (1971).

CHAPTER IV

$M^+F_2^-$

Introduction

Castner and Kanzig [1] and Woodruff and Kanzig [2] investigated the structure of the V_k-center in alkali fluoride crystals and showed that this center consisted of an electron hole trapped in an alkali vacancy in the crystal. It effectively behaved as an F_2^- molecule-ion. Its structure, as determined via ESR, placed the odd electron in a $^2\Sigma_u$ ground state that consisted of s- and pσ-orbitals with the largest contribution being made by the p-orbitals. They obtained this center by X-ray irradiation of the corresponding alkali fluoride. They found that the hyperfine tensor of F_2^- consisted of a large parallel contribution (of the order of 890 G) and smaller perpendicular contributions (of the order of 58 G). The crystal they used for their study was LiF. They also determined that the g-tensor contained a parallel component very close to $g_o = 2.0023$ and a perpendicular component that indicated that the ground state was mixed with an excited $^2\Pi_u$ inverted state, since $g_\perp > g_o$. It was also found that a second-order solution to the spin Hamiltonian was not sufficient for the determination of all the magnetic parameters, but that an exact solution was required because the parallel components of the hyperfine tensor were so large, meaning that the off-diagonal elements of the spin Hamiltonian matrix were very large.

Later Kanzig [3] domonstrated the existence of an analog of the F-center which he called a V_F-center, in which the molecule-ion is associated with a nearby alkali metal ion, causing an effective "bending" of the F-F bond in the direction away from the cation and the p-Π orbitals in the direction toward the cation. The properties of F_2^- vary only slightly. The most salient change was found in the nature of the g-tensor; it was essentially transformed from a two g-component problem ($g_{\parallel}$ and $g_{\perp}$) to a three g-component problem (g_x, g_y, g_z). This caused variations in the spectra (see Observed Spectra of $M^+F_2^-$) that led to the determination of the bending angle as about 4°.

Theoretical investigations have been carried out by Balint-Kurti and Karplus [4] and Balint-Kurti [5] to analyze the behavior of the $Li^+F_2^-$ species in the LiF crystal and in the collision of Li atoms with F_2 molecules, respectively. Balint-Kurti [5] was able to show that in the collisional approach of Li atoms and F_2 molecules there is a region in which an electron jumps from Li to the F_2 molecule, forming the $Li^+F_2^-$ complex. He found that the electron-jump distance between Li and F_2 is a rapidly increasing function of the F-F separation around the calculated equilibrium position (2.8 a.u.). It was also noticed that the electron-jump distance was a function of direction of approach of the Li atom to the F_2 molecule.

Ikenberry, Jette and Das [6] showed theoretically that the explanation of the negative transferred hyperfine constants at nuclei of ions surrounding the V_k-center is due to exchange polarization of the ligand cores by the unpaired σ_u electron of the molecule-ion. Gilbert and Wahl [7] performed calculations for the ground state of F_2^-. They found that the equilibrium distance was 3.6 a.u. Jette, Gilbert and Das [8] calculated properties of the ground state and some of the excited states for F_2^-. They also found that the equilibrium distance between the two F atoms was 3.6 a.u. They also predicted some of the magnetic properties of this molecule-ion. In their calculation of the excited states, they did not proceed farther out than a distance very close to the equilibrium distance in the ground state and, therefore, found no minimum in the potential energy functions for them. It was also established that the equilibrium internuclear distance between the metal ion and F_2^- increased with increasing atomic number of the alkali metal chosen. It was also found that the value of $A_\perp$ was negative. Yarkony, Hunt and Schaefer [9] studied the relationship between the structure of the complexes formed upon reaction between a metal atom and a halogen molecule and the observed chemiluminescence (Ham and Chang [10]).

Optical studies were conducted by Delbecq, Hayes and Yuster [11] to elucidate the structure of F_2^-. They related the properties of the ${}^2\Sigma_u$ ground state to the excited states for which transitions were observed, i.e., a ${}^2\Sigma_g$ and a ${}^2\Sigma_u$. The configurations of these states are:

${}^2\Sigma_u$ (ground state): $\sigma_g^2\ \pi_u^4\ \pi_g^4\ \sigma_u^1$
${}^2\Sigma_g$ (excited state): $\sigma_g^1\ \pi_u^4\ \pi_g^4\ \sigma_u^2$
${}^2\Pi_g$ (excited state): $\sigma_g^2\ \pi_u^4\ \pi_g^3\ \sigma_u^2$
${}^2\Pi_u$ (excited state): $\sigma_g^2\ \pi_u^3\ \pi_g^4\ \sigma_u^2$.

The transition to the ${}^2\Pi_u$ was not observed since it is forbidden.

Electron-Nuclear Double Resonance (ENDOR) studies were carried out by Gazzinelli and Mieher [12]. They observed negative contact hyperfine constants and explained them by exchange polarization of the closed-shell molecular orbitals.

ESR studies were conducted by Bailey [13], Otto and Gilliam [14], and Schoemaker [15]. Schoemaker carried out a complete experimental and theoretical analysis of all the $(\text{halogen})_2^-$ ions and showed in detail that, although an orthorombic g-tensor was really involved, two of the g-values were very close, so that an axially symmetric treatment was warranted. He also found the values of $A_\perp$ to be negative through theoretical considerations.

The first isolation of the F_2^- entity in matrices that has been reported was performed by Howard and Andrews [16]. They identified the interaction between F_2^- and the associated M^+ ion.

The results obtained for the Cl_2^- case, as well as the results summarized previously, challenge us to study the $M^+F_2^-$ complex isolated in rare gas matrices. The main assumption underlying these experiments is that the complex is extremely ionic and that it can be treated essentially as an ion pair in which F_2^- would be a $^2\Sigma_u$, which makes it observable via ESR. The presence of the metal ion and its effect can be deduced from the perturbations it causes on the F_2^- lines.

Experimental

Method of Preparation of $M^+F_2^-$

In view of the results obtained for the $M^+Cl_2^-$ case described in Chapter III, a mixture of 5% F_2 in Ar was obtained from Matheson Gas Products and used without further purification. The gas mixture was passed through ¼" copper tubing connected to the gas tank regulator and leading into the chamber where the sapphire rod was located. The copper tubing was first treated with a solution of HF in order to cover its surface with a coat of fluoride and minimize the chances for F_2 reacting with the metal. The pressure at which the matrix gas was desposited was maintained at about 3×10^{-5} torr by adjusting the tank's regulator and monitoring it with an ion gauge.

The metals were deposited at different temperatures using a Chromel-Alumel thermocouple attached to the Knudsen cell. The temperature was chosen to produce a vapor pressure of about 10^{-1} torr. The metals used were obtained from the same sources as those for the Cl_2^- experiments (see Table I, Chapter III). The temperature was recorded using a Leeds and Northrup potentiometer with a cold junction immersed in an ice-water bath.

The metals used were Na, K, Cs, Mg and Ba. Cs was obtained by reacting Cs_2CrO_4 and Si following the Scheer and Fine [16] procedure. Cs_2CrO_4, obtained from Matheson, Coleman and Bell, was reagent quality. Si was obtained from Alfa Inorganics.

Observed Spectra of $M^+F_2^-$

Figures 24, 25, 27, 28 and 29 show the spectra obtained when Na, K, Cs, Mg and Ba, respectively, were co-deposited with the F_2:Ar mixture. In all cases, two widely separated lines were identified about 2000 G apart and centered about $g_o = 2.0023$. These lines had the characteristic shape of parallel lines. Two more lines, having the characteristic shape of perpendicular lines, were found in the region closed to g_o and about 120 G apart. They had, however, the wrong direction if they were associated with the previously described parallel lines. In the regular derivative ESR spectrum, the peak of the perpendicular line associated with a parallel line, must point in the opposite direction to the maximum of the parallel line. In the $M^+F_2^-$ case they pointed in the same direction.

F consists entirely of a single isotope with I = ½. For a pure first-order spectrum, three parallel lines widely separated and centered about g_o should be observed. Likewise, three perpendicular lines with a narrower splitting should also be observed. This, however, was not observed in the crystal work or in our case. In Woodruff and Kanzig's work [2] three widely separated lines were observed for $\theta = 0°$, where θ is the angle between the molecular axis and the magnetic field. Four lines were observed for the case in which $\theta = 90°$. These four lines consisted of a doublet of doublets. The main doublet was separated by about 120 G and the smaller one by about 24 G. In Kanzig's work [5] on the antimorph of the F-center [3] he found three widely separated lines for the $\theta = 0°$ case and either two or three lines for $\theta = 90°$, depending on the orientation of the magnetic field with respect to the crystalline axes. This latter one resembled the spectra obtained in this work. There was, however, a major difference. The position of

$g_\perp$ for all the previously observed spectra, including the V_F-center work, indicated that it had a value approximately equal to 2.023. In our case, though, the spectra could only be compatible with a $g_\perp$ equal to about 1.97.

A computer program (see Appendix D) was written utilizing the scheme discussed by Golding and Tennant [17] for non-collinear g- and A-tensors. This, associated with the subroutines in Appendix E for a nonlinear, least-squares fitting of the lines, was run by using as variables $g_\perp$, $A_\perp$, and α, where α is the angle by which the system varied from linearity. No set of parameters could be found that could explain completely the spectrum observed, unless $\alpha = 0$. In this case, two lines very close together were found in two different positions. One at the point where $g_\perp$ is located and the other about 120 G downfield.

Furthermore, if a powder pattern were to be imposed on Kanzig's V_F-center spectrum [3], two perpendicular peaks in the same direction would be observed, rather than one in one direction and the other in the opposite direction. The only possibility of observing a spectrum similar to the one found was to have $g_\perp$ at a higher field ($g_\perp < g_\parallel$) and the two perpendicular doublets distributed about $g_\parallel$, one on each side (see Fig. 26).

In view of this, a computer program was written (see Appendix E) to minimize the difference between the calculated line positions and the observed ones. When the matrix elements were written (see Appendix E for a complete listing), it was noticed that the matrix could be broken down into two blocks of 3×3 and one of 2×2 for the $\theta = 90°$ case, the latter one with no off-diagonal elements (see Appendix E). This fixed the position of $g_\perp$, which falls where the third line of the spectrum for $\theta = 90°$ is. This line should correspond to where the high-field strong perpendicular line is encountered. With this information obtained directly from the spectra, as well as with a value for $A_\parallel$ determined as half the distance between the two parallel lines, and a value for $g_\parallel$ calculated at the midpoint of the two parallel lines, the program was run varying the value of $A_\perp$ until a fit was found. This occurred when $A_\perp$ was of the order of 3 G. It was observed that the main splitting of the perpendicular lines, of the order of about 120 G, was due to second- and higher-order terms in $A_\parallel$ and that the perpendicular splitting was so small that it did not split the two doublets at each position. Furthermore, since the outer perpendicular lines were associated with the outer parallel lines, their intensities would be significantly smaller than the one obtained for the two inner ones (see Fig. 26). This explained both the existence of only two lines and their direction relative to the parallel lines. It was also noticed that a complete solution of the spin Hamiltonian matrix was required since the off-diagonal elements were not small and could not be neglected for a lower-order solution. When $\theta = 0°$, the matrix is tri-diagonal with off-diagonal elements very small compared with the diagonal elements (see Appendix F). Therefore, a first-order solution suffices for the determination of the position of the parallel lines.

In order to confirm these results, a solution of the problem was attempted using the MAGNSPEC 3 program (Quantum Chemistry Program Exchange #150), suitably modified to operate on an IBM 370/165 machine for the potassium case. In Figure 23 the θ vs. H graph is shown as obtained directly from this program and in Fig. 26 the powder pattern obtained is compared with the experimentally determined one. No other runs were done with the MAGNSPEC 3 program since the cost of its operation is extremely high.

In Table XXI, a list of the magnetic parameters calculated from the spectra is summarized.

Since the matrix obtained for the spin Hamiltonian is diagonally symmetric, there is no evidence as to the sign of the different elements of the A-tensor. Therefore, their absolute values are reported here.

No variation of the spectra was observed when the angle made by the rod with the magnetic field was varied. It is assumed, then, that the ion-pairs were completely random in their orientation.

Θ vs. H_Θ for F_2^-

	Θ 0°	15°	30°	45°	60°	75°	90°
H(G)	2437.6	2475.3	2550.2	2674.5	2845.3	3055.7	3293.1
	3349.2	3343.5	3330.0	3314.0	3303.5	3300.5	3293.2
	3349.2	3353.8	3366.2	3383.4	3400.9	3413.9	3418.7
	4260.8	4216.7	4123.1	3971.9	3772.2	3539.3	3418.7

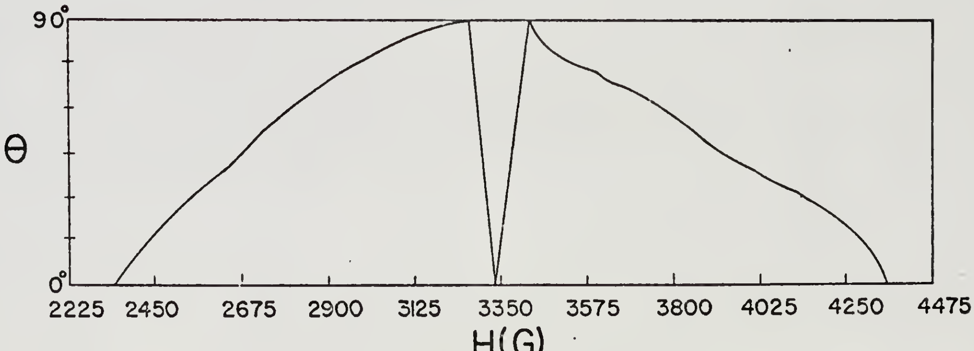

Figure 23

TABLE XXI

MAGNETIC PARAMETERS FOR $M^+F_2^-$

Metal	$\lvert A_\parallel \rvert$ (G)	$\lvert A_\perp \rvert$ (G)	$g_\parallel$	$g_\perp$
Na	892.7	2.9	2.0016	1.9654
K	911.4	3.0	2.0043	1.9666
Cs	920.6	3.0	2.0048	1.9662
Mg	854.2	2.8	2.0036	1.9676
Ba	899.5	3.0	2.0004	1.9768

All $A_\parallel$ values are within ± 1.0 G, $A_\perp$ within ± 2.0 G and all g-values are within ± 0.001.

No variation of the spectra was encountered when Ar was co-deposited with the gas mixture and the metal. This was done to assure the fact that the trapping of the $M^+F_2^-$ had been done, essentially, at infinite dilution, in spite of the large initial concentration of F_2.

In none of these spectra could the alkaline-earth metal ions be identified as separate entities, as they were in the case of $M^+Cl_2^-$.

In the case of $Mg^+F_2^-$ only, the presence of the monofluoride (MgF) was observed.

In all these spectra a large amount of methyl radicals was observed. This is believed to be due to the reaction of F_2 with some hydrocarbon impurity present in the argon or in the system.

$\underline{Na^+F_2^-}$

In Figure 24 the lines observed when Na was co-deposited with the F_2 and Ar mixture are shown. Two parallel lines, separated by a distance of 1785.4 with a value of $A_\parallel$ of 892.7 ± 1.0 G and a calculated $g_\parallel = 2.0016 + 0.001$ were observed. The high field perpendicular line is located at 3408.5 ± 0.5 G with $g_\perp = 1.9654$. The computed value for $A_\perp$ is equal to 2.9 ± 2.0 G.

In Table XXII the values obtained experimentally as well as the calculated ones for the field positions are listed.

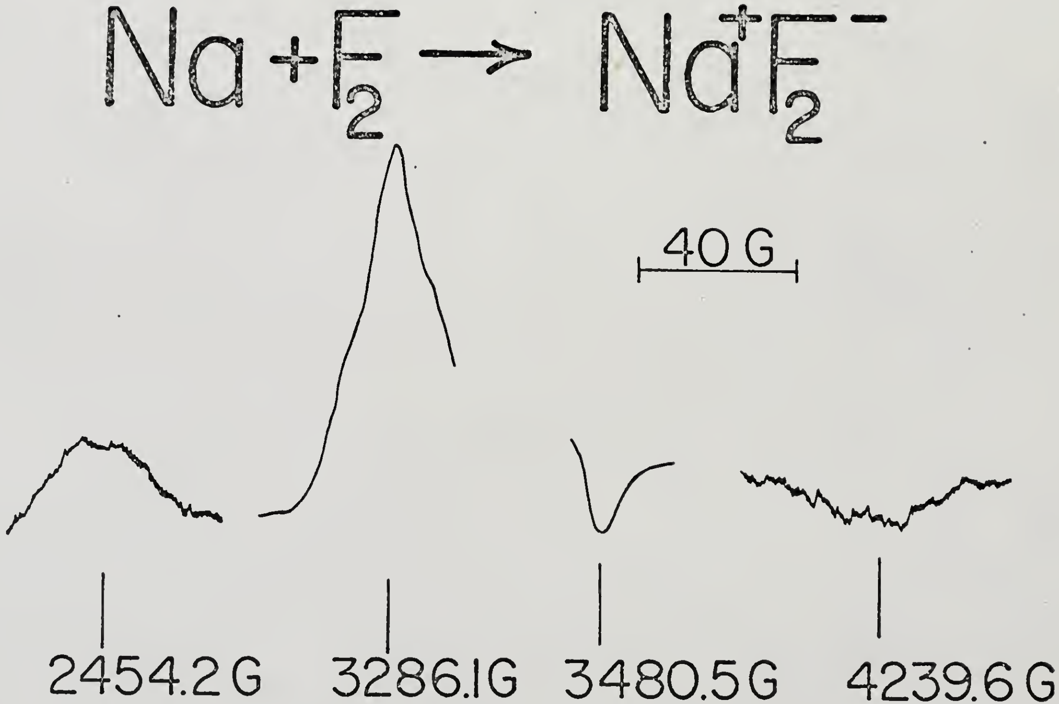

The intensity ratio between the two inside lines and the two outside ones is 100:1.

Figure 24

TABLE XXII

MAGNETIC FIELD POSITION FOR $Na^+F_2^-$

Angle	Experimental (G)	Program (App. E)(G)
0°	2454.2	2454.2
		3346.9
		3346.9
	4239.6	4239.6
90°	3286.1	3284.6
		3285.1
	3408.5	3408.5
		3408.8

All experimental values are within ± 0.5 G.

It can be seen that the two perpendicular lines on the lower end of the field are superimposed, as well as those at the higher end of the field. This essentially accounts for the presence of two lines only and their shapes.

$K^+F_2^-$

In Figure 25 the lines observed when K was co-deposited with F_2 and Ar mixture are shown. Again, two parallel and two perpendicular lines were observed. The parallel lines were separated by a distance of 1822.8 G with a value of $A_{\parallel} = 911.4 \pm 1.0$ G. The calculated $g_{\parallel} = 2.0043 \pm 0.001$. The high field perpendicular line is located at 3418.5 ± 0.5 G with a value of $g_{\perp} = 1.9666 \pm 0.001$. The computed value of $A_{\perp}$ is equal to 3.0 ± 2.0 G.

In Table XXIII, the values for the field positions obtained experimentally, and through calculation, are listed. It can be seen that the two low-field perpendicular lines are superimposed, as well as the two high-field ones. This accounts for the presence of only two lines rather than four.

For this case a computer simulation was carried out with the MAGNSPEC 3 program. Once the values of $A_{\parallel}$, $A_{\perp}$, $g_{\parallel}$, and $g_{\perp}$ were set by means of the program in Appendix D, they were introduced into MAGNSPEC 3 to obtain a simulation. In Figure 26 the simulated spectrum is compared with the experimentally determined one. The shape of the perpendicular lines with respect to the parallel lines is justified due

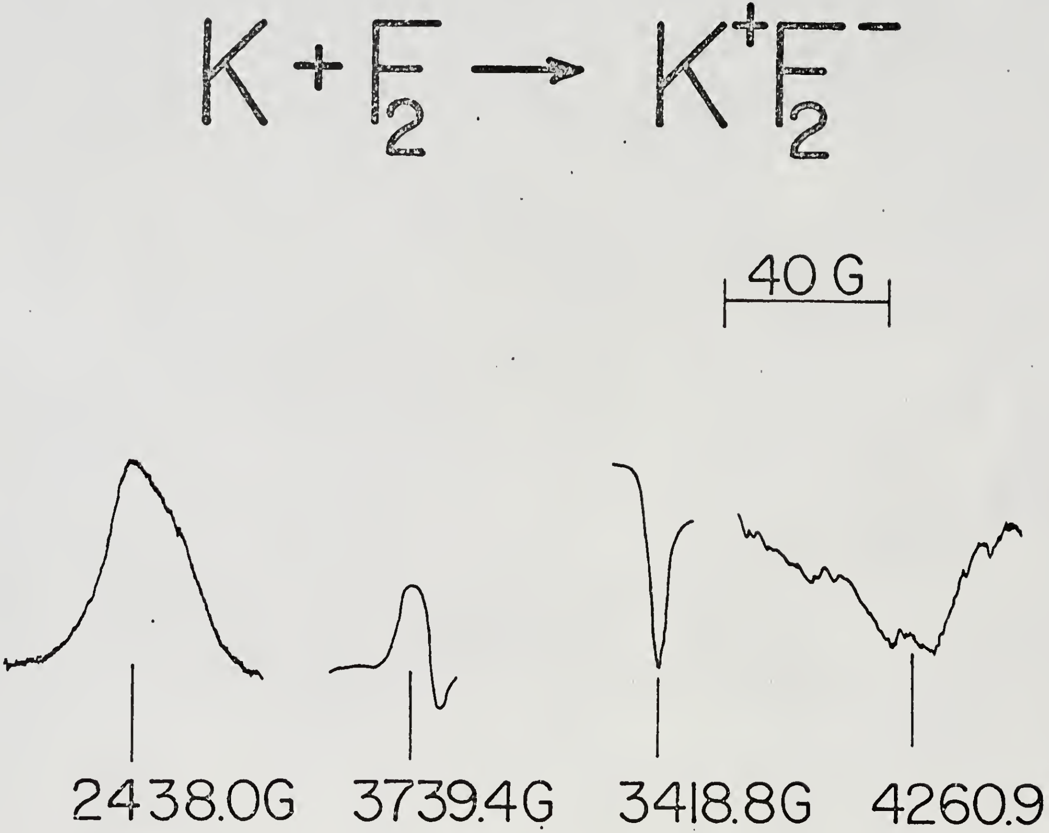

The intensity ratio between the two inside lines and the two outside ones is 100:1.

Figure 25

TABLE XXIII

MAGNETIC FIELD POSITION FOR $K^+F_2^-$

Angle	Experimental (G)	Program (App. E)(G)	MAGNSPEC 3(G)
0°	2438.0	2438.0	2437.6
		3349.4	3349.4
		3349.4	3349.4
	4260.9	4260.9	4260.8
90°	3293.4	3292.9	3293.1
		3293.4	3293.1
	3418.8	3418.3	3418.7
		3418.8	3418.7

All experimental values are within ± 0.5 G.

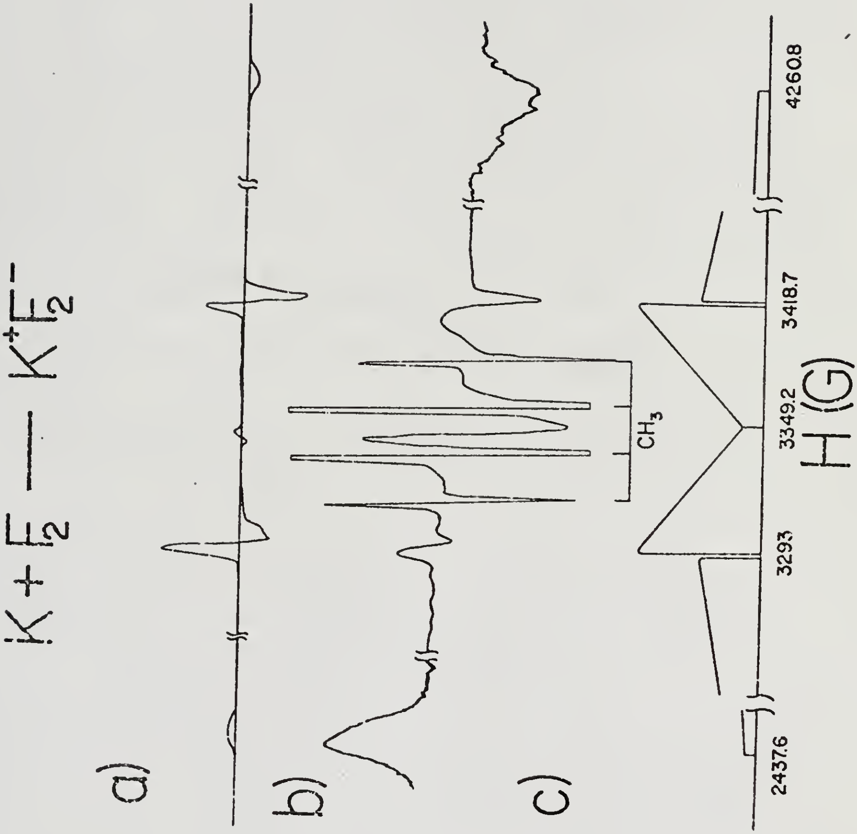

Figure 26

to the superposition of the two low-field ones and the two high-field ones as can be seen in Figure 26. The low-field perpendicular line points in the same direction as the parallel line rather than the opposite direction as it should, but intensity considerations as well as superposition of the other line accounts for the apparent discrepancy. The same is observed in the high-field parallel and perpendicular lines (see discussion).

$Cs^+F_2^-$

The spectrum obtained when Cs atoms are allowed to react with the F_2 and Ar mixture is shown in Figure 27. The salient features of it are again those of the F_2^- ion. Two parallel and two perpendicular lines are observed. The two parallel lines are separated by a distance of 1841.2 G with $A_{\parallel} = 920.6 \pm 1.0$ G and $g_{\parallel} = 2.0048 \pm 0.001$. The high-field perpendicular line is at 3415.6 ± 0.5 G with $g_{\perp} = 1.9662 \pm 0.001$. The computed value of $A_{\perp}$ is 3.0 ± 2.0 G.

In Table XXIV the values obtained experimentally and computationally for the field positions are listed. It can be seen that the two low-field perpendicular lines overlap and the two high-field ones are very close. This accounts for the presence of only two lines and their shapes.

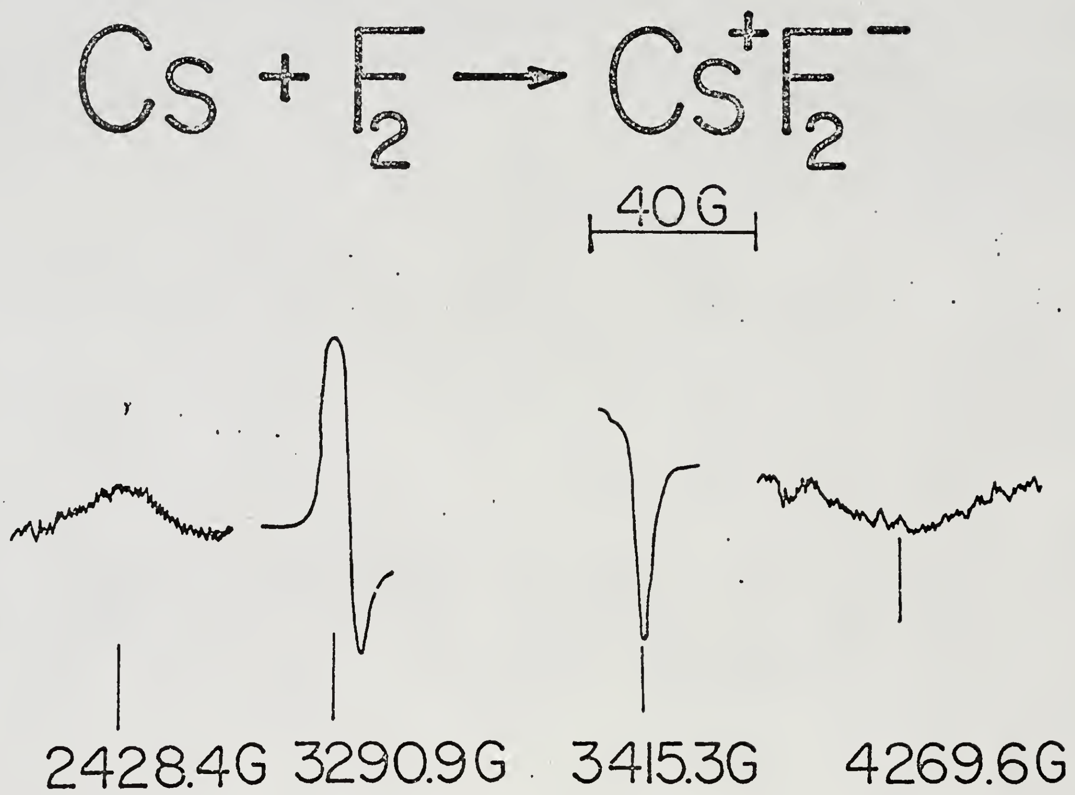

The intensity ratio between the two inside lines and the two outside ones is 100:1.

Figure 27

TABLE XXIV

MAGNETIC FIELD POSITION FOR $Cs^+F_2^-$

Angle	Experimental (G)	Program (App. E) (G)
0°	2428.4	2428.4
		3349.0
		3349.0
	4269.6	4269.6
90°	3295.5	3295.2
		3295.6
	3409.3	3409.3
		3409.5

All experimental values are within ± 0.5 G.

$Mg^+F_2^-$

The spectrum obtained when Mg atoms were allowed to react with the F_2 and Ar mixture is shown in Figure 28. The spectrum corresponds to the F_2^- ion. Two parallel and two perpendicular lines are, again, observed. The two parallel lines are separated by a distance of 1708.4 G with $A_\parallel = 854.2 \pm 1.0$ G and $g_\parallel = 2.0036 \pm 0.001$. The high-field perpendicular line is located at 3411.7 ± 0.5 G with $g_\perp = 1.9676 \pm 0.001$. The computed value for $A_\perp$ is 2.8 G.

In Table XXV the values obtained experimentally and computationally for the field positions are listed. It can be seen again that the two low-field perpendicular lines are very close, as well as the two high-field ones; therefore, we expect only two lines in the spectrum.

In this spectrum the presence of MgF is detected for both Mg isotopes. The ^{nat}MgF consists of two parallel and two perpendicular lines, since ^{nat}Mg has $I = 0$ and F will be the splitter. From these lines the values of $A_\parallel = 112.6 \pm 1.0$ G and $A_\perp = 53.4 \pm 1.0$ G, for the F nucleus and $g_\parallel = 2.0006 \pm 0.001$ and $g_\perp = 1.9998 \pm 0.001$ for the molecule. ^{25}MgF consists of 6 doublets. The doublets are produced by F ($I = \frac{1}{2}$) and the sextet is produced by ^{25}Mg ($I = 5/2$, natural aboundance 10.13%). The value for A_{iso} obtained for ^{25}Mg is 116.5 ± 1.0 G. In Table XXVI the observed and calculated values of the line positions are listed. The values for

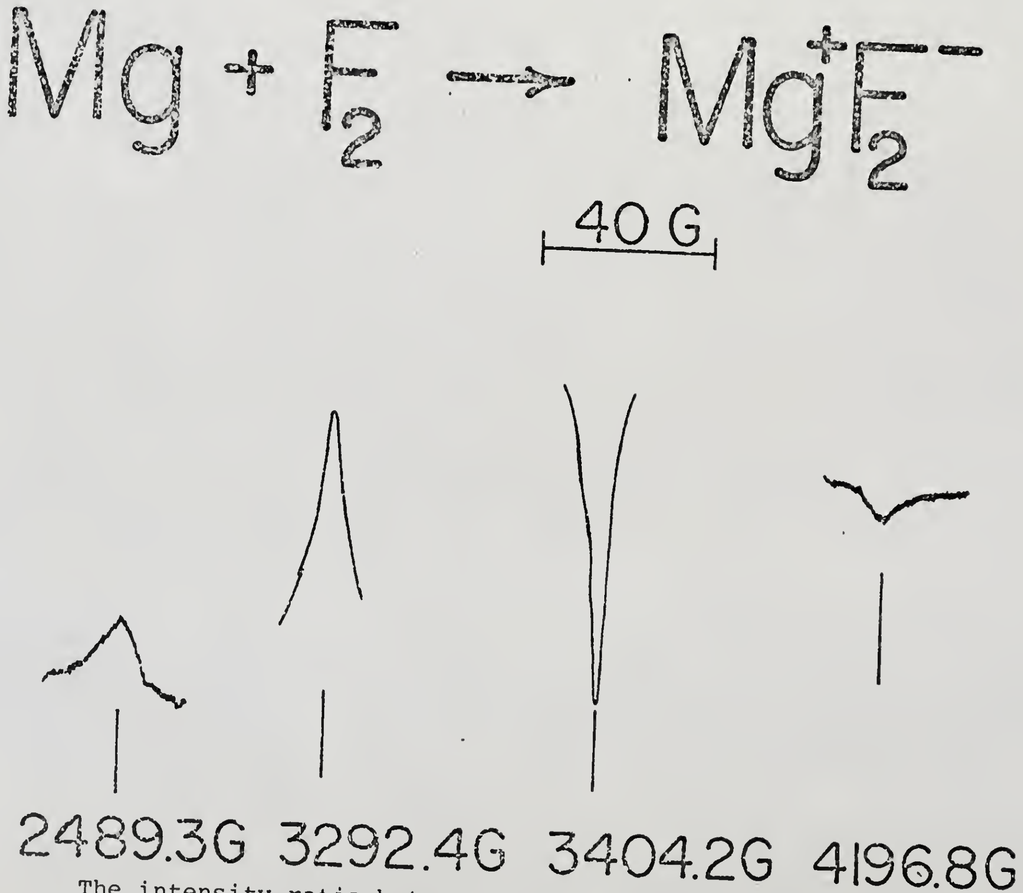

The intensity ratio between the two inside lines and the two outside ones is 100:1.

Figure 28

TABLE XXV

MAGNETIC FIELD POSITIONS FOR $Mg^{+}F_{2}^{-}$

Angle	Experimental (G)	Program (App. E)(G)
0°	2489.3	2489.3
		3343.1
		3343.1
	4196.8	4196.8
90°	3291.1	3291.9
		3292.4
	3404.2	3404.2
		3404.8

All experimental values are within ± 0.5 G.

TABLE XXVI

MAGNETIC FIELD POSITIONS FOR MgF

^{nat}MgF			Experimental	Calculated
	Parallel Lines		3299.1	3299.1
			3411.7	3411.7
	Perpendicular Lines		3329.5	3329.5
			3382.9	3382.9
^{25}MgF	$m_1^{^{25}Mg}$	m_1^F		
	-5/2	-1/2	3033.3	3033.2
	-5/2	1/2	3087.7	3086.6
	-3/2	-1/2	3141.1	3141.6
	-3/2	1/2	3194.5	3195.0
	-1/2	-1/2	3253.8	3254.1
	-1/2	1/2	*	3307.5
	1/2	-1/2	*	3370.6
	1/2	1/2	3423.8	3424.0
	3/2	-1/2	3491.0	3491.1
	3/2	1/2	3543.8	3544.5
	5/2	-1/2	3615.2	3615.7
	5/2	1/2	3668.8	3669.1

All experimental lines have an uncertainty of ± 0.5 G.

*Too much overlap to make an assignment.

^{nat}MgF agree with those obtained by Knight, Easley, Weltner and Wilson [18].

$Ba^+F_2^-$

The spectrum obtained when Ba atoms are allowed to react with the F_2 and Ar mixture is shown in Figure 29. The salient features are those of the F_2^- ion. Two parallel and two perpendicular lines are observed. The two parallel lines are separated by a distance of 1799.0 G with $A_\parallel = 899.5 \pm 1.0$ G and $g_\parallel = 2.0004 \pm 0.001$. The high-field perpendicular line is at 3418.1 ± 0.5 G with $g_\perp = 1.9768 \pm 0.001$. The computed value of $A_\perp$ is 3.0 ± 2.0 G.

In Table XXVII the values obtained experimentally and computationally for the field positions are listed. It can be seen that the two low-field perpendicular lines, as well as the two high-field ones, are very close. This accounts for the presence of only two lines and for their shapes.

Discussion

In the following discussion of the experimental spectra, the main assumption made is that the experimental results can be explained by treating the complex as two loosely bound entities, M^+ and F_2^-, and that they can be treated independently of one another.

$$Ba + F_2 \rightarrow Ba^+F_2^-$$

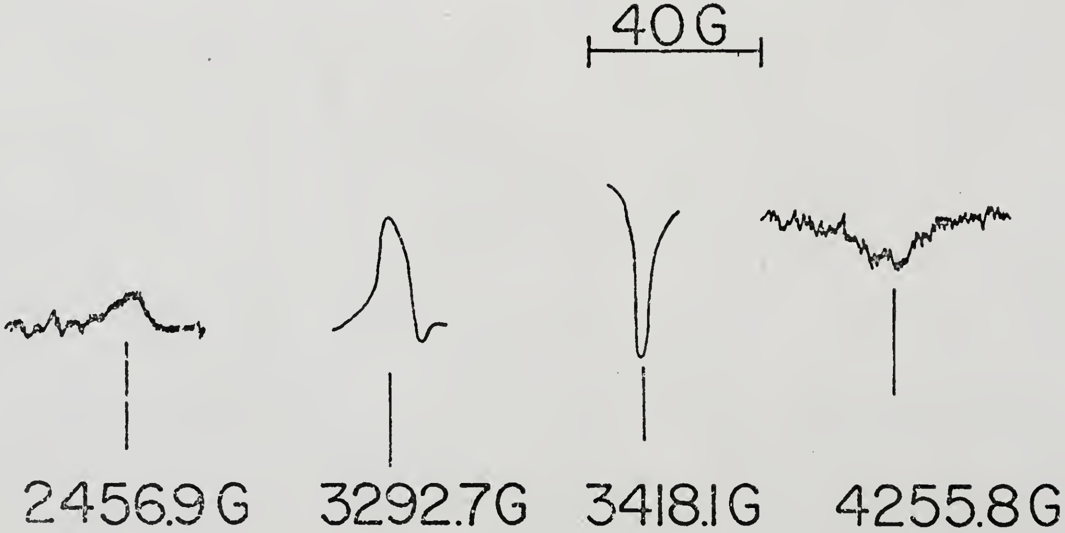

The intensity ratio between the two inside lines and the two outside ones is 100:1.

Figure 29

TABLE XXVII

MAGNETIC FIELD POSITION FOR $Ba^{+}F_2^{-}$

Angle	Experimental (G)	Program (App. E) (G)
0°	2456.9	2456.9
		3356.4
		3356.4
	4255.8	4255.8
90°	3292.7	3292.1
		3292.7
	3397.2	3397.2
		3397.2

All experimental values are within ± 0.5 G.

1. Hyperfine Tensor

The spin Hamiltonian used to describe the behavior of a linear molecule in a magnetic field can be written (Eq. (16)) as

$$\mathcal{H} = g\beta_o H S_z + K S_z I_z + Y(S^+ + S^-)I_z + X^-(S^+I^+ + S^-I^-) + X^+(S^+I^- + S^-I^+)$$

where

$$X^{\pm} = \frac{A_\parallel A_\perp}{4K} \pm \frac{A_\perp}{4} \quad \text{and} \quad Y = \frac{A_\perp^2 - A_\parallel^2}{2K} \frac{g_\parallel g_\perp}{g} \cos\theta \sin\theta .$$

In Appendix E the matrix elements and the Hamiltonian matrix are derived for basis eigenvectors of the type $|S,M\rangle|I,m\rangle$ where S, M, I, and m have their usual meaning. The diagonal elements of largest magnitude involve terms of the type $F \pm \frac{1}{2}K$, where $F = gH/2g_o$. The off-diagonal elements depend upon $X^{\pm}$ and Y. For the $\theta = 0°$ case, F = 1650 G for a typical field of about 3300 G, $K = A_\parallel = 900$ G, $X^+ = 1.5$ G, $X^- = 0$ and Y = 0. For the $\theta = 90°$ case, however, F = 1623 G for the same typical field intensity, $K = A_\perp = 3$ G, $X^+ = 226$, $X^- = 224$, and Y = 0. It can be seen that as we approach $\theta = 90°$, the values of the off-diagonal elements increase; therefore, they cannot be neglected. Y equals zero at the extreme points because of the angular dependence, but it is not equal to zero in the intermediate orientations, so it must also be counted in those.

From the values of $A_{\parallel}$ and $A_{\perp}$ thus determined the values of A_{iso} and A_{dip} can be obtained from Eqs. (3 & 7) by

$$A_{iso} = (A_{\parallel} + 2A_{\perp})/3 \quad \text{and} \quad A_{dip} = (A_{\parallel} - A_{\perp})/3.$$

A_{iso} is correlated with the Fermi contact term. It measures the spin density of the odd electron at the nucleus. A_{dip} is a measure of the anisotropy of the hyperfine tensor. It is usually correlated with the amount of p-character of the wavefunction describing the system. The values obtained for A_{iso} and A_{dip} are listed in Table XXVIII for all the different complexes studied. It is interesting to notice that, due to the smallness of $A_{\perp}$, A_{iso} and A_{dip} are very close in value.

The values of A_{iso} and A_{dip} can be correlated with fundamental properties of the molecule via the Dirac equation, as discussed in detail in Chapter II. As was shown there (Eqs. (3 & 7))

$$A_{iso} = \frac{8\pi}{3} g \beta_o g_o g_n \beta_n |\psi(o)|^2$$

and

$$A_{dip} = g \beta_o g_n \beta_n \left\langle \frac{3 \cos^2\theta - 1}{2r^3} \right\rangle$$

The values of $|\psi(o)|^2$ and $\left\langle \frac{3 \cos^2\theta - 1}{2r^3} \right\rangle$ are listed in Table XXIX for the values of A_{iso} and A_{dip} found in Table XXVIII.

TABLE XXVIII

MAGNETIC PARAMETERS FOR F_2^-

Metal	A_{iso}(MHz)*	A_{dip}(MHz)**
Na	826	821.
K	847	839
Cs	856	847
Mg	794	786
Ba	838	830

*All these values are within ± 4 MHz.

**All these values are within ± 2 MHz.

TABLE XXIX

MOLECULAR PARAMETERS FOR F_2^-

Metal	$\lvert\psi_{(o)}\rvert$ (a.u.)*	$\langle\frac{3\cos^2\theta-1}{2r^3}\rangle$ (a.u.)**
Na	0.197	1.64
K	0.202	1.67
Cs	0.204	1.69
Mg	0.189	1.57
Ba	0.199	1.65

*All these values are within ± 0.0001.

**All these values are within ± 0.001.

If the wavefunction ψ for the ground state of the F_2^- ion is assumed to be expandable by an LCAO in terms of the atomic orbitals ϕ of the F atoms, it can be shown that

$$\psi = C_1\phi_s^{(1)} + C_2\phi_{p\sigma}^{(1)} + C_3\phi_s^{(2)} + C_4\phi_{p\sigma}^{(2)}$$

where the superscripts identify the atomic center involved and the subscripts the character of the atomic orbital. The Cs are the weighting coefficients. If the two F atoms are identical, then $C_1 = C_3$ and $C_2 = C_4$. If the wavefunction is normalized, then $\sum_i C_i^2 = 1$ and it is assumed that the cross-terms, C_iC_j $(i \neq j)$, are small. It can be shown, following the procedure outlined in Eq. (II-18), that

$$C_1^2 = C_3^2 = \frac{A_{iso}}{A_{iso}^{atom}} \quad \text{and} \quad C_2^2 = C_4^2 = \frac{A_{dip}}{A_{dip}^{atom}} .$$

The values of these coefficients were obtained utilizing the atomic values given by Ayscough [19] and are tabulated in Table XXX. From the nature of the wavefunction, its coefficients can be interpreted as the percent character of its given parts. It can be seen, then, that the wavefunction consists of very small (of the order of 2%) s-character and a larger contribution (of the order of 48%) for the p-character for each F atom.

If the s in density values C_1^2 and C_2^2 are plotted against the ionization potential of the metal donor, two straight lines are obtained. They indicate that as the

TABLE XXX

MO-WAVEFUNCTION COEFFICIENTS FOR F_2^-

Metal	Ionization Potential (eV)	C_1^2 *	C_2^2 **
Na	5.12	0.0157	0.467
K	4.32	0.0161	0.477
Cs	3.89	0.0163	0.481
Mg	7.61	0.0151	0.447
Ba	5.19	0.0160	0.472

All these values are per F atom.

Atomic values used (Ayscough [19]).

A_{iso}^{atom} = 52500 MHz.

A_{dip}^{atom} = 1760 MHz .

*These values are within ± 0.0005.

**These values are within ± 0.005.

ionization potential of the metal decreases, the amount of electronic density lying on F_2^- increases. This is an indication that an ion-pair, $M^+F_2^-$, is formed. Although its presence is felt only to a small degree, the metal ion does influence the spin density and bonding of the halogen anion. In Figure 30 the spin density for both s-character and p-character (called there the non-s-character) is plotted against the ionization potential of the metal. It should be noted that the scale used for the s-character in Figure 30 is larger than for p-character in order to show the small variations.

The lines going through the experimental points can be found by a least-squares fitting program. This program is listed in Appendix C. The lines obtained were

s-character: $Y = -3.08 \times 10^3 X + 5.40 \times 10^1$

non-s-character: $Y = -1.06 \times 10^2 X + 5.50 \times 10^1$.

Here Y is the ionization potential in eV and X is the corresponding s- or non-s-spin density in atomic units.

The relatively large value of A_{dip} and the large percentage of p-character in the wavefunction indicates that the odd electron is in a predominantly p-orbital. This is to be expected if the electronic configuration of the ground state of F_2^- ion is

$$(\sigma_g 2s)^2 (\sigma_u 2s)^2 (\sigma_g 2p)^2 (\pi_u 2p)^4 (\pi_g 2p)^4 (\sigma_u 2p)^1$$

in agreement with past work [1-15].

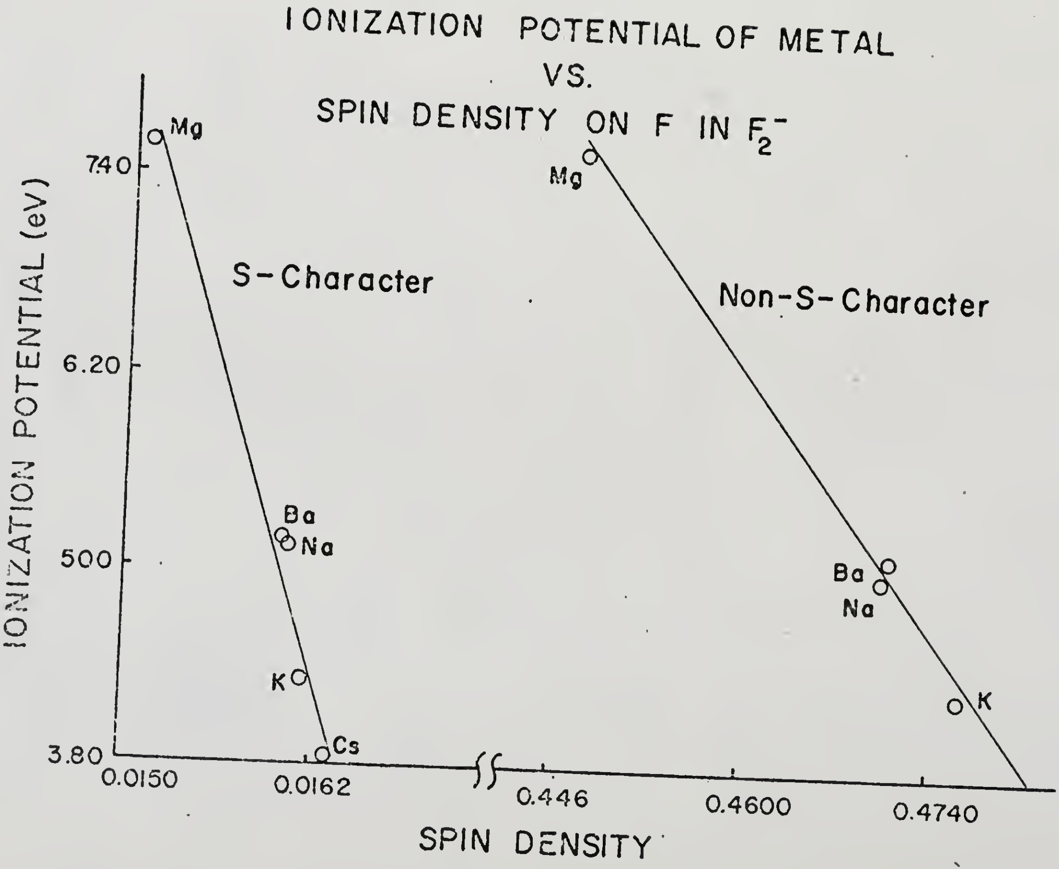
IONIZATION POTENTIAL OF METAL
VS.
SPIN DENSITY ON F IN F2−
IONIZATION POTENTIAL (eV)
7.40
6.20
5.00
3.80
Mg
S-Character
Ba
Na
K
Cs
Mg
Non-S-Character
Ba
Na
K
0.0150
0.0162
0.446
0.4600
0.4740
SPIN DENSITY

Figure 30

If the values of $A_\perp$ are compared with those obtained in the crystal work, e.g., Woodruff and Kanzig [2] or Kanzig [3] ($A_\perp$ = 58 G), it can be seen that the values obtained in this work are significantly smaller than those found there. This indicates that the species that is being dealt with here is slightly more anisotropic than the one present in the crystal case. It is believed, then, that the presence of a crystal field of positive ions surrounding the F_2^- tends to make it more isotropic than the presence of a single cation on one side of the molecule-ion.

If the values of $A_\perp$ in the crystal and those obtained in this work for Cl_2^- are also compared (see Table II, Chapter II), it can be seen that this difference is not found there. Therefore, it can be concluded that the Cl_2^- ion is not as polarizable as the F_2^- ion, since, in going from the crystal to the matrix environment, no significant increase in the anisotropy of the species is found. The large polarizability of the F_2^- has been predicted by Balint-Kurti [5].

2. g-Tensor

The deviations from g_o = 2.0023 in the g-values for the molecules studied can be accounted for by mixing of $^2\Pi$ states with the $^2\Sigma$ ground state. As was discussed in the derivation of Eqs. (17a and b), this mixing of excited states enters the wavefunction via spin-orbit coupling.

The changes in $g_\perp$ were shown to be, to second-order perturbation theory,

$$g_\perp - g_o = -2 \sum_n \frac{\langle n|\xi L_x|0\rangle \langle 0|L_x|n\rangle}{E_n - E_0} .$$

On the other hand, the mixing of excited states affects $g_\parallel$ only in higher order so that the changes in $g_\parallel$ are believed to be due to matrix effects. If it is assumed that the matrix effects will be the same for both $g_\parallel$ and $g_\perp$, then it might be more meaningful to study $g_\perp - g_\parallel$ rather than $g_\perp - g_o$, but, since the values of $\Delta g_\parallel$ are very small, the conventional way of treating this problem will be used here.

The experimentally determined values of $g_\parallel$ and $g_\perp$ are listed in Table XXI. In Table XXXI the values for $\Delta g_\parallel$ and $\Delta g_\perp$ are listed. It can be seen there that the deviations of $g_\parallel$ from g_o are indeed very small. However, the deviations of $g_\perp$ from g_o are approximately two orders of magnitude larger and indicate that there are some low-lying $^2\Pi$ states that are mixed with the gound state.

In the optical work done by Delbecq, Hayes and Yuster [11], two low-lying $^2\Pi$ states were identified. They are

$$^2\Pi_u: (\sigma_g 2s)^2(\sigma_u 2s)^2(\sigma_g 2p)^2(\Pi_u 2p)^3(\sigma_g 2p)^4(\sigma_u 2p)^2$$

and

$$^2\Pi_g: (\sigma_g 2s)^2(\sigma_u 2s)^2(\sigma_g 2p)^2(\Pi_u 2p)^4(\Pi_g 2p)^3(\sigma_u 2p)^2 .$$

TABLE XXXI

Δg FOR F_2^-

Metal	$g_\parallel$	$g_\perp$
Na	-0.0007	-0.0369
K	0.0020	-0.0357
Cs	0.0025	-0.0361
Mg	0.0013	-0.0347
Ba	-0.0019	-0.0255

All Δg values are within ± 0.001.

This is in agreement with the work done by Schoemaker [14]. Both of these states are inverted; therefore, they will yield $\Delta g_\perp$ values that will always be positive. This is in agreement with all the work done in this field until now [1-15]. On the other hand, only the $^2\Pi_u$ state could be mixed with the ground state due to conservation of parity.

It is interesting to notice, however, that in this work, since all the values of $\Delta g_\perp$ are negative, a low-lying $^2\Pi_u$ state is mixed with the $^2\Sigma_u$ ground state but that it must be regular rather than inverted. This is in agreement with a state of the following configuration:

$$^2\Pi_u\colon\ (\sigma_g 2s)^2(\sigma_u 2s)^2(\sigma_g 2p)^2(\Pi_u 2p)^4(\Pi_g 2p)^4(\Pi'_u 3p)^1.$$

A state of this type is difficult to accept, but bending the F-F bond, changing the sign of $A_\perp$, and making the two fluorines completely non-equivalent by forming a linear $M^+F_2^-$ species would not produce a change in $g_\perp$ that would be compatible with the spectrum or that would approach the value observed in the irradiated crystal. The latter has to be the case if the F_2^- molecule is linear. If the metal ion is incorporated into the model, the molecule changes from a $D_{\infty h}$ to a C_{2v} symmetry group and the ground state goes from $^2\Sigma_u$ to $^2B_1$. Correspondingly, the excited state goes from $^2\Pi_u$ to $^2A_1$. This is true provided that the metal ion is placed on the perpendicular bisector of the F-F bond. In Balint-Kurti's calculation [5], he observed for this same configuration, a $^2B_1$ ground state that was mainly ionic at all $Li^+ - F_2^-$ distances. In the excited $^2A_1$ state, however, there was a crossing over from a purely ionic state (F_2^-; $^2\Sigma_u$ and Li^+; ^1S) to a covalent state (F_2; $^1\Sigma_g$ and Li; ^2S). This state decomposes to the F_2 molecule and the Li atom. The distance between the Li atom and the center of the F_2 bond at which the crossing occurs is approximately 4.8 a.u. At distances lower than this, the ionic configuration prevails; at larger ones, the covalent configuration prevails. The calculation suggests that the electron in the excited state is associated, no matter how weakly, with the metal more than in the ground state. This may explain the observed $g_\perp$ since it is reasonable to assume that higher states in F_2^- must contribute significantly to the excited state of the overall molecule for it to dissociate into its F_2 and Li components.

Linewidths

The linewidths of the observed spectra are listed in Table XXXII. All linewidths are measured at half-height for the low-field parallel line. It can be seen that those metals whose magnetic moment is not zero broaden the F_2^- lines significantly. On the other hand, those with no magnetic moments have relatively narrow lines. A graph in which magnetic moment is plotted against linewidth is presented in Fig. 31 for the alkali-metal complexes.

TABLE XXXII

LINEWIDTHS AND MAGNETIC MOMENTS FOR METAL DONORS IN F_2^-

Metal	Linewidth (G)	Magnetic Moment (magnetons)
Na	26.9	2.216
K	23.7	0.391
Cs	28.2	2.56
Mg	11.2	0.0
Ba	11.2	0.0

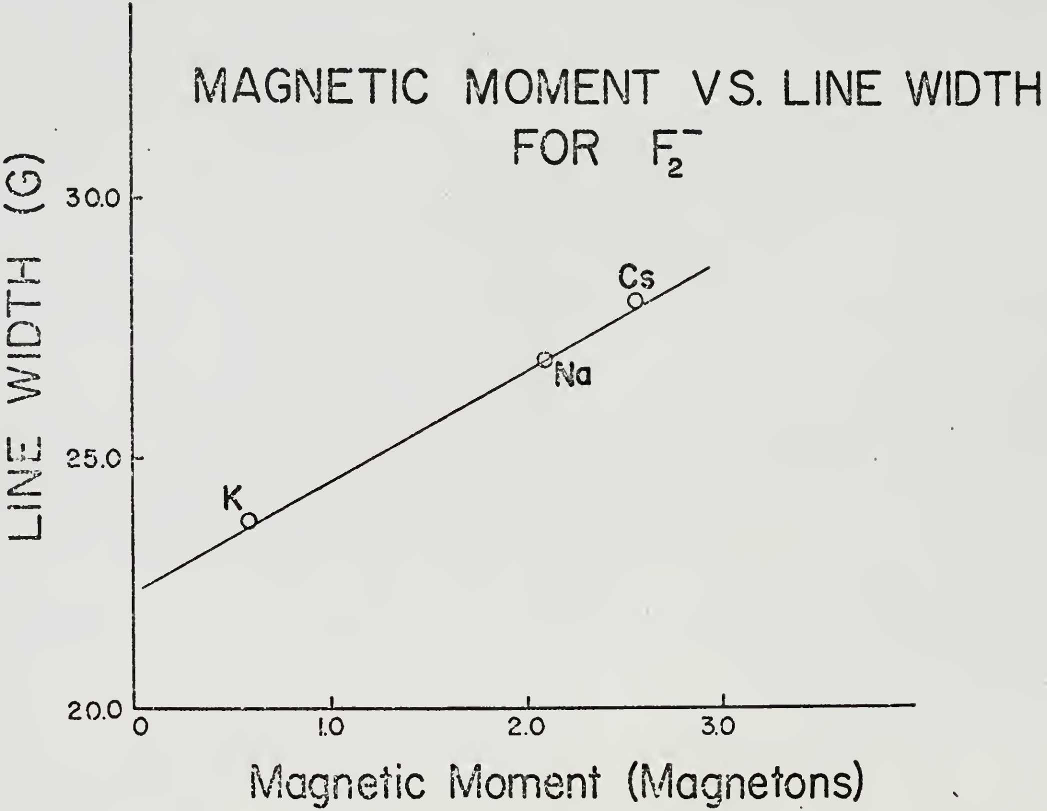
MAGNETIC MOMENT VS. LINE WIDTH FOR F_2^-
LINE WIDTH (G)
30.0
25.0
20.0
0
1.0
2.0
3.0
Magnetic Moment (Magnetons)
K
Na
Cs

Figure 31

The interpretation given to the increase in linewidths is the metal associated with the F_2^- ion, possessing a magnetic moment of its own, will cause further hyperfine splitting of the F_2^- lines. These splittings, however, will not be large, since as it has been mentioned previously, the complex is extremely ionic in its ground state and little interaction exists between the metal ion and the F_2^- ion. Therefore, this splitting is mostly unresolved and only broadening of the F_2^- lines is observed. This has been observed previously in the ESR spectra of ion-pairs (see Szwarc [20]).

INDO Calculation

INDO has been used previously to compare experimentally determined ESR parameters with those predicted by a simple calculation with relative success by Knight, Brom and Weltner [21].

An INDO calculation was carried out to understand better the properties of the F_2^- ion. The internuclear distance was varied until a minimum in the total energy for the system was found. The distance for which the minimum energy occurred was 1.42 Å, which is not too different from other more refined calculations (Balint-Kurti [5]) in which an equilibrium internuclear distance of 2.8 a.u. (1.5 Å) was found. The hyperfine parameters were A_{iso} = 1176 MHz and A_{dip} = -8.775 MHz. The value for A_{dip} was obtained using the spin-density matrix provided by INDO and the method discussed by Beveridge and

McIver [22]. If the values of the molecular parameters predicted from this calculation are compared with those listed in Table XXVIII, it can be seen that there is very poor agreement. This was expected to a large extent since INDO is notoriously poor in treating fluorine-containing compounds (see Pople and Beveridge [23]).

M^+ Ions

It was noticeably curious that, in the spectra of the alkaline-earth metal and F_2 experiments, the signal corresponding to the M^+ ion was absent. In the Cl_2^- case, this line was a prominent one and appeared in all cases. This can be understood, however, if it is realized that in the $M^+F_2^-$ case, a stronger interaction is present between the metal ion and the F_2^- ion than in the $M^+Cl_2^-$ (see the discussion of the hyperfine and g-tensors). It is assumed, then, that the alkaline-earth metal ion signals are broadened beyond recognition in these experiments.

Summary

The ESR spectrum of the trapped intermediates in the reaction between some alkali- and alkaline-earth metals and F_2 has been observed at 4 K. The observed spectra imply that an ion pair, $M^+F_2^-$, is formed in which the two species retain, to a large extent, their individual identity, although not to the extent observed in the $M^+Cl_2^-$ case.

The variation of the magnetic parameters of the F_2^- ions with the ionization potential of the metal donor was studied.

The dependence of the observed linewidths on the magnetic moment of the donor metal was analyzed in terms of the broadening of the F_2^- lines due to the hyperfine interaction in these metals.

The g-tensor was analyzed in terms of mixing of excited $^2A_1$ states with the $^2B_1$ ground state of the complex. The necessity to consider perturbing effects of the metal cation on the magnetic parameters of the halogen anion is taken as an indication that the interaction between the metal ion and the F_2^- ion is stronger than the one encountered between the metal ion and the Cl_2^- ion.

References

[1] Castner, T. G., and Kanzig, W., J. Phys. Chem. Solids, 3, 178 (1957).

[2] Woodruff, T. O., and Kanzig, W., J. Phys. Chem. Solids, 5, 268 (1958).

[3] Kanzig, W., J. Phys. Chem. Solids, 17, 80 (1960).

[4] Balint-Kurti, G. G., and Karplus, M., J. Chem. Phys., 50, 478 (1969).

[5] Balint-Kurti, G. G., Mol. Phys., 25, 393 (1973).

[6] Ikenberry, D., Jette, A. N., and Das, T. P., Phys. Rev. B, 1, 2785 (1970).

[7] Gilbert, T. L., and Wahl, A. C., J. Chem. Phys., 55, 5247 (1971).

[8] Jette, A. N., Gilbert, T. L., and Das, T. P., Phys. Rev., 184, 884 (1969).

[9] Yarkony, D. R., Hunt, W. J., and Schaefer, H. F., Mol. Phys., 26, 941 (1973).

[10] Ham, D. O., and Chang, H. W., Chem. Phys. Letters, 24, 579 (1974).

[11] Delbecq, C. J., Hayes, W., and Yuster, P. H., Phys. Rev., 121, 1043 (1961).

[12] Gazzinelli, R., and Mieher, R. L., Phys. Rev. 175, 395 (1968).

[13] Bailey, C. E., Phys. Rev., 136, A1311 (1964).

[14] Otto, F. B., and Gilliam, O. R., Phys. Rev., 154, 244 (1967).

[15] Schoemaker, D., Phys. Rev. B, 7, 786 (1973).

[16] Howard, W. F., and Andrews, L., J. Am. Chem. Soc., 95, 3045 (1973).

[17] Golding, R. M., and Tennant, W. C., Mol. Phys., 25, 1163 (1973).

[18] Knight, L. B., Easley, W. C., Weltner, W., Jr., and Wilson, M., J. Chem. Phys., 54, 322 (1971).

[19] Ayscough, P. B., Electron Spin Resonance in Chemistry, Methuen & Co., London (1967).

[20] Szwarc, M., Ions and Ion Pairs in Organic Reactions, Wiley and Sons, New York (1972).

[21] Knight, L. B., Brom, J. M., and Weltner, W., Jr., J. Chem. Phys., 56, 1152 (1972).

[22] Beveridge, D. L., and McIver, J. W., J. Chem Phys., 54, 4681 (1971).

[23] Pople, J. A., and Beveridge, D. L., Approximate Molecular Orbital Theory, McGraw-Hill, New York (1970).

APPENDIX A

PROGRAM TO SIMULATE THE ESR SPECTRUM OF $^2\Sigma$ MOLECULES TO SECOND-ORDER PERTURBATION THEORY

```
C     ELECTRON RESONANCE LINESHAPE  (EPRSIG)      MAIN PROGRAM
C
C***********************************************************************
C
C     THE DATA CARDS SHOULD BE AS FOLLOWS
C
C***********************************************************************
C
C     THE FIRST CARD
C        COLS. 71-72   -1 IF CALCOMP PLOTS ARE DESIRED
C
C     THE SECOND CARD
C        COLS.  1-70   TITLE
C
C     THE THIRD CARD
C        COLS.  1-10   ELECTRON SPIN
C        COLS.  11-20  G(1) PARALLEL COMPONENT OF G TENSOR
C        COLS.  21-30  G(2) PERPENDICULAR COMPONENT OF G TENSOR
C        COLS.  31-40  LEAVE BLANK UNLESS PROBLEM HAS ORTHORHOMBIC SYMMETRY
C        COLS.  41-50  ZERO FIELD SPLITTING
C        COLS.  51-60  ORTHORHOMBIC COMPONENT OF ZERO FIELD SPLITTING
C
C     THE FOURTH CARD(INCLUDE ONE OF THESE CARDS FOR EACH NON-EQUIVALENT
C        NUCLEUS)
C        COLS.  1-2    NUMBER OF THIS TYPE,NOTE: FOR N<10 PUNCH NUMBER IN COL 2
C        COLS.  3-10   NUCLEAR SPIN (PUNCH DECIMAL)
C        COLS.  11-20  PARALLEL COMPONENT OF COUPLING TENSOR(PUNCH DECIMAL)
C        COLS.  21-30  PERPENDICULAR COMPONENT OF COUPLING TENSOR
C        COLS.  31-40  ORTHORHOMBIC COMPONENT OF COUPLING TENSOR
```

```
C          COLS.  41-50 QUADRUPOLE CONSTANT Q'**2 IN LOWE'S
C
C       AFTER THE LAST CARD FOR THE NON-EQUIVALENT NUCLEUS
C       INSERT A BLANK CARD
C
C       THE NEXT CARD CONTAINS SPECTROMETER PARAMETERS
C          COLS.  3-10   FREQUENCY IN MEGACYCLES
C          COLS.  11-20  MINIMUM SENSITIVITY(SET TO .001 UNLESS PUNCHED)
C          COLS.  21-30  NUMBER OF STEPS IN THETA (100 UNLESS PUNCHED)
C
C       THE NEXT CARD SETS THE RANGE AND RESOLUTION OF THE SWEEP
C          COLS.  1-10   INITIAL FIELD IN GAUSS
C          COLS.  11-20  TERMINAL FIELD IN GAUSS
C          COLS.  21-30  RESOLUTION IN GAUSS
C
C       THE NEXT CARD CONTAINS :
C          COLS.  31-40  LINEWIDTH IN GAUSS (DELTA FUNCTION UNLESS PUNCHED)
C          COLS.  41-50  WEIGHTING FACTOR (1.0 UNLESS PUNCHED)
C
C       THE NEXT CARD DETERMINES THE RED FUNCTION
C          COLS.  1-10   INITIAL COEFFICIENT OF R(THETA)
C          COLS.  11-20  COEFFICIENT OF THETA
C          COLS.  21-30  COEFFICIENT OF THETA ** 2
C          COLS.  31-40  COEFFICIENT OF THETA ** 3
C          COLS.  41-50  COEFFICIENT OF THETA ** 4
C          COLS.  51-60  COEFFICIENT OF THETA ** 5
C          COLS.  71-72  NUMBER OF NON ZERO COEFFICIENTS YOU LISTED NOT COUNTING
C                        THE INITIAL COEFFICIENT.MUST AT LEAST EQUAL 2
C
```

```
C     PUNCH -999 IN COLUMNS 1-4 OF THE NEXT CARD IF ANOTHER SPECTRUM
C     IS TO BE SUPERIMPOSED OF THE LAST ONE, IN WHICH CASE YOU WOULD
C     START WITH THE TITLE OF YOUR SPECTRUM AND SET UP THE NEW
C     DATA STATEMENTS.   OTHERWISE LEAVE THIS CARD BLANK.
C
C     THE FINAL CARD OF THE DATA STATEMENTS IS FOR THE CALCOMP PLOTTER
C        COLS.  6-10   NUMBER OF POINTS IN THE SPECTRUM TO BE PRINTED
C        COLS.  11-15  NUMBER OF THETA VS. H PLOTS DESIRED. IF NEGATIVE
C                      NO OTHER PLOTS ARE MADE.
C        COL.      20  POSITIVE NUMBER PLOTS INTEGRALS
C        COLS.  21-30  NUMBER OF GAUSS PER INCH DESIRED ON PLOT
C
C*********************************************************************
C
C     THIS PROGRAM APPEARS IN KASAI, P.H., WHIPPLE, E.B., AND WELTNER,JR.
C     W., TECHNICAL REPORT, UNION CARBIDE, SEPTEMBER 1965.
      DIMENSION TITLE(12),G(3),NPOP(10),SPIN(10),A(10,3),RESLIN(1000),
     *HPRIM(100),XINT(100),SIGNAL(30000),BUFFER(1024),X(1200),
     *JUNK(22),SIG2(30000),QUAD(10)
      COMMON TITLE,S,G,D,E,NPOP,SPIN,A,FREQ,SMIN,DTHETA,HMIN,HMAX,DH,NUC
     *LEI,ISTOP,LINES,IFTAPE,JUNK
      COMMON/B/PHI
      COMMON/C/IDUMMB
      COMMON/D/QUAD
      DO 774 I=1,100
      HPRIM(I)=0.
  774 XINT(I)=0.
      DO 775 I=1,1200
  775 X(I)=0.
```

```
      DO 776 I=1,1000
  776 RESLIN(I)=0.
      DO 777 I=1,30000
      SIGNAL(I)=0.
  777 SIG2(I)=0.
      ICNT=0
      READ (5,1004)IFTAPE
      IF(IFTAPE+1)20,21,20
   20 CONTINUE
      GO TO 1
   21 REWIND 9
    1 READ(5,1000) (TITLE(I),I=1,12)
       IDUMME=0
      READ (5,1001)S,(G(I),I=1,3),D,E
      NUCLEI=1
    2 READ(5,1002)NPOP(NUCLEI),SPIN(NUCLEI),(A(NUCLEI,J),J=1, 3),QUAD(NU
     *CLEI)
      IF(NPOP(NUCLEI))5,5,3
    3 NUCLEI=NUCLEI+1
      GO TO 2
    5 CONTINUE
      NUCLEI=NUCLEI-1
      READ(5,1001)FREQ,SMIN,DTHETA
      IF(DTHETA)6,4,6
    4 DTHETA=1.57079633E-02
      LPSTOP=101
      GO TO 7
    6 LPSTOP=IFIX(DTHETA+0.1)+1
      DTHETA=1.57079633/DTHETA
    7 IF(SMIN)8,8,9
    8 SMIN=1.0E-03
    9 WRITE(6,2000) (TITLE(I),I=1,12)
      IF(IFTAPE+1)23,22,23
   22 WRITE(9) (TITLE(I),I=1,12)
      WRITE(9)LPSTOP
   23 WRITE (6,2001)FREQ,SMIN
      WRITE (6,2002)(I,G(I),I=1,3)
      IF(NUCLEI)15,15,13
   13 WRITE(6,2003)
      DO 14 I=1,NUCLEI
   14 WRITE (6,2004)I,SPIN(I),(A(I,J),J=1,3),QUAD(I)
   15 READ (5,1001)HMIN,HMAX,DH
       IF(DH.EQ.0.0)DH=.0001
22222 DUMMY=HMAX-HMIN
      ISTOP=DUMMY/DH+0.5
      THETA=0.
   25 IF(ISTOP-29950)17,17,16
   16 ISTOP=29950
      DH=DUMMY/29950
   17 WRITE (6,2005)HMIN,HMAX,DH
      CALL SHAPE (RESLIN)
      IF(JUNK(2)+1)82,81,82
   81 SYM=-1.0
      GO TO 83
   82 SYM=1.0
   83 MSTEP=400
  100 DO 200 LOOP=1,LPSTOP
      CALL HRES(THETA,PHI,MSTEP,HPRIM,XINT)
      WT1=RED(THETA,PHI)
      WT2=GREEN(THETA)
      DO 140 L=1,LINES
      IF (HPRIM(L)-HMAX)110,140,140
  110 SIG=HPRIM(L)-HMIN
      MIDDLE=SIG/DH+0.5
      IF (MIDDLE)140,140,120
  120 SIGNAL (MIDDLE)=SIGNAL (MIDDLE)+RESLIN(1000)*WT1*XINT(L)
52525 SIG2(MIDDLE)=SIG2(MIDDLE)+RESLIN(1000)*XINT(L)*WT2
52526 DUMMY=XINT(L)*WT1
52527 SIG=DUMMY*RESLIN(1000)
      DO 125 I=1,999
52528 INDEX=1000-I
52529 SAVE=SIG
52520 SIG=RESLIN(INDEX)*DUMMY
63524 IF(SIG-SMIN)124,122,122
  124 IF(SIG-SAVE)126,126,122
  122 INDEX=MIDDLE+I
      IF(INDEX-ISTOP)123,123,992
  123 SIGNAL(INDEX)=SIGNAL(INDEX)+SYM*SIG
      INDEX=MIDDLE-I
      IF(INDEX)992,992,125
  125 SIGNAL(INDEX)=SIGNAL(INDEX)+SIG
      GO TO 991
  126 DUMMY=XINT(L)*WT2
      SIG=DUMMY*RESLIN(1000)
      DO 130 I=1,999
      INDEX=1000-I
      SAVE=SIG
      SIG=RESLIN(INDEX)*DUMMY
      IF(SIG-SMIN)128,127,127
  128 IF(SIG-SAVE)140,140,127
  127 INDEX=MIDDLE+I
      SIG2(INDEX)=SIG2(INDEX)+SYM*SIG
      INDEX=MIDDLE-I
  130 SIG2(INDEX)=SIG2(INDEX)+SIG
      GO TO 991
  140 CONTINUE
  200 THETA=THETA+DTHETA
201   READ (5,1003)IFTO
      IF(IFTAPE+1)206,205,206
  205 WRITE (9)IFTO
  206 IF(IFTO+999)208,1,208
  208 CONTINUE
      CALL OUTPUT(X,SIGNAL,SIG2)
      IF(IFTAPE+1)210,209,210
  209 END FILE 9
 210  CONTINUE
      DO 301 I=1,ISTOP
      SIGNAL(I)=0.
  301 SIG2(I)=0
      GO TO 1
  991 WRITE (6,2010)L,LOOP,THETA,PHI
      STOP
  992 WRITE (6,2011)L,LOOP,HPRIM(L),MIDDLE,INDEX,RESLIN(INDEX),SIG
      WRITE(6,2009)
      DH=DH*1.1
      ICNT=ICNT+1
      IF(ICNT.GT.4)STOP 6
      HMIN=HMIN-DUMMY/25.
      HMAX=HMAX+DUMMY/25.
      DO 333 III=1,30000
      SIGNAL(III)=0.
  333 SIG2(III)=0.
      GO TO 22222
 1000 FORMAT(12A4)
 1001 FORMAT(6F10.5)
 1002 FORMAT(I2,F8.4,4F10.5)
 1003 FORMAT(I4)
 1004 FORMAT(70X,I2)                                                                204
 2000 FORMAT('1',9X,12A4,//)
 2001 FORMAT(10X,'SPECTROMETER FREQUENCY =  ',F8.2,'M.C., SENSITIVITY =
     *  ',F10.3     )
 2002 FORMAT('0',20X3('G(',I1,') = ',F10.8,3X)/)
 2003 FORMAT('0',10X,'NUCLEUS',5X,'SPIN',6X,'A(1)',6X,'A(2)',6X,'A(3)',
     *5X,'QUAD',/)
 2004 FORMAT(14X,I1,8X,F4.2,3X,4(1X,F8.3,1X))
 2005 FORMAT('0'/9X,'MAGNETIC FIELD SWEPT FROM ',F8.2,' GAUSS TO ',F8.2,
     *' GAUSS WITH RESOLUTION OF ',F8.4,' GAUSS  ')
 2009 FORMAT('1',10X,'RESTART ATTEMPTED - NEW RANGE ASSUMED')
 2010 FORMAT('0',10X'SIGNAL FAILS TO VANISH IN WINGS FOR LINE ',I2,' IN
     *LOOP ',I4,/,10X,'CURRENT VALUE OF THETA IS ',F8.5,' PHI = ',F8.5)
 2011 FORMAT('0',5X,'SIGNAL EXCEEDS RANGE FOR LINE ',I2,'ON LOOP NUMBER'
     *,I4,/,10X,'LINE CENTER AT ',F8.2,'GAUSS IS IN',I4,'TH CELL OF SIGN
     *AL',/,10X,'RESLIN(',I3,') = ',E12.5,' SIGNAL LEVEL = ',E12.5)
      END
```

```
C     GREEN (NUMERICAL INTEGRATION)          (FUNCTION)
       FUNCTION GREEN(THETA)
      EXTERNAL GOFX
      DIMENSION CLIST(100),SPACE(250),DATA(100)
      COMMON DATA
      COMMON/B/PHI
      DATA CLIST/100*0./,SPACE/250*0./
      IF(PHI+9.99)9,3,6
    3 PHI=0.
      NORDER=5
      SCALE=1.0
      GREEN=0.
      VALUE=0.
      WRITE(6,2000)
 2000 FORMAT('0',5X,' VALUES OF WEIGHTING FUNCTIONS AT 5-DEGREE INTERVAL
     *S'/,22X,'THETA',14X,'R(THETA)',15X,'RED',14X,'G(THETA)',14X,'GREEN
     *'/)
      TEST=0.
      SAVE=0.
      GO TO 8
    6 CALL GG5 (SAVE,PHI,GOFX,ANS)
      SAVE=PHI
       VALUE=VALUE+ANS
      GREEN=SCALE*PHI*ABS (VALUE)
      IF(THETA-TEST)9,3,8
    8 RED=PHI*DATA(100)
      WRITE (6,2001)THETA,DATA(100),RED,VALUE,GREEN
 2001 FORMAT(21X5(F12.5,8X))
      TEST=TEST+.08726
```

```
9 RETURN
  END
```

```
C     HRES(AXIAL)           SUBROUTINE
      SUBROUTINE HRES (THETA,PHI,MSTEP,HPRIM,XINT)
C************************************************************************
C
C     SUBROUTINE HRES CALCULATES THE POSITION OF THE LINES AND PRINTS
C     THESE OUT TOGETHER WITH THEIR NUMBER AND INTENSITIES.
C     THE HAMILTONIAN USED IS FOR AXIALLY SYMMETRIC MOLECULES UP TO
C     SECOND ORDER INCLUDING QUADRUPOLE INTERACTION.
C     REFERENCE: WILLIAM LOW, PARAMAGNETIC RESONANCE IN SOLIDS,
C     ACADEMIC PRESS, N.Y., 1960, PAGE 60
C
C************************************************************************
      DIMENSION G(3),SPIN(10),A(10,3),HPRIM(100),XINT(100),NPOP(10),
     *SZ(10),TITLE(12),NOEGEN(72),SKIP5(5),SKIP6(6)
      DATA SZ/10*0./,NOEGEN/72*0/
      COMMON TITLE,S,G,D,E,NPOP,SPIN,A,FREQ,SKIP5,NUCLEI,IFOOL,LINES,IFT
     *APE,SKIP6,C,P,Q
      C=COS(THETA)**2
      S=1.-C
      P=C*G(1)**2
      Q=S*G(2)**2
      G(3)=SQRT(P+Q)*1.39965
      IF(MSTEP-400)99,10,100
   99 STOP
   10 XINT(1)=1.
      LINES=1
      IF(NUCLEI)99,20,11
   11 DO 15 I=1,NUCLEI
      CALL NEONUC(NPOP(I),SPIN(I),NOEGEN,LENGTH)
      SPIN(I)=SPIN(I)*FLOAT(NPOP(I))
      M=1
      DO 13 J=1,LENGTH
      DO 13 K=1,LINES
      XINT(M)=XINT(K)*FLOAT(NDEGEN(J))
   13 M=M+1
   15 LINES=LINES*LENGTH
   20 WRITE(6,2001) LINES
      WRITE (6,2002) (I,XINT(I),I=1,LINES)
      IHSTOP=LINES
      ISTOP=IFIX(2.*SPIN(NUCLEI)+1.1)
      MSTEP=500
      IF(IFTAPE+1)100,25,100
   25 WRITE (9) LINES
      WRITE (9) (XINT(I),I=1,LINES)
  100 LINES=1
      DO 102 I=1,NUCLEI
  102 SZ(I)=SPIN(I)
  101 H=FREQ/G(3)
      ITURN=NUCLEI-1
      IF(ITURN)198,105,120
  198 HPRIM(LINES)=H
  197 IF(IFTAPE+1)200,199,200
  199 WRITE (9)(HPRIM(I),I=1,LINES)
  200 IF(THETA.EQ.0.0) GO TO 201
      TEMP=ABS(THETA-1.57076)
      IF(TEMP.LT.0.0001) GO TO 204
      GO TO 203
  201 WRITE(6,2003)
```

```
      GO TO 206
  204 WRITE(6,2005)
  206 WRITE(6,2004)(I,HPRIM(I),I=1,IHSTOP)
  203 RETURN
  105 SZ(NUCLEI)=SPIN(NUCLEI)
      DO 108 I=1,ISTOP
      HPRIM(LINES)=H-DELTAH(NUCLEI,SZ,THETA)
      LINES=LINES+1
  108 SZ(NUCLEI)=SZ(NUCLEI)-1.
  109 IF(ITURN)99,197,110
  110 IF(SZ(ITURN)+SPIN(ITURN))112,112,115
  112 SZ(ITURN)=SPIN(ITURN)
      ITURN=ITURN-1
      GO TO 109
  115 SZ(ITURN)=SZ(ITURN)-1.
      GO TO 101
  120 DO 122 I=1,ITURN
  122 H=H-DELTAH(I,SZ,THETA)
      GO TO 105
 2001 FORMAT('0'//10X'NORMALIZED INTENSITIES OF THE   ',I3,' ALLOWED LINE
     *S   '//)
 2002 FORMAT('0',20X'I(',I2,') = ',E15.7)
 2003 FORMAT(//,10X,'THE PARALLEL LINES ARE LOCATED AT:',//)
 2005 FORMAT(//,10X,'THE PERPENDICULAR LINES ARE LOCATED AT:',//)
 2004 FORMAT(30X,I3,5X,F20.4,/)
      END
```

```
C                                                                       QG5  001
C     ..................................................................QG5  002
C                                                                       QG5  003
C        SUBROUTINE QG5                                                 QG5  004
C                                                                       QG5  005
C        PURPOSE                                                        QG5  006
C           TO COMPUTE INTEGRAL(FCT(X), SUMMED OVER X FROM XL TO XU)    QG5  007
C                                                                       QG5  008
C        USAGE                                                          QG5  009
C           CALL QG5 (XL,XU,FCT,Y)                                      QG5  010
C           PARAMETER FCT REQUIRES AN EXTERNAL STATEMENT                QG5  011
C                                                                       QG5  012
C        DESCRIPTION OF PARAMETERS                                      QG5  013
C           XL     - THE LOWER BOUND OF THE INTERVAL.                   QG5  014
C           XU     - THE UPPER BOUND OF THE INTERVAL.                   QG5  015
C           FCT    - THE NAME OF AN EXTERNAL FUNCTION SUBPROGRAM USED.  QG5  016
C           Y      - THE RESULTING INTEGRAL VALUE.                      QG5  017
C                                                                       QG5  018
C        REMARKS                                                        QG5  019
C           NONE                                                        QG5  020
C                                                                       QG5  021
C        SUBROUTINES AND FUNCTION SUBPROGRAMS REQUIRED                  QG5  022
C           THE EXTERNAL FUNCTION SUBPROGRAM FCT(X) MUST BE FURNISHED   QG5  023
C           BY THE USER.                                                QG5  024
C                                                                       QG5  025
C        METHOD                                                         QG5  026
C           EVALUATION IS DONE BY MEANS OF 5-POINT GAUSS QUADRATURE     QG5  027
C           FORMULA, WHICH INTEGRATES POLYNOMIALS UP TO DEGREE 9        QG5  028
C           EXACTLY.                                                    QG5  029
```

```
C        FOR REFERENCE, SEE                                              QG5  030
C        V.I.KRYLOV, APPROXIMATE CALCULATION OF INTEGRALS,               QG5  031
C        MACMILLAN, NEW YORK/LONDON, 1962, PP.100-111 AND 337-338,       QG5  032
C     ..................................................................QG5  034
C                                                                        QG5  035
      SUBROUTINE QG5(XL,XU,FCT,Y)                                        QG5  036
C                                                                        QG5  037
C                                                                        QG5  038
      A=.5*(XU+XL)                                                       QG5  039
      B=XU-XL                                                            QG5  040
      C=.4530899*B                                                       QG5  041
      Y=.1184634*(FCT(A+C)+FCT(A-C))                                     QG5  042
      C=.2692347*B                                                       QG5  043
      Y=Y+.2393143*(FCT(A+C)+FCT(A-C))                                   QG5  044
      Y=B*(Y+.2844444*FCT(A))                                            QG5  045
      RETURN                                                             QG5  046
      END                                                                QG5  047
```

```
C     DELTA H (SECOND-ORDER)          FUNCTION
C*****************************************************************************
C
C     SUBROUTINE DELTAH CALCULATES THE POSITIONS OF THE LINES TO SECOND
C     ORDER PERTURBATION THEORY, INCLUDING QUADRUPOLE. IF NO QUADRUPOLE
C     IS DESIRED A 0.0 SHOULD BE ENTERED FOR THE VALUE OF QUAD. THIS
C     CALCULATION IS DONE IN THIS SUBROUTINE FOR DOUBLET SIGMA MOLECULES
C     OTHERWISE, SOME CARDS SHOULD BE CHECKED. SEE LOWE'S BOOK AND
C     INTRODUCE HIS M'S.
C
C*****************************************************************************
      FUNCTION DELTAH (INDEX,SZ,CONST)
      DIMENSION G(3),SPIN(10),A(10,3),HPRIM(100),XINT(100),NPOP(10),
     *SZ(10),TITLE(12),NDEGEN(72),SKIP5(5),SKIP6(6),TERM2(10),TERM3(10),
     *QUAD(10),TERM4(10),TERM5(10)
      COMMON TITLE,S,G,D,E,NPOP,SPIN,A,FREQ,SKIP5,NUCLEI,IFOCL,LINES,IFT
     *APE,SKIP6,C,P,Q
      COMMON/D/QUAD
      DATA TERM2/10*0./,TERM3/10*0./,TERM4/10*0./,TERM5/10*0./
      IF(CONST)5,2,1
    1 IF(CONST-SAVE)2,5,2
    2 SAVE=CONST
      R=G(1)*G(2)/(P+Q)
      DO 4  I=1,NUCLEI
      A(I,3)=(P*A(I,1)**2+Q*A(I,2)**2)/(P+Q)
      TERM2(I)=(A(I,1)**2/A(I,3)+1.)*A(I,2)**2*G(3)/(4.*FREQ)
      TERM3(I)=R*A(I,3)*C*S*G(3)/FREQ*((A(I,1)**2-A(I,2)**2)/A(I,3))**2
      TERM4(I)=2.*QUAD(I)*C*S/A(I,3)*(A(I,1)*A(I,2)*R/A(I,3))**2
      A(I,3)=SQRT(A(I,3))
```

```
4 TERM5(I)=QUAD(I)*S**2/(2.*A(I,3))*(A(I,2)*G(2)/(A(I,3)*(P+Q)))**2
5 DELTAH=A(INDEX,3)*SZ(INDEX)+TERM2(INDEX)*(SPIN(INDEX)*(SPIN(INDEX)
 *+1.)-SZ(INDEX)**2)+TERM3(INDEX)*SZ(INDEX)**2-TERM4(INDEX)*SZ(INDEX
 1)*(4.*SPIN(INDEX)*(SPIN(INDEX)+1.)-8.*SZ(INDEX)**2-1.)+TERM5(INDEX
 2)*SZ(INDEX)*(2.*SPIN(INDEX)*(SPIN(INDEX)+1.)-2.*SZ(INDEX)**2-1.)
6 RETURN
  END
```

```
C      NEONUC (SUBROUTINE FOR HRES-I)
       SUBROUTINE NEONUC(N,S,NDEGEN,LENGTH)
       DIMENSION NDEGEN(72),NSTOR(72),NSPIN(8)
       JSTOP=IFIX(2.*S+1.1)
       DATA NSTOR/72*0/,NSPIN/8*0/
       LENGTH=JSTOP
       DO 1 I=1,JSTOP
       NSPIN(I)=1
       NDEGEN(I)=1
     1 NSTOR(I)=0
       M=JSTOP+1
       DO 2 I=M,72
       NDEGEN(I)=0
     2 NSTOR(I)=0
       M=1
     3 IF(N-M)99,10,4
     4 DO 6 I=1,64
       IF(NDEGEN(I))99,11,5
     5 DO 6 J=1,JSTOP
       K=I+J-1
     6 NSTOR(K)=NSTOR(K)+NDEGEN(I)
       LENGTH=71
    10 RETURN
    11 LENGTH=JSTOP+I-2
       DO 12 I=1,LENGTH
       NDEGEN(I)=NSTOR(I)
    12 NSTOR(I)=0
       M=M+1
       GO TO 3
```

```
  99 WRITE (6,2000)
2000 FORMAT('0',' ILLOGICAL INSTRUCTION ENCOUNTERED IN SUBROUTINE NEQNU
    *C      ')
     STOP
     END
```

```
C     SHAPE  (DERIVATIVE OF LORENTZIAN)      (SUBROUTINE)
      SUBROUTINE SHAPE (RESLIN)
      DIMENSION RESLIN(1000),DATA(100),MDATA(100)
      COMMON DATA
      COMMON/C/IDUMME
      EQUIVALENCE (DATA(1),MDATA(1))
      MDATA(80)=-1
      DH=DATA(74)
      IF(IDUMME.EQ.1)GO TO 11
   10 READ (5,1001)WIDTH,ABUND
 1001 FORMAT(30X,2F10.5)
   11 IF(ABUND)1,3,1
    3 ABUND=1.0
    1 DX=DH/WIDTH
      ABUND=2.*ABUND/3.1415927
      X=0.
      K=1000
      RESLIN(1)=0.0
      DO 4 I=1,999
      RESLIN(K)=ABUND*X/(1.+X*X)**2
      K=K-1
    4 X=X+DX
      WRITE(6,2001)WIDTH
 2001 FORMAT('0',10X,'A LORENTZIAN LINESHAPE WITH A HALFWIDTH OF ',F6.3,
     *' GAUSS IS ASSUMED.          ')
      RETURN
      END
```

```
C      RED (UP TO FIFTH ORDER POLYNOMIAL)            (FUNCTION)
       FUNCTION RED(/THETA/,/PHI/)
       DIMENSION DATA(93),A(5)
       COMMON DATA,A0,A,VALUE
       COMMON/C/IDUMME
       IF(THETA)9,3,6
     3 PHI=-9.99
       IF(IDUMME.EQ.1)GO TO 11
    10 READ(5,1001)A0,(A(I),I=1,5),ISTOP
       IDUMME=1
    11 WRITE (6,2001)A0,A(1),(A(I),I,I=2,ISTOP)
       VALUE=A0
       RED=0.
       GO TO 9
     6 SUM=0.
       K=5
       DO 7 I=1,5
       SUM=THETA*(SUM+A(K))
     7 K=K-1
       VALUE=SUM+A0
       IF(VALUE)91,8,8
     8 PHI=SIN(THETA)
       RED=10.*PHI*VALUE
     9 RETURN
    91 WRITE (6,2002)THETA
    99 STOP
  1001 FORMAT(6F10.5,10XI2)
  2001 FORMAT('0',5X,'P(THETA) = ',F8.4,' + ',F8.4,'*THETA + ',(F8.4,'*TH
      *ETA**',I1,' + '))
```

```
2002 FORMAT('0',5X,'FUNCTION RED GOES NEGATIVE AT THETA = ',F8.5)
     END
```

```
C     GOFX (UP TO FIFTH ORDER POLYNOMIAL)          (FUNCTION)
       FUNCTION GOFX(X)
      DIMENSION DATA(53),A(5)
      COMMON DATA,A0,A
      COMMON/B/PHI
      PRMTR=ARCOS(X)
      SUM=0.
      K=5
      DO 2 I=1,5
      SUM=PRMTR*(SUM+A(K))
    2 K=K-1
      SUM=SUM+A0
      XX=SQRT(ABS(PHI**2-X**2))
      IF(XX)10,10,11
   10 GOFX=0.0
      WRITE(6,12)PHI,X
   12 FORMAT(2E20.10)
      RETURN
   11 GOFX=SUM/XX
      RETURN
      END
```

```
C     OUTPUT-V  (SPECTRUM,INTEGRAL,AND THETA VS. H)
      SUBROUTINE OUTPUT(X,Y,Z)
       DIMENSION X(1200),Y(5000),Z(5000),XINT(100),G(1200),XP(1200),
     1YP(1200),DATA(100),MDATA(100),ZP(1200), TITLF(12)
      REAL * 8 B
       COMMON DATA
      WRITE(6,4004) (DATA(IPX),IPX=13,100)
4004  FORMAT(' S= ', E13.4, '   G= ',3E13.4, '   D= ', E13.4, '  E=  ',
     *  E13.4,/,' NPOP=  ',10I10,/,' SPIN=  ',10E12.3,/,' A=  ',
     *  3(10E12.3/),' FREQ, SMIN, DTHETA, HMIN, HMAX, DH, NUCLEI, ISTOP
     *, LINES, IFTAPE'/,6E12.3,4I10/,' JUNK= ',10E12.3,/,5X,10E12.3,/,
     *5X, 10E12.3)
      EQUIVALENCE(DATA(1),MDATA(1))
      DO 772 I=1,1200
  772 G(I)=0.
      DO 773 I=1,100
  773 XINT(I)=0.
      CALL SETTIM
      A=TIME(2)
      CALL PLSTRT(0562,10)
      A=TIME(2)
      WRITE(6,9009)A
 9009 FORMAT(' THE TIME IT TOOK THE OPERATOR TO MOUNT A CALCOMP TAPE WAS
     $  ',F8.3,'  SECONDS')
      CALL PLOT(5.,5.,-3)
    1 READ(5,1001)            JBNC,NPRINT,IFPLOT,INT,GPI
      YDIM=8.
      XDIM=10.
      ORIGIN=XDIM+4
      IF(IFPLOT)29,2,2
    2 ZTEST=0.
      NDATA=MDATA(76)
      NSTEP=0
    3 NSTEP=NSTEP+1
      NDX=IFIX(100.*XDIM    )
      NTEST=NDATA/NSTEP
      IF(NTEST-NDX)4,3,3
    4 DX=XDIM/FLOAT(NTEST)
      YINT=0.
      ZINT=0.
      K=1
      DO 15 I=1,NDATA,NSTEP
      JSTOP=I+NSTEP-1
      DO 14 J=I,JSTOP
      YINT=YINT+Y(J)
   14 ZINT=ZINT+Z(J)
      X(K)=YINT
      G(K)=ZINT
      Y(K)=Y(I)
      Z(K)=Z(I)
   15 K=K+1
      NPOINT=K-1
      TEST1=Y(1)
      TEST2=Z(1)
      TEST3=X(1)
      TEST4=G(1)
      DO 12 I=2,NPOINT
      IF (TEST1-Y(I))6,6,5
    5 TEST1=Y(I)
    6 IF(TEST2-Z(I))8,8,7
    7 TEST2=Z(I)
    8 IF(TEST3-X(I))10,10,9
    9 TEST3=X(I)
   10 IF(TEST4-G(I))12,12,11
   11 TEST4=G(I)
   12 CONTINUE
      DO 13 I=1,NPOINT
      Y(I)=Y(I)-TEST1
      Z(I)=Z(I)-TEST2
      X(I)=X(I)-TEST3
   13 G(I)=G(I)-TEST4
      COUNT=0.
      ISTOP=NPOINT*2
      ISTART=NPOINT+1
      K=1
      DO 16 I=ISTART,ISTOP
      Y(I)=X(K)
      X(K)=COUNT
      Z(I)=G(K)
      G(K)=0.
      COUNT=COUNT+DX
      ZTEST=ZTEST+Z(K)
   16 K=K+1
      WRITE(6,2000) (DATA(I),I=1,12)
      INDEX=12
      DO 17 I=1,6
      SWAP=DATA(I)
      DATA(I)=DATA(INDEX)
      DATA(INDEX)=SWAP
   17 INDEX=INDEX-1
      MSTEP=0
      IF(NPRINT)21,21,18
   18 MSTEP=MSTEP+1
      MTEST=NPOINT/MSTEP
      IF(MTEST-NPRINT)19,19,18
19    DH=DATA(74)*FLOAT(MSTEP*NSTEP)
      WRITE(6,2001)
      H=DATA(72)
      WRITE(6,5001)NPOINT,MSTEP,NPRINT,MTEST
 5001 FORMAT('0',5X,'DEBUG TEST NPOINT = ',I5,5X,'MSTEP =',I5,5X,'NPRINT
     * = ',I5,'MTEST = ',I5)
      DO 20 I=1,NPOINT,MSTEP
      INDEX=NPOINT+I
      WRITE(6,2002)I,H,Y(I),Y(INDEX),Z(I),Z(INDEX)
   20 H=H+DH
   21 K=1
      CALL SCALAR(X,1,NPOINT,10.,XMAX,XMIN)
      CALL SCALAR(Y,1,  NPOINT,5.0,YMAX,YMIN)
      XMAX=DATA(73)
      XMIN=DATA(72)
      GNIN=(XMAX-XMIN)/GPI
      DO 2020 IIII=1,NPOINT
 2020 X(IIII)=X(IIII)*GNIN/10.
      CALL PLOT(0., 5.,-3)
   22 CALL LINE1(X(1),Y(K),NPOINT)
      IF(INT)5543,5543,5542
```

```
5542 CALL PLOT(0.,-5.,-3)
5543 CALL AXIS2(0.,0.,GNIN,0.,GNIN/10.)
     CALL AXIS3(GNIN,0.,10.,90.,100.,0.)
     CALL AXIS3(GNIN,10.,GNIN,180.,100.,0.)
     CALL AXIS2(0.,10.,10.,270.,1.)
     XIN =(XMAX-XMIN)/5.
     YINT=(YMAX-YMIN)/5.
     XX=-.25
     PX=XMIN
     DO 557 I=1,6
     INTEG=PX
     CALL ZBCDIN(J,INTEG)
     CALL CPRINT(J,4,XX,-.5,.1,0.)
     PX=PX+XIN
 557 XX=XX+GNIN/5.
     PY=YMIN
     YY=-.05
     DO 668 I=1,6
     CALL $$$FIX(PY,B,4,8,4)
     CALL CPRINT(B,8,-.85,YY,.1,0.)
     PY=PY+YINT
 668 YY=YY+2.
     CALL CPRINT('MAGNETIC FIELD',14,2.0,-.85,.15,0.)
     CALL CPRINT(DATA(1 ),32,-1.,2.,.15,90.)
     CALL PLOT(GNIN+10.,0.,-3)
     IF(INT)24,24,23
  23 K=NPOINT+1
     INT=-INT
     CALL SCALAR(Y,K,2*NPOINT,10.,YMAX,YMIN)
```

```
      GO TO 22
   24 IF(ZTEST)28,28,25
   25 CALL SCALAR(Z,1,  NPOINT,10.,YMAX,YMIN)
      K=1
   26 CONTINUE
      CALL LINE1(X(1),Z(K),NPOINT)
      CALL AXIS2(0.,0.,GNIN,0.,GNIN/10.)
      CALL AXIS3(GNIN,0.,10.,90.,100.,0.)
      CALL AXIS3(GNIN,10.,GNIN,180.,100.,0.)
      CALL AXIS2(0.,10.,10.,270.,1.)
      XIN =(XMAX-XMIN)/5.
      YINT=(YMAX-YMIN)/5.
      XX=-.25
      PX=XMIN
      DO 556 I=1,6
      INTEG=PX
      CALL ZBCDIN(J,INTEG)
      CALL CPRINT(J,4,XX,-.5,.1,0.)
      PX=PX+XIN
  556 XX=XX+GNIN/5.
      PY=YMIN
      YY=-.05
      DO 667 I=1,6
      CALL $$$FIX(PY,B,4,8,4)
      CALL CPRINT(B,8,-.85,YY,.1,0.)
      PY=PY+YINT
  667 YY=YY+2.
      CALL CPRINT('MAGNETIC FIELD',14,2.,-.85,.15,0.)
      CALL CPRINT('GREEN ORIENTATION',17,-1.,2.,.15,90.)
      CALL PLOT(GNIN+10.,0.,-3)
      IF(INT) 27,28,28
   27 INT=-INT
      K=NPOINT+1
      CALL SCALAR(Z,K,2*NPOINT,10.,YMAX,YMIN)
      GO TO 26
   28 IF(IFPLOT)29,40,29
   29 X(1)=0.
      IFPLOT=IABS(IFPLOT)
      REWIND 9
   33 READ(9)(TITLE(I),I=1,12)
      WRITE(6,2000)(TITLE(I),I=1,12)
      READ(9)NREC
      READ(9)LINES
      WRITE(6,2011)NREC,LINES
      READ(9)(XINT(I),I=1,LINES)
      THETA=0.
      DX=8.0/FLOAT(NREC)
      WRITE(6,2003)(I,I=1,LINES)
      MATRIX=NREC*LINES
      DY=XDIM/(DATA(73)-DATA(72))
      DO 30 I=1,NREC
      READ(9)(Y(J),J=I,MATRIX,NREC)
      WRITE(6,2004)THETA,(Y(J),J=I,MATRIX,NREC)
      DO 31 J=I,MATRIX,NREC
   31 Y(J)=DY*(Y(J)-DATA(72))
      THETA=THETA+DATA(71)
   30 X(I+1)=X(I)+DX
      ISTART=1
      CALL SCALAR(X,1,NREC,10.,YMAX,YMIN)
      CALL SCALAR(Y,1,MATRIX,10.,XMAX,XMIN)
   32 CONTINUE
      CALL LINE1(Y(ISTART),X(1),NREC)
      ISTART=ISTART+NREC
      IF(ISTART-MATRIX)32,34,34
   34 CONTINUE
      CALL AXIS2(0.,0.,10.,0.,1.)
      CALL AXIS3(10.,0.,10.,90.,100.,0.)
      CALL AXIS3(10.,10.,10.,180.,100.,0.)
      CALL AXIS2(0.,10.,10.,270.,1.)
      XIN =(XMAX-XMIN)/5.
      YINT=(YMAX-YMIN)/5.
      XX=-.25
      PX=XMIN
      DO 555 I=1,6
      INTEG=PX*100.
      CALL ZBCDIN(J,INTEG)
      CALL CPRINT(J,4,XX,-.5,.1,0.)
      PX=PX+XIN
  555 XX=XX+2.
      PY=YMIN
      YY=-.05
      DO 666 I=1,6
      PP=PY*.1
      CALL $$$FIX(PP,8,4,8,4)
      CALL CPRINT(8,8,-.85,YY,.1,0.)
      PY=PY+YINT
  665 YY=YY+2.
```

```
      CALL CPRINT('RESONANT FIELD',14,1.,-.85,.15,0.)
      CALL CPRINT('ANGLE (RADIANS)',15,-1.,2.,.15,90.)
      CALL PLOT(15.,0.,-3)
      READ(9)NPOINT
      IF(NPOINT+999)40,35,40
   35 IFPLOT=IFPLOT-1
      IF(IFPLOT)40,40,36
   36 CONTINUE
      GO TO 33
 1001 FORMAT(4I5,F10.0)
 2000 FORMAT('1',10X,12A4)
 2001 FORMAT('0'/34X,'RED SPECTRUM',27X,'GREEN SPECTRUM',/,3X,'POINT',4
     *X,'FIELD',9X,'SPECTRUM',12X,'SPECTRUM',12X,'INTEGRAL',/)
 2002 FORMAT(2XI4,6XF6.1,4(7XF11.4))
 2011 FORMAT('0',5X,I4,'RECORDS OF',I4,' WORDS CONTAIN RESONANCE LINE PO
     *SITIONS.      ')
 9853 FORMAT(1H ,10X,'CHECK PT.')
 2003 FORMAT('0',10X,'RESONANT FIELD VS ANGLE',//,4X,'THETA',3X,10(2X,'L
     *INE(',I2,')  '))
 2004 FORMAT(3XF6.4,3X10(3XF6.1,3X))
   40 CALL PLTEND
      RETURN
      END
```

```
  SUBROUTINE SCALAR(X,I,N,Y,XMAX,XMIN)
  DIMENSION X(1)
  Z=X(I)
  ZZ=X(I)
  ZZZ=X(I)
   L=N-1
   DO1 K=I,L
  ZZ=AMIN1(X(K+1),ZZ)
  ZZZ=AMAX1(X(K+1),ZZZ)
  A=ABS(X(K+1))
  B=ABS(Z)
1 Z=AMAX1(A,B)
  A=Y/Z
  DO2K=I,N
2 X(K)=X(K)*A
  XMIN=ZZ
  XMAX=ZZZ
  RETURN
  END
```

APPENDIX B

MATRIX ELEMENTS FOR THE SPIN HAMILTONIAN OF Cl_2^-

The spin Hamiltonian for a linear molecule was shown to be (Eq. (16))

$$\mathcal{H} = g\beta_0 H S_z + K S_z I_z + Y(S_+ + S_-)I_z + X^-(S_+I_+ + S_-I_-) + X^+(S_+I_- + S_-I_+)$$

where

$$X^{\pm} = \frac{A_{\parallel}A_{\perp}}{4} \pm \frac{A_{\perp}}{4} \quad \text{and} \quad Y = \frac{A_{\perp}^2 - A_{\parallel}^2}{2K}\,\frac{g_{\parallel}g_{\perp}}{g}\cos\theta\sin\theta .$$

Let the eigenvectors be of the type $|S,M\rangle|I,m\rangle$ so they can be written

$|1\rangle = |1/2,1/2\rangle\,|3,3\rangle$
$|2\rangle = |1/2,-1/2\rangle\,|3,3\rangle$
$|3\rangle = |1/2,1/2\rangle\,|3,2\rangle$
$|4\rangle = |1/2,1/2\rangle\,|2,2\rangle$
$|5\rangle = |1/2,1/2\rangle\,|3,1\rangle$
$|6\rangle = |1/2,-1/2\rangle\,|2,2\rangle$
$|7\rangle = |1/2,-1/2\rangle\,|3,2\rangle$
$|8\rangle = |1/2,1/2\rangle\,|2,1\rangle$
$|9\rangle = |1/2,1/2\rangle\,|1,1\rangle$
$|10\rangle = |1/2,1/2\rangle\,|3,0\rangle$
$|11\rangle = |1/2,1/2\rangle\,|2,0\rangle$
$|12\rangle = |1/2,1/2\rangle\,|1,0\rangle$
$|13\rangle = |1/2,1/2\rangle\,|0,0\rangle$
$|14\rangle = |1/2,-1/2\rangle\,|1,1\rangle$
$|15\rangle = |1/2,-1/2\rangle\,|2,1\rangle$
$|16\rangle = |1/2,-1/2\,|3,1$
$|17\rangle = |1/2,-1/2\rangle\,|3,0\rangle$
$|18\rangle = |1/2,-1/2\rangle\,|2,0\rangle$
$|19\rangle = |1/2,-1/2\rangle\,|1,0\rangle$
$|20\rangle = |1/2,-1/2\rangle\,|0,0\rangle$
$|21\rangle = |1/2,1/2\rangle\,|1,-1\rangle$
$|22\rangle = |1/2,1/2\rangle\,|2,-1\rangle$
$|23\rangle = |1/2,1/2\rangle\,|3,-1\rangle$
$|24\rangle = |1/2,1/2\rangle\,|3,-2\rangle$
$|25\rangle = |1/2,1/2\rangle\,|2,-2\rangle$
$|26\rangle = |1/2,-1/2\rangle\,|3,-1\rangle$
$|27\rangle = |1/2,-1/2\rangle\,|2,-1\rangle$
$|28\rangle = |1/2,-1/2\rangle\,|1,-1\rangle$
$|29\rangle = |1/2,1/2\rangle\,|3,-3\rangle$
$|30\rangle = |1/2,-1/2\rangle\,|3,-2\rangle$
$|31\rangle = |1/2,-1/2\rangle\,|2,-2\rangle$
$|32\rangle = |1/2,-1/2\,|3,-3$

The only nonvanishing matrix elements for the spin Hamiltonian are

$$\langle M|S_z|M\rangle = M, \quad \langle m|I_z|m\rangle = m$$

$$\langle M\pm 1,m|S_{\pm}I_z|M,m\rangle = m[S(S+1)-M(M\pm 1)]^{\frac{1}{2}}$$

$$\langle M\pm 1,m\pm 1|S_{\pm}I_{\pm}|M,m\rangle = [S(S+1)-M(M\pm 1)]^{\frac{1}{2}}[I(I+1)-m(m\pm 1)]^{\frac{1}{2}}$$

$$\langle M\pm 1,m\mp 1|S_{\pm}I_{\mp}|M,m\rangle = [S(S+1)-M(M_{\pm}1)]^{\frac{1}{2}}[I(I+1)-m(m\mp 1)]^{\frac{1}{2}} .$$

Therefore, for the operator $A = g\beta_o HS_z + KS_zI_z$ we obtain (if $F = \frac{1}{2}g\beta_o H$),

$\langle 1|A|1\rangle = F + (3/2)K$

$\langle 2|A|2\rangle = -F + K$

$\langle 3|A|3\rangle = F + K$

$\langle 4|A|4\rangle = F + K$

$\langle 5|A|5\rangle = F + (1/2)K$

$\langle 6|A|6\rangle = -F - K$

$\langle 7|A|7\rangle = -F - K$

$\langle 8|A|8\rangle = F + (1/2)K$

$\langle 9|A|9\rangle = F + (1/2)K$

$\langle 10|A|10\rangle = F$

$\langle 11|A|11\rangle = F$

$\langle 12|A|12\rangle = F$

$\langle 13|A|13\rangle = F$

$\langle 14|A|14\rangle = -F - (1/2)K$

$\langle 15|A|15\rangle = -F - (1/2)K$

$\langle 16|A|16\rangle = -F - (1/2)K$

$\langle 17|A|17\rangle = -F$

$\langle 18|A|18\rangle = -F$

$\langle 19|A|19\rangle = -F$

$\langle 20|A|20\rangle = -F$

$\langle 21|A|21\rangle = F - (1/2)K$

$\langle 22|A|22\rangle = F - (1/2)K$

$\langle 23|A|23\rangle = F - (1/2)K$

$\langle 24|A|24\rangle = F - K$

$\langle 25|A|25\rangle = F - K$

$\langle 26|A|26\rangle = -F + K$

$\langle 27|A|27\rangle = -F + K$

$\langle 28|A|28\rangle = -F + K$

$\langle 29|A|29\rangle = F - (3/2)K$

$\langle 30|A|30\rangle = -F + K$

$\langle 31|A|31\rangle = -F + K$

$\langle 32|A|32\rangle = -F + (3/2)K$

For the operator $B_\pm = S_\pm I_z$, we obtain

$\langle 1|B_+|2\rangle = 3$

$\langle 2|B_-|1\rangle = 3$

$\langle 4|B_+|6\rangle = 2$

$\langle 6|B_-|4\rangle = 2$

$\langle 3|B_+|7\rangle = 2$

$\langle 7|B_-|3\rangle = 2$

$\langle 9|B_+|14\rangle = 1$

$\langle 14|B_-|9\rangle = 1$

$\langle 8|B_+|15\rangle = 1$

$\langle 15|B_-|8\rangle = 1$

$\langle 5|B_+|16\rangle = 1$

$\langle 16|B_-|5\rangle = 1$

$\langle 23|B_+|26\rangle = -1$

$\langle 26|B_-|23\rangle = -1$

$\langle 22|B_+|27\rangle = -1$

$\langle 27|B_-|22\rangle = -1$

$\langle 21|B_+|28\rangle = -1$

$\langle 28|B_-|21\rangle = -1$

$\langle 24|B_+|30\rangle = -2$

$\langle 30|B_-|24\rangle = -2$

$\langle 25|B_+|31\rangle = -2$

$\langle 31|B_-|25\rangle = -2$

$\langle 29|B_+|32\rangle = -3$

$\langle 32|B_-|29\rangle = -3$

For the operator $C_\pm = S_\pm I_\pm$, we obtain

$\langle 1|C_+|7\rangle = \sqrt{6}$

$\langle 7|C_-|1\rangle = \sqrt{6}$

$\langle 4|C_+|15\rangle = 2$

$\langle 15|C_-|4\rangle = 2$

$\langle 3|C_+|16\rangle = \sqrt{10}$

$\langle 16|C_-|3\rangle = \sqrt{10}$

$\langle 5|C_+|17\rangle = \sqrt{12}$

$\langle 17|C_-|5\rangle = \sqrt{12}$

$\langle 8|C_+|18\rangle = \sqrt{6}$

$\langle 18|C_-|8\rangle = \sqrt{6}$

$\langle 9|C_+|19\rangle = \sqrt{2}$

$\langle 19|C_-|9\rangle = \sqrt{2}$

$\langle 10|C_+|26\rangle = \sqrt{12}$

$\langle 26|C_-|10\rangle = \sqrt{12}$

$\langle 11|C_+|27\rangle = \sqrt{6}$

$\langle 27|C_-|11\rangle = \sqrt{6}$

$\langle 12|C_+|28\rangle = \sqrt{2}$

$\langle 28|C_-|12\rangle = \sqrt{2}$

$\langle 23|C_+|30\rangle = \sqrt{10}$

$\langle 30|C_-|23\rangle = \sqrt{10}$

$\langle 22|C_+|31\rangle = 2$

$\langle 31|C_-|22\rangle = 2$

For the operator $D_{\pm} = S_{\pm} I_{\mp}$, we obtain

$$\langle 3|D_+|2\rangle = \sqrt{6}$$

$$\langle 2|D_-|3\rangle = \sqrt{6}$$

$$\langle 5|D_+|7\rangle = \sqrt{10}$$

$$\langle 7|D_-|5\rangle = \sqrt{10}$$

$$\langle 12|D_+|14\rangle = \sqrt{2}$$

$$\langle 14|D_-|12\rangle = \sqrt{2}$$

$$\langle 11|D_+|15\rangle = \sqrt{6}$$

$$\langle 15|D_-|11\rangle = \sqrt{6}$$

$$\langle 10|D_+|16\rangle = \sqrt{12}$$

$$\langle 16|D_-|10\rangle = \sqrt{12}$$

$$\langle 23|D_+|17\rangle = \sqrt{12}$$

$$\langle 17|D_-|23\rangle = \sqrt{12}$$

$$\langle 22|D_+|18\rangle = \sqrt{6}$$

$$\langle 18|D_-|22\rangle = \sqrt{6}$$

$$\langle 21|D_+|19\rangle = \sqrt{2}$$

$$\langle 19|D_-|21\rangle = \sqrt{2}$$

$$\langle 24|D_+|26\rangle = \sqrt{10}$$

$$\langle 26|D_-|24\rangle = \sqrt{10}$$

$$\langle 25|D_+|27\rangle = 2$$

$$\langle 27|D_-|25\rangle = 2$$

$$\langle 29|D_+|30\rangle = \sqrt{6}$$

$$\langle 30|D_-|29\rangle = \sqrt{6}$$

APPENDIX C

LEAST-SQUARES FIT FOR A LINEAR FUNCTION

```
      DIMENSION X(100),Y(100),Z(100)
      READ(5,5)N
      READ(5,10)(Y(I),X(I),Z(I),I=1,N)
    5 FORMAT(I5)
   10 FORMAT(3F15.8)
      CALL LINE(X,Y,N,B,A,PA,PB)
      DO 15 I=1,N
      X(I)=Z(I)
   15 CONTINUE
      CALL LINE(X,Y,N,B,A,PA,PB)
      STOP
      END
      SUBROUTINE LINE (X,Y,N,B,A,PA,PB)
C THIS SUBROUTINE CALCULATES LEAST SQUARES FITS FIRST USING Y AS THE DEPENDENT
C VARIABLE (FORM - Y = AX + B AND Y/A = X + B/A) AND THEN X AS THE DEPENDENT
C VARIABLE (FORM - X = CY + D AND X/C = Y + D/C).  PROBABLE ERRORS IN CALCULATED
C VALUES OF X AND Y AS WELL AS THE SLOPE AND INTERCEPT ARE CALCULATED (SEE
C MARGENAU AND MURPHY, MATHEMATICS OF PHYSICS AND CHEMISTRY, I, 519, VAN
C NOSTRAND AND CO.).  INTEGRAL POINTS ARE ALSO CALCULATED FOR EASE IN PLOTTING.
C ONLY THE VALUES OF A AND B, NOT C AND D, ARE USED IN THE MAIN PROGRAM.
C MAXIMUM NUMBER OF POINTS = 100
C     THIS SUBROUTINE WAS WRITTEN BY DR. N.H.F. BEEBE, QUANTUM THEORY
C     PROJECT UNIVERSITY OF FLORIDA, GAINESVILLE, FLA.
      DIMENSION X(100),Y(100),V(100),W(100),VCALC(100),YCALC(100),
     1PY(100),PX(100),YC(100),VC(100),XDIFSQ(100),WDIFSQ(100),AX(100),
     2AY(100),AW(100),AV(100),YY(100),XX(100),VV(100),WW(100)
      SUMX = 0.
      SUMY = 0.
      SUMXY = 0.
      SUMX2 = 0.
      SUMV = 0.
      SUMW = 0.
      SUMVW = 0.
      SUMW2 = 0.
      AN = N
      DO 1  I = 1,N
      V(I) = X(I)
      W(I) = Y(I)
      SUMX = SUMX + X(I)
      SUMY = SUMY + Y(I)
      SUMV = SUMV + V(I)
      SUMW  = SUMW + W(I)
      SUMXY = SUMXY + X(I)*Y(I)
      SUMVW = SUMVW + V(I)*W(I)
      SUMX2 = SUMX2 + X(I)**2
    1 SUMW2 = SUMW2 + W(I)**2
      A = (SUMXY-(SUMX*SUMY)/AN)/(SUMX2-(SUMX**2)/AN)
      B = (SUMX*SUMXY-SUMY*SUMX2)/(SUMX**2-AN*SUMX2)
      C = (SUMVW-(SUMV*SUMW)/AN)/(SUMW2-(SUMW**2)/AN)
      D = (SUMW*SUMVW-SUMV*SUMW2)/(SUMW**2-AN*SUMW2)
      AA = 1./A
      BB = B/A
      CC = 1./C
      DD = D/C
      YDIFSQ = 0.
      VDIFSQ = 0.
      XDIFSQ(1) = 0.
      WDIFSQ(1) = 0.
      DO 2  I = 1,N
      YCALC(I) = A*X(I) + B
      VCALC(I) = C*W(I) + D
      YC(I) = Y(I) - YCALC(I)
      VC(I) = V(I) - VCALC(I)
      YDIFSQ = YDIFSQ + YC(I)**2
    2 VDIFSQ = VDIFSQ + VC(I)**2
      RY = .6745*SQRT(YDIFSQ/(AN-2.))
      RV = .6745*SQRT(VDIFSQ/(AN-2.))
      DY = AN*SUMX2 - SUMX**2
      DV = AN*SUMW2 - SUMW**2
      EB = RY*SQRT(SUMX2/DY)
      PA = RY*SQRT(AN/DY)
      PC = RV*SQRT(AN/DV)
      PD = RV*SQRT(SUMW2/DV)
      DO 3  J = 1,N
      DO 3  I = 1,N
      XDIFSQ(J) = XDIFSQ(J) + (X(I)-X(J))**2
    3 WDIFSQ(J) = WDIFSQ(J) + (W(I)-W(J))**2
      DO 4  I = 1,N
      PY(I) = RY*SQRT(XDIFSQ(I)/DY)
    4 PX(I) = RV*SQRT(WDIFSQ(I)/DV)
      M = N/3
      DO 5  I = 1,N,M
      AX(I) = AINT(X(I))
      AY(I) = AINT(Y(I))
      AW(I) = AINT(W(I))
      AV(I) = AINT(V(I))
      YY(I) = A*AX(I) + B
      XX(I) = (AY(I) - B)/A
      VV(I) = C*AW(I) + D
    5 WW(I) = (AV(I) - D)/C
      WRITE (6,6)
      WRITE (6,7) (X(I),Y(I),VCALC(I),YCALC(I),VC(I),YC(I),PX(I),PY(I),
     1 I = 1,N)
      WRITE (6,8) (AX(I),YY(I), I = 1,N,M), (XX(I),AY(I),I = 1,N,M)
      WRITE (6,9) (AW(I),VV(I), I = 1,N,M),(WW(I),AV(I),I = 1,N,M)
      IF (B) 14,15,15
   14 IF (A) 16,17,17
   16 B = ABS(B)
      WRITE (6,20) A,B,AA,BB,PA,PB
      GO TO 18                                                          LINE078
   17 B = ABS(B)                                                        LINE079
      BB = ABS(BB)                                                      LINE080
      WRITE (6,11) A,B,AA,BB,PA,PB                                      LINE081
      GO TO 18                                                          LINE082
   15 IF (A) 21,22,22                                                   LINE083
   21 BB = ABS(BB)                                                      LINE084
      WRITE (6,23) A,B,AA,BB,PA,PB                                      LINE085
      GO TO 18                                                          LINE086
   22 WRITE (6,10) A,B,AA,BB,PA,PB                                      LINE087
   18 IF (D) 24,25,25                                                   LINE088
   24 IF (C) 26,27,27                                                   LINE089
   26 D = ABS(D)                                                        LINE090
      WRITE (6,31) C,D,CC,DD,PC,PD                                      LINE091
      GO TO 19                                                          LINE092
   27 D = ABS(D)                                                        LINE093
      DD = ABS(DD)                                                      LINE094
      WRITE (6,13) C,D,CC,DD,PC,PD                                      LINE095
      GO TO 19                                                          LINE096
   25 IF (C) 28,29,29                                                   LINE097
   28 DD = ABS(DD)                                                      LINE098
      WRITE (6,30) C,D,CC,DD,PC,PD                                      LINE099
      GO TO 19                                                          LINE100
   29 WRITE (6,12) C,D,CC,DD,PC,PD                                      LINE101
    6 FORMAT (1H0/7X,1HX,14X,1HY,8X,12HCALCULATED X,15H    CALCULATED Y, LINE102
     14X,9HX - XCALC,6X,9HY - YCALC,18H    PROBABLE ERROR,15H PROBABLE E LINE103
     2RROR/96X,4HIN X,11X,4HIN Y/)                                      LINE104
    7 FORMAT (1H ,1PE12.4,7E15.4)                                       LINE105
    8 FORMAT (1H ,1PE12.4,C45.4)                                        LINE106
```

```
 9 FORMAT (1H ,1PE27.4,E15.4)
10 FORMAT (1H0,3HY =,1PE11.4,4H X +,E11.4,E14.4,8H Y = X +,E11.4,16H
 1    ERROR IN A =,E11.4,16H    ERROR IN B =,E11.4)
11 FORMAT (1H0,3HY =,1PE11.4,4H X -,E11.4,E14.4,8H Y = X -,E11.4,16H
 1    ERROR IN A =,E11.4,16H    ERROR IN B =,E11.4)
12 FORMAT (1H0,3HX =,1PE11.4,4H Y +,E11.4,E14.4,8H X = Y +,E11.4,16H
 1    ERROR IN C =,E11.4,16H    ERROR IN D =,E11.4)
13 FORMAT (1H0,3HX =,1PE11.4,4H Y -,E11.4,E14.4,8H X = Y -,E11.4,16H
 1    ERROR IN C =,E11.4,16H    ERROR IN D =,E11.4)
20 FORMAT (1H0,3HY =,1PE11.4,4H X -,E11.4,E14.4,8H Y = X +,E11.4,16H
 1    ERROR IN A =,E11.4,16H    ERROR IN B =,E11.4)
23 FORMAT (1H0,3HY =,1PE11.4,4H X +,E11.4,E14.4,8H Y = X -,E11.4,16H
 1    ERROR IN A =,E11.4,16H    ERROR IN B =,E11.4)
31 FORMAT (1H0,3HX =,1PE11.4,4H Y -,E11.4,E14.4,8H X = Y +,E11.4,16H
 1    ERROR IN C =,E11.4,16H    ERROR IN D =,E11.4)
30 FORMAT (1H0,3HX =,1PE11.4,4H Y +,E11.4,E14.4,8H X = Y -,E11.4,16H
 1    ERROR IN C =,E11.4,16H    ERROR IN D =,E11.4)
19 RETURN
   END
```

APPENDIX D

MATRIX ELEMENTS AND PROGRAM FOR BENT F_2^- NON-COLLINEAR A- AND g-TENSORS

When the A- and g-tensors are not collinear, the nuclei must be treated separately and, therefore, the basis vectors used were of the type $|S,M\rangle$, $|I_1,m_1\rangle$, $|I_2,m_2\rangle$, where the variables have their customary meaning. For the case of interest they are

$$|1\rangle = |1/2,1/2\rangle\,|1/2,1/2\rangle\,|1/2,1/2\rangle$$
$$|2\rangle = |1/2,1/2\rangle\,|1/2,1/2\rangle\,|1/2,-1/2\rangle$$
$$|3\rangle = |1/2,1/2\rangle\,|1/2,-1/2\rangle\,|1/2,1/2\rangle$$
$$|4\rangle = |1/2,-1/2\rangle\,|1/2,-1/2\rangle\,|1/2,-1/2\rangle$$
$$|5\rangle = |1/2,-1/2\rangle\,|1/2,1/2\rangle\,|1/2,-1/2\rangle$$
$$|6\rangle = |1/2,-1/2\rangle\,|1/2,-1/2\rangle\,|1/2,1/2\rangle$$
$$|7\rangle = |1/2,1/2\rangle\,|1/2,-1/2\rangle\,|1/2,-1/2\rangle$$
$$|8\rangle = |1/2,-1/2\rangle\,|1/2,1/2\rangle\,|1/2,1/2\rangle$$

For the operator $O = g\beta_o HS_z + KS_zI_z$ we obtain, if $F = \frac{1}{2}g\beta_o H$, $S_z = S_z^1 + S_z^2$, and $I_z = I_z^1 + I_z^2$

$$\langle 1|O|1\rangle = F + (1/4)(K_1+K_2)$$
$$\langle 2|O|2\rangle = F + (1/4)(K_1-K_2)$$
$$\langle 3|O|3\rangle = F - (1/4)(K_1-K_2)$$
$$\langle 4|O|4\rangle = -F - (1/4)(K_1+K_2)$$
$$\langle 5|O|5\rangle = -F + (1/4)(K_1-K_2)$$
$$\langle 6|O|6\rangle = -F - (1/4)(K_1-K_2)$$
$$\langle 7|O|7\rangle = F - (1/4)(K_1+K_2)$$
$$\langle 8|O|8\rangle = -F + (1/4)(K_1+K_2)$$

For the operator $\frac{A}{4}(S_+I_+ + S_-I_-) = P$, where $I_\pm = I_\pm^1 + I_\pm^2$, we obtain

$\langle 1|P|5\rangle = (1/4)A_1$

$\langle 5|P|1\rangle = (1/4)A_1$

$\langle 1|P|6\rangle = (1/4)A_2$

$\langle 6|P|1\rangle = (1/4)A_2$

$\langle 2|P|8\rangle = (1/4)A_1$

$\langle 8|P|2\rangle = (1/4)A_1$

$\langle 3|P|8\rangle = (1/4)A_2$

$\langle 8|P|3\rangle = (1/4)A_2$

For the operator $\frac{B}{4}(I_+S_- + I_-S_+) = Q$, where $I_\pm = I_\pm^1 + I_\pm^2$, we obtain

$\langle 2|Q|4\rangle = (1/4)B_2$

$\langle 4|Q|2\rangle = (1/4)B_2$

$\langle 3|Q|4\rangle = (1/4)B_1$

$\langle 4|Q|3\rangle = (1/4)B_1$

$\langle 5|Q|7\rangle = (1/4)B_2$

$\langle 7|Q|5\rangle = (1/4)B_2$

$\langle 6|Q|7\rangle = (1/4)B_1$

$\langle 7|Q|6\rangle = (1/4)B_1$

For the operator $\frac{C}{2}(I_z S_+ + I_z S_-) = R$, where $I_z = I_z^1 + I_z^2$, we obtain

$$\langle 1|R|4\rangle = (1/4)(C_1+C_2)$$
$$\langle 4|R|1\rangle = (1/4)(C_1+C_2)$$
$$\langle 2|R|6\rangle = (1/4)(C_1-C_2)$$
$$\langle 6|R|2\rangle = (1/4)(C_1-C_2)$$
$$\langle 3|R|5\rangle = (1/4)(C_1-C_2)$$
$$\langle 5|R|3\rangle = (1/4)(C_1-C_2)$$
$$\langle 7|R|8\rangle = (1/4)(C_1+C_2)$$
$$\langle 8|R|7\rangle = (1/4)(C_1+C_2)$$

A, B, and D are defined by the following equations:

$$g^2 = (l_\alpha g_{\beta\alpha})^2$$
$$g^2K^2 = (l_\alpha g_{\beta\alpha} A_{\gamma\beta})^2$$
$$g^2K^2K_1' = (l_\alpha g_{\beta\alpha} A_{\gamma\delta} A_{\delta\beta})^2 - g^2K^2$$
$$+ K^2\{l_\alpha l_\beta g_{\gamma\alpha} g_{\delta\beta} A_{\varepsilon\gamma} X_{\varepsilon\delta} - g^2 A_{\alpha\beta} A_{\alpha\beta}\}$$
$$g^2K^2K_2' = -g^2K^4 + (l_\alpha g_{\beta\alpha} A_{\gamma\delta} A_{\delta\beta})^2$$
$$KK_3' = -\tfrac{1}{2}A_{\alpha\alpha}A_{\beta\gamma}A_{\beta\gamma} + (1/3)A_{\alpha\beta}A_{\gamma\alpha}A_{\beta\gamma} + (1/6)A_{\alpha\alpha}A_{\beta\beta}A_{\gamma\gamma}$$

where

$$g_{ij} = g_{ii}\delta_{ij}$$

$$A_{ij}X_{ik} = A_{ij}^2\delta_{ik}.$$

A_{ij} are the elements of the A-tensor, and l_{ij} are the direction cosines of the g-tensor with respect to the magnetic field; then

$$A^2 + B^2 = -2K_1', \quad B^2 - A^2 = 4K_3' \quad \text{and} \quad C^2 = K_2'.$$

The subscripts of A, B, C and K refer to nucleus 1 or 2.

BENT F_2^- SPIN HAMILTONIAN MATRIX

$$
\begin{array}{c|cccccccc}
 & |1\rangle & |2\rangle & |3\rangle & |4\rangle & |5\rangle & |6\rangle & |7\rangle & |8\rangle \\
\langle 1| & F+\frac{1}{4}(K_1+K_2) & 0 & 0 & \frac{1}{4}(C_1+C_2) & \frac{1}{4}A_1 & \frac{1}{4}A_2 & 0 & 0 \\
\langle 2| & 0 & F+\frac{1}{4}(K_1-K_2) & 0 & B_2 & 0 & \frac{1}{4}(C_1-C_2) & 0 & \frac{1}{4}A_1 \\
\langle 3| & 0 & 0 & F-\frac{1}{4}(K_1-K_2) & B_1 & -\frac{1}{4}(C_1-C_2) & 0 & 0 & \frac{1}{4}A_2 \\
\langle 4| & \frac{1}{4}(C_1+C_2) & \frac{1}{4}B_2 & \frac{1}{4}B_1 & -F-\frac{1}{4}(K_1+K_2) & 0 & 0 & 0 & 0 \\
\langle 5| & \frac{1}{4}A_1 & 0 & -\frac{1}{4}(C_1-C_2) & 0 & -F+\frac{1}{4}(K_1-K_2) & 0 & \frac{1}{4}B_2 & 0 \\
\langle 6| & \frac{1}{4}A_2 & \frac{1}{4}(C_1-C_2) & 0 & 0 & 0 & -F-\frac{1}{4}(K_1-K_2) & \frac{1}{4}B_1 & 0 \\
\langle 7| & 0 & 0 & 0 & 0 & \frac{1}{4}B_2 & \frac{1}{4}B_1 & F-\frac{1}{4}(K_1+K_2) & -\frac{1}{4}(C_1+C_2) \\
\langle 8| & 0 & \frac{1}{4}A_1 & \frac{1}{4}A_2 & 0 & 0 & 0 & \frac{1}{4}(C_1+C_2) & -F+\frac{1}{4}(K_1+K_2)
\end{array}
$$

```
C
C
C  PROGRAM TO CALCULATE THE EIGENVALUES OF THE F2- MATRIX ASSUMING
C NON-COLLINEARITY OF THE G AND THE A TENSORS
C
C
      IMPLICIT REAL*8 (A-H,O-Z)
      DIMENSION H(200),AI(5),AMAX(5),AM(20,5),CONST1(20,3),TITLE(20),AA(
     15),BB(5),CC(5),ELEM(50,50),EIG(50),VEC(50,50),DIFF(50)
      COMMON B(3,5),G(3,5),GSQ(5),GI(5),A(3,3,5),SQK(5),SK(5),ONE(5),TWO
     *K(5),X(3,3),THREEK(5),ALPHA(5),BETA(5),ATEN(3,5),THETA,PHI,N
      EXTERNAL SIN,COS,SQRT,ABS
    1 READ(5,3)(TITLE(I),I=1,20)
    3 FORMAT(20A4)
      READ(5,5)N,NP,IFIN,FREQ,HSTART,STEP
    5 FORMAT(3I5,3F10.5)
      READ(5,10)(AI(K),ALPHA(K),BETA(K),K=1,N)
   10 FORMAT(3F10.5)
      READ(5,15)((G(I,K),ATEN(I,K),I=1,3),K=1,N)
   15 FORMAT(6F10.5)
      ICOUNT=0
   76 WRITE(6,30)(TITLE(I),I=1,20)
   30 FORMAT(1H1,20A4,///)
      WRITE(6,110)((ATEN(I,K),I=1,3),K=1,N)
  110 FORMAT(10X,'AX= ',E20.10,'AY= ',E20.10,'AZ= ',E20.10,/)
      DO 13 K=1,N
   11 BETA(K)=BETA(K)*3.1416/180.0
   13 ALPHA(K)=ALPHA(K)*3.1416/180.0
      KFLAG=0
      IFLAG=0
      DO 200 ITHETA=1,IFIN
      READ(5,14)THETA,PHI
   14 FORMAT(2F10.5)
      PHII=PHI
      PHI=PHI*3.1416/180.0
      THETA=THETA*3.1416/180.0
      CALL CALCEL
      WRITE(6,41)
   41 FORMAT(//,10X,'TRANSFORMED A-TENSOR',//)
      WRITE(6,40) (((A(I,J,K),J=1,3),I=1,3),K=1,N)
   40 FORMAT(3(E20.10,10X,E20.10,10X,E20.10,/),//)
      WRITE(6,45)(ONE(K),TWOK(K),THREEK(K),SK(K),K=1,N)
   45 FORMAT(10X,'ONE =',E20.10,'TWOK= ',E20.10,'THREEK = ',E20.10,'SK =
     1',E20.10,/)
      DO 60 K=1,N
      AA(K)=SQRT(-2.0*THREEK(K)-ONE(K))
   62 BB(K)=SQRT(2.0*THREEK(K)-ONE(K))
      IF(TWOK(K).LT.0.0) TWOK(K)=0.0
      CC(K)=SQRT(TWOK(K))
   60 CONTINUE
      NN=8
      G0=2.00229
      DO 65 I=1,NN
      DO 65 J=1,NN
   65 ELEM(I,J)=0.0
      DELT=714.484*FREQ/2.00229
      WRITE(6,100) DELT
  100 FORMAT(10X,'DELT =',F20.10,//)
```

```
SKS=SK(1)+SK(2)
SKD=SK(1)-SK(2)
AAS=AA(1)+AA(2)
AAD=AA(1)-AA(2)
BBS=BB(1)+BB(2)
BBD=BB(1)-BB(2)
CCS=CC(1)+CC(2)
CCD=CC(1)-CC(2)
ELEM(1,4)=0.25*CCS
ELEM(1,5)=0.25*AA(1)
ELEM(1,6)=0.25*AA(2)
ELEM(2,4)=0.25*BB(2)
ELEM(2,6)=0.25*CCD
ELEM(2,8)=0.25*AA(1)
ELEM(3,4)=0.25*BB(1)
ELEM(3,5)= -0.25*CCD
ELEM(3,8)=0.25*AA(2)
ELEM(5,7)=0.25*BB(2)
ELEM(6,7)=0.25*BB(1)
ELEM(7,8)=-0.25*CCS
H(1)=HSTART
DO 50 ITEMP=1,NF
F=0.5*GI(1)*H(ITEMP)/GO
ELEM(1,1)=F+0.25*SKS
ELEM(2,2)=F+0.25*SKD
ELEM(3,3)=F-0.25*SKD
ELEM(4,4)=-F-0.25*SKS
ELEM(5,5)=-F+0.25*SKD
ELEM(6,6)=-F-0.25*SKD
```

```
      ELEM(7,7)=F-0.25*SKS
      ELEM(8,8)=-F+0.25*SKS
      DO 70 I=1,NN
      DO 70 J=1,NN
   70 ELEM(J,I)=ELEM(I,J)
      WRITE(6,46)((ELEM(I,J),J=1,NN),I=1,NN)
   46 FORMAT(//,3X,8E16.10,/)
      CALL EIGN(NN,ELEM,EIG,VEC,IND)
      K=0
      INN=NN-1
      DO 75 I=1,INN
      IM=I+1
      DO 75 J=IM,NN
      K=K+1
      DIFF(K)=EIG(I)-EIG(J)
      WRITE(6,80)I,J,DIFF(K)
   80 FORMAT(10X,'THE DIFFERENCE BETWEEN EIGRNVALUE',I3,'AND EIGENVALUE'
     1,I3,'  IS',E20.10)
   75 CONTINUE
      WRITE(6,85)H(ITEMP),GI(1),IND
   85 FORMAT(//,5X,'H = ',F16.10,5X,'G PERPENDICULAR = ',E16.10,5X,'IND
     1=',I5,//)
      WRITE(6,90)(EIG(I),I=1,NN)
   90 FORMAT(//,10X,'THE EIGENVALUES ARE',//,8(20X,E20.10,/))
      WRITE(6,95)((VEC(I,J),J=1,NN),I=1,NN)
   95 FORMAT(//,10X,'THE EIGENVECTORS ARE:',//,20X,8(20X,E20.10,/),//)
      H(ITEMP+1)=H(ITEMP)+STEP
   50 CONTINUE
      DO 77 K=1,N
      ALPHA(K)=ALPHA(K)*180.0/3.1416
   77 BETA(K)=BETA(K)*180.0/3.1416
      WRITE(6,105)(ALPHA(K),BETA(K),K=1,N)
  105 FORMAT(10X,'ALPHA(1)= ',E20.10,'BETA(1)= ',E20.10,'ALPHA(2)= ',E20
     1.10,'BETA(2)= ',F20.10,//)
      THETA=THETA*180.0/3.1416
      WRITE(6,35) THETA,PHII
   35 FORMAT(10X,'THETA = ',F20.5,10X,' PHI = ',F20.5,//)
  200 CONTINUE
      GO TO 1
  500 STOP
      END
      SUBROUTINE CALCEL
C
C
C     THIS SUBROUTINE USES THE METHOD DESCRIBED BY GOLDING, R.M., AND
C     TENNANT, W.C., MOL. PHYS. 25, 1163,(1973).
C
C
      IMPLICIT REAL*8 (A-H,O-Z)
      DIMENSION D(3,3),DE(3,3),E(3,3),T(3,3),TINV(3,3)
      COMMON B(3,5),G(3,5),GSQ(5),GI(5),A(3,3,5),SQK(5),SK(5),ONE(5),TWO
     *K(5),X(3,3),THREEK(5),ALPHA(5),BETA(5),ATEN(3,5),THETA,PHI,N
      EXTERNAL SIN,COS,SQRT,ABS
      DO 1000 K=1,N
      T(1,1)=-COS(ALPHA(K))*COS(BETA(K))
      T(1,2)=-COS(ALPHA(K))*SIN(BETA(K))
      T(1,3)=SIN(ALPHA(K))
      T(2,1)=SIN(BETA(K))
      T(2,2)=-COS(BETA(K))
      T(2,3)=0.0
      T(3,1)=SIN(ALPHA(K))*COS(BETA(K))
      T(3,2)=SIN(ALPHA(K))*SIN(BETA(K))
      T(3,3)=COS(ALPHA(K))
      DO 5 I=1,3
      DO 5 J=1,3
      TINV(I,J)=T(J,I)
    5 D(I,J)=0.0
      DO 6 I=1,3
    6 D(I,I)=ATEN(I,K)
      WRITE(6,100)((T(I,J),J=1,3),I=1,3)
      WRITE(6,100)((D(I,J),J=1,3),I=1,3)
      WRITE(6,100)((TINV(I,J),J=1,3),I=1,3)
      CALL MULT(D,T,E)
      CALL MULT(TINV,E,DE)
      WRITE(6,100)((E(I,J),J=1,3),I=1,3)
      WRITE(6,100)((DE(I,J),J=1,3),I=1,3)
  100 FORMAT(//,10X,3(E20.10,10X,E20.10,10X,E20.10,/),//)
      DO 7 I=1,3
      DO 7 J=1,3
    7 A(I,J,K)=DE(I,J)
      B(1,K)=SIN(THETA)*COS(PHI)
      B(2,K)=SIN(THETA)*SIN(PHI)
      B(3,K)=COS(THETA)
      SUM1=0.0
      DO 10 I=1,3
   10 SUM1=SUM1+(B(I,K)*G(I,K))*B(I,K)*G(I,K)
      GSQ(K)=SUM1
      GI(K)=SQRT(GSQ(K))
      SUM2=0.0
      DO 16 IGAMMA=1,3
      SUM1=0.0
      DO 15 IALPHA=1,3
   15 SUM1=SUM1+B(IALPHA,K)*G(IALPHA,K)*A(IGAMMA,IALPHA,K)
   16 SUM2=SUM2+SUM1*SUM1
      SQK(K)=SUM2/GSQ(K)
      SK(K)=SQRT(SQK(K))
      CONST=GSQ(K)*SQK(K)
      SUM2=0.0
      DO 21 IGAMMA=1,3
    SUM1=0.0
    DO 20 IALPHA=1,3
    DO 20 IDELT=1,3
 20 SUM1=SUM1+B(IALPHA,K)*G(IALPHA,K)*A(IGAMMA,IDELT,K)*A(IDELT,IALPHA
   1,K)
 21 SUM2=SUM2+SUM1*SUM1
    TERM1=SUM2/CONST
    DO 22 I=1,3
    DO 22 J=1,3
 22 X(I,J)=0.0
    DO 23 I=1,3
    SUM=0.0
    DO 24 J=1,3
 24 SUM=SUM+A(I,J,K)
 23 X(I,I)=SUM
    SUM1=0.0
    DO 25 IBETA=1,3
    DO 25 IALPHA=1,3
    DO 25 IEPS=1,3
 25 SUM1=SUM1+B(IALPHA,K)*B(IBETA,K)*G(IALPHA,K)*G(IBETA,K)*A(IEPS,IAL
   1PHA,K)*X(IEPS,IBETA)
    TERM2=SUM1/GSC(K)
    SUM=0.0
    DO 30 IALPHA=1,3
    DO 30 IBETA=1,3
 30 SUM=SUM+A(IALPHA,IBETA,K)*A(IALPHA,IBETA,K)
    TERM3=SUM
    WRITE(6,55)TERM1,TERM2,TERM3
    ONE(K)=TERM1+TERM2-TERM3-1.0
```

```
      SUM2=0.0
      DO 36 IGAMMA=1,3
      SUM1=0.0
      DO 35 IALPHA=1,3
      DO 35 IDELTA=1,3
   35 SUM1=SUM1+B(IALPHA,K)*G(IALPHA,K)*A(IGAMMA,IDELTA,K)*A(IDELTA,IALP
     1HA,K)
   36 SUM2=SUM2+SUM1*SUM1
      TWOK(K)=SUM2/CONST-SOK(K)
      SUM=0.0
      DO 40 IALPHA=1,3
      DO 40 IBETA=1,3
      DO 40 IGAMMA=1,3
   40 SUM=SUM+A(IALPHA,IALPHA,K)*A(IBETA,IGAMMA,K)*A(IBETA,IGAMMA,K)
      TERM1=0.5*SUM/SK(K)
      SUM=0.0
      DO 45 IALPHA=1,3
      DO 45 IBETA=1,3
      DO 45 IGAMMA=1,3
   45 SUM=SUM+A(IALPHA,IBETA,K)*A(IGAMMA,IALPHA,K)*A(IBETA,IGAMMA,K)
      TERM2=SUM/(3.0*SK(K))
      SUM=0.0
      DO 50 IALPHA=1,3
      DO 50 IBETA=1,3
      DO 50 IGAMMA=1,3
   50 SUM=SUM+A(IALPHA,IALPHA,K)*A(IBETA,IBETA,K)*A(IGAMMA,IGAMMA,K)
      TERM3=SUM/(6.0*SK(K))
      WRITE(6,55)TERM1,TERM2,TERM3
   55 FORMAT(3X,'TERM1 = ',E20.10,3X,'TERM2 = ',E20.10,3X,'TERM3 = ',E20
     1.10./)
      THREEK(K)=-TERM1+TERM2+TERM3
 1000 CONTINUE
      RETURN
      END
      SUBROUTINE EIGN(NN,A,EIG,VEC,IND)                                 EIGN0010
C         NN= SIZE OF MATRIX                                            EIGN0020
C         A = MATRIX (ONLY LOWER TRIANGLE IS USED + THIS IS DESTROYED)  EIGN0030
C         EIG = RETURNED EIGENVALUES IN ALGEBRAIC DESCENDING ORDER      EIGN0040
C         VEC = RETURNED EIGENVECTORS IN COLUMNS                        EIGN0050
C         IND = ERROR RETURN INDICATOR                                  EIGN0060
C                0 FOR NORMAL RETURN                                    EIGN0070
C                1 SUM OF EIGENVALUES NOT EQUAL TO TRACE                EIGN0080
C                2 SUM OF EIGENVALUES SQUARED NOT EQUAL TO NORM         EIGN0090
C                3 BOTH OF THESE ERRORS                                 EIGN0100
      IMPLICIT REAL*8 (A-H,O-Z)
      DIMENSION A(50,50),GAMMA(50),BETA(50),BETASQ(50),EIG(50)          EIGN0110
      DIMENSION W(49),VEC(50,50)                                        EIGN0120
C     THE FOLLOWING DIMENSIONED VARIABLES ARE EQUIVALENCED              EIGN0130
      DIMENSION P(49),Q(49)                                             EIGN0140
      EXTERNAL SIN,COS,SQRT,ABS
      EQUIVALENCE (P(1),BETA(1)),(Q(1),BETA(1))                         EIGN0150
      DIMENSION IPOSV(50),IVPOS(50),IORD(50)                            EIGN0160
      EQUIVALENCE (IPOSV(1),GAMMA(1)),(IVPOS(1),BETA(1)),               EIGN0170
     1(IORD(1),BETASQ(1))                                               EIGN0180
      N=NN                                                              EIGN0190
C     RESET ERROR RETURN INDICATOR                                      EIGN0200
      IND=0                                                             EIGN0210
      IF(N .EQ. 0) GO TO 560                                            EIGN0220
      N1=N-1                                                            EIGN0230
      N2=N-2                                                            EIGN0240
C     COMPUTE THE TRACE AND EUCLIDIAN NORM OF THE INPUT MATRIX          EIGN0250
C     LATER CHECK AGAINST SUM AND SUM OF SQUARES OF EIGENVALUES         EIGN0260
      ENORM=0.                                                          EIGN0270
      TRACE=0.                                                          EIGN0280
      DO 110 J=1,N                                                      EIGN0290
      DO 100 I=J,N                                                      EIGN0300
  100 ENORM=ENORM+A(I,J)**2                                             EIGN0310
      TRACE=TRACE+A(J,J)                                                EIGN0320
  110 ENORM=ENORM-.5*A(J,J)**2                                          EIGN0330
      ENORM=ENORM+ENORM                                                 EIGN0340
      GAMMA(1)=A(1,1)                                                   EIGN0350
      IF(N2) 280,270,120                                                EIGN0360
  120 DO 260 NR=1,N2                                                    EIGN0370
      B=A(NR+1,NR)                                                      EIGN0380
      S=0.                                                              EIGN0390
      DO 130 I=NR,N2                                                    EIGN0400
  130 S=S+A(I+2,NR)**2                                                  EIGN0410
C     PREPARE FOR POSSIBLE BYPASS OF TRANSFORMATION                     EIGN0420
      A(NR+1,NR)=0.                                                     EIGN0430
      IF(S) 250,250,140                                                 EIGN0440
  140 S=S+B*B                                                           EIGN0450
      SGN=+1.                                                           EIGN0460
      IF(B) 150,160,160                                                 EIGN0470
  150 SGN=-1.                                                           EIGN0480
  160 SQRTS=SQRT(S)                                                     EIGN0490
      D=SGN/(SQRTS+SQRTS)                                               EIGN0500
      TEMP=SQRT(0.5+B*D)                                                EIGN0510
      W(NR)=TEMP                                                        EIGN0520
      A(NR+1,NR)=TEMP                                                   EIGN0530
      D=D/TEMP                                                          EIGN0540
      B=-SGN*SQRTS                                                      EIGN0550
C     D IS FACTOR OF PROPORTIONALITY. NOW COMPUTE AND SAVE W VECTOR.    EIGN0560
```

```
C       EXTRA SINGLY SUBSCRIPTED W VECTOR USED FOR SPEED.                 EIGN0570
        DO 170 I=NR,N2                                                    EIGN0580
        TEMP=C*A(I+2,NR)                                                  EIGN0590
        W(I+1)=TEMP                                                       EIGN0600
    170 A(I+2,NR)=TEMP                                                    EIGN0610
C       PREMULTIPLY VECTOR W BY MATRIX A TO OBTAIN P VECTOR.              EIGN0620
C       SIMULTANEOUSLY ACCUMULATE DOT PRODUCT WP,(THE SCALAR K)           EIGN0630
        WTAW=0.                                                           EIGN0640
        DO 220 I=NR,N1                                                    EIGN0650
        SUM=0.                                                            EIGN0660
        DO 180 J=NR,I                                                     EIGN0670
    180 SUM=SUM+A(I+1,J+1)*W(J)                                           EIGN0680
        I1=I+1                                                            EIGN0690
        IF(N1-I1) 210,190,190                                             EIGN0700
    190 DO 200 J=I1,N1                                                    EIGN0710
    200 SUM=SUM+A(J+1,I+1)*W(J)                                           EIGN0720
    210 P(I)=SUM                                                          EIGN0730
    220 WTAW=WTAW+SUM*W(I)                                                EIGN0740
C       P VECTOR AND SCALAR K NOW STORED. NEXT COMPUTE Q VECTOR           EIGN0750
        DO 230 I=NR,N1                                                    EIGN0760
    230 Q(I)=P(I)-WTAW*W(I)                                               EIGN0770
C       NOW FORM PAP MATRIX, REQUIRED PART                                EIGN0780
        DO 240 J=NR,N1                                                    EIGN0790
        QJ=Q(J)                                                           EIGN0800
        WJ=W(J)                                                           EIGN0810
        DO 240 I=J,N1                                                     EIGN0820
    240 A(I+1,J+1)=A(I+1,J+1)-2.*(W(I)*QJ+WJ*Q(I))                        EIGN0830
    250 BETA(NR)=B                                                        EIGN0840
        BETASQ(NR)=B*B                                                    EIGN0850
```

```
  260 GAMMA(NR+1)=A(NR+1,NR+1)
  270 B=A(N,N-1)
      BETA(N-1)=B
      BETASQ(N-1)=B*B
      GAMMA(N)=A(N,N)
  280 BETASQ(N)=0.
C     ADJOIN AN IDENTITY MATRIX TO BE POSTMULTIPLIED BY ROTATIONS.
      DO 300 I=1,N
      DO 290 J=1,N
  290 VEC(I,J)=0.
  300 VEC(I,I)=1.
      M=N
      SUM=0.
      NPAS=1
      GO TO 400
  310 SUM=SUM+SHIFT
      COSA=1.
      G=GAMMA(1)-SHIFT
      PP=G
      PPBS=PP*PP+BETASQ(1)
      PPBR=SQRT(PPBS)
      DO 370 J=1,M
      COSAP=COSA
      IF(PPBS .NE. 0.) GO TO 320
      SINA=0.
      SINA2=0.
      COSA=1.
      GO TO 350
  320 SINA=BETA(J)/PPBR
```

```
      SINA2=BETASQ(J)/PPBS                                              EIGN1150
      COSA=PP/PPBR                                                      EIGN1160
C     POSTMULTIPLY IDENTITY BY P-TRANSPOSE MATRIX                       EIGN1170
      NT=J+NPAS                                                         EIGN1180
      IF(NT .GE. N) NT=N                                                EIGN1190
  330 DO 340 I=1,NT                                                     EIGN1200
      TEMP=COSA*VEC(I,J)+SINA*VEC(I,J+1)                                EIGN1210
      VEC(I,J+1)=-SINA*VEC(I,J)+COSA*VEC(I,J+1)                         EIGN1220
  340 VEC(I,J)=TEMP                                                     EIGN1230
  350 DIA=GAMMA(J+1)-SHIFT                                              EIGN1240
      U=SINA2*(G+DIA)                                                   EIGN1250
      GAMMA(J)=G+U                                                      EIGN1260
      G=DIA-U                                                           EIGN1270
      PP=DIA*COSA-SINA*COSAP*BETA(J)                                    EIGN1280
      IF(J .NE. M) GO TO 360                                            EIGN1290
      BETA(J)=SINA*PP                                                   EIGN1300
      BETASQ(J)=SINA2*PP*PP                                             EIGN1310
      GO TO 380                                                         EIGN1320
  360 PPBS=PP*PP+BETASQ(J+1)                                            EIGN1330
      PPBR=SQRT(PPBS)                                                   EIGN1340
      BETA(J)=SINA*PPBR                                                 EIGN1350
  370 BETASQ(J)=SINA2*PPBS                                              EIGN1360
  380 GAMMA(M+1)=G                                                      EIGN1370
C     TEST FOR CONVERGENCE OF LAST DIAGONAL ELEMENT                     EIGN1380
      NPAS=NPAS+1                                                       EIGN1390
      IF(BETASQ(M) .GT. 1.E-21) GO TO 410                               EIGN1400
  390 EIG(M+1)=GAMMA(M+1)+SUM                                           EIGN1410
  400 BETA(M)=0.                                                        EIGN1420
      BETASQ(M)=0.                                                      EIGN1430
      M=M-1                                                             EIGN1440
      IF(M .EQ. 0) GO TO 430                                            EIGN1450
      IF(BETASQ(M) .LE. 1.E-21) GO TO 390                               EIGN1460
C     TAKE ROOT OF CORNER 2 BY 2 NEAREST TO LOWER DIAGONAL IN VALUE     EIGN1470
C     AS ESTIMATE OF EIGENVALUE TO USE FOR SHIFT                        EIGN1480
  410 A2=GAMMA(M+1)                                                     EIGN1490
      R2=.5*A2                                                          EIGN1500
      R1=.5*GAMMA(M)                                                    EIGN1510
      R12=R1+R2                                                         EIGN1520
      DIF=R1-R2                                                         EIGN1530
      TEMP= SQRT(DIF*DIF+BETASQ(M))                                     EIGN1540
      R1=R12+TEMP                                                       EIGN1550
      R2=R12-TEMP                                                       EIGN1560
      DIF=ABS(A2-R1)-ABS(A2-R2)                                         EIGN1570
      IF(DIF .LT. 0.) GO TO 420                                         EIGN1580
      SHIFT=R2                                                          EIGN1590
      GO TO 310                                                         EIGN1600
  420 SHIFT=R1                                                          EIGN1610
      GO TO 310                                                         EIGN1620
  430 EIG(1)=GAMMA(1)+SUM                                               EIGN1630
C     INITIALIZE AUXILIARY TABLES REQUIRED FOR REARRANGING THE VECTORS  EIGN1640
      DO 440 J=1,N                                                      EIGN1650
      IPOSV(J)=J                                                        EIGN1660
      IVPOS(J)=J                                                        EIGN1670
  440 IORD(J)=J                                                         EIGN1680
C     USE A TRANSPOSITION SORT TO ORDER THE EIGENVALUES                 EIGN1690
      M=N                                                               EIGN1700
      GO TO 470                                                         EIGN1710
  450 DO 460 J=1,M                                                      EIGN1720
```

```
      IF(EIG(J) .GE. EIG(J+1)) GO TO 460
      TEMP=EIG(J)
      EIG(J)=EIG(J+1)
      EIG(J+1)=TEMP
      ITEMP=IORD(J)
      IORD(J)=IORD(J+1)
      IORD(J+1)=ITEMP
  460 CONTINUE
  470 M=M-1
      IF(M .NE. 0) GO TO 450
      IF(N1 .EQ. 0) GO TO 500
      DO 490 L=1,N1
      NV=IORD(L)
      NP=IPOSV(NV)
      IF(NP .EQ. L) GO TO 490
      LV=IVPOS(L)
      IVPOS(NP)=LV
      IPOSV(LV)=NP
      DO 480 I=1,N
      TEMP=VEC(I,L)
      VEC(I,L)=VEC(I,NP)
  480 VEC(I,NP)=TEMP
  490 CONTINUE
  500 ESUM=0.
      ESSQ=0.
C     BACK TRANSFORM THE VECTORS OF THE TRIPLE DIAGONAL MATRIX
      DO 550 NRR=1,N
      K=N1
  510 K=K-1
```

```
      IF(K .LE. 0) GO TO 540                                            EIGN2020
      SUM=0.                                                            EIGN2030
      DO 520 I=K,N1                                                     EIGN2040
  520 SUM=SUM+VEC(I+1,NRR)*A(I+1,K)                                     EIGN2050
      SUM=SUM+SUM                                                       EIGN2060
      DO 530 I=K,N1                                                     EIGN2070
  530 VEC(I+1,NRR)=VEC(I+1,NRR)-SUM*A(I+1,K)                            EIGN2080
      GO TO 510                                                         EIGN2090
  540 ESUM=ESUM+EIG(NRR)                                                EIGN2100
  550 ESSQ=ESSQ+EIG(NRR)**2                                             EIGN2110
      TEMP= ABS(128.*TRACE)                                             EIGN2120
      IF((ABS(TRACE-ESUM)+TEMP)-TEMP .NE. 0.) IND=IND+1                 EIGN2130
      TEMP=256.*ENORM                                                   EIGN2140
      IF((ABS(ENORM-ESSQ)+TEMP)-TEMP .NE. 0.) IND=IND+2                 EIGN2150
  560 RETURN                                                            EIGN2160
      END                                                               EIGN2170
      SUBROUTINE MULT(A,B,C)
      IMPLICIT REAL*8 (A-H,O-Z)
      DIMENSION A(3,3),B(3,3),C(3,3)
      DO 10 I=1,3
      DO 10 J=1,3
      SUM=0.0
      DO 15 K=1,3
   15 SUM=SUM+A(I,K)*B(K,J)
   10 C(I,J)=SUM
      RETURN
      END
```

```
FUNCTION SIN(X)
IMPLICIT REAL*8 (A-H,O-Z)
SIN=DSIN(X)
RETURN
END
```

```
FUNCTION COS(X)
IMPLICIT REAL*8 (A-H,O-Z)
COS=DCOS(X)
RETURN
END
```

```
FUNCTION SQRT(X)
IMPLICIT REAL*8 (A-H,O-Z)
SQRT=DSQRT(X)
RETURN
END
```

```
FUNCTION ABS(X)
IMPLICIT REAL*8 (A-H,O-Z)
ABS=DABS(X)
RETURN
END
```

APPENDIX E

MATRIX ELEMENTS AND PROGRAM FOR LINEAR F_2^- COLLINEAR A- AND g-TENSORS

Let the eigenvectors be of the type $|S,M\rangle|I,m\rangle$, so they can be written:

$$|1\rangle = |1/2,1/2\rangle|1,1\rangle$$

$$|2\rangle = |1/2,1/2\rangle|1,-1\rangle$$

$$|3\rangle = |1/2,-1/2\rangle|1,0\rangle$$

$$|4\rangle = |1/2,-1/2\rangle|1,-1\rangle$$

$$|5\rangle = |1/2,-1/2\rangle|1,1\rangle$$

$$|6\rangle = |1/2,1/2\rangle|1,0\rangle$$

$$|7\rangle = |1/2,1/2\rangle|0,0\rangle$$

$$|8\rangle = |1/2,-1/2\rangle|0,0\rangle$$

For the operator $A = g\beta_o HS_z + KS_zI_z$, we obtain (if $F = \frac{1}{2}g\beta_o H$

$$\langle 1|A|1\rangle = F + (1/2)K$$

$$\langle 2|A|2\rangle = F - (1/2)K$$

$$\langle 3|A|3\rangle = -F$$

$$\langle 4|A|4\rangle = -F + (1/2)K$$

$$\langle 5|A|5\rangle = -F - (1/2)K$$

$$\langle 6|A|6\rangle = F$$

$$\langle 7|A|7\rangle = F$$

$$\langle 8|A|8\rangle = -F$$

For the operator $B_\pm = S_\pm I_z$, we obtain

$$\langle 2|B_+|4\rangle = -1$$

$$\langle 4|B_-|2\rangle = -1$$

$$\langle 1|B_+|5\rangle = 1$$

$$\langle 5|B_-|1\rangle = 1$$

For the operator $C_\pm = S_\pm I_\pm$, we obtain

$$\langle 1|C_+|3\rangle = \sqrt{2}$$

$$\langle 3|C_-|1\rangle = \sqrt{2}$$

$$\langle 6|C_+|4\rangle = \sqrt{2}$$

$$\langle 4|C_-|6\rangle = \sqrt{2}$$

For the operator $D_\pm = S_\pm I_\mp$, we obtain

$$\langle 2|D_+|3\rangle = \sqrt{2}$$

$$\langle 3|D_-|2\rangle = \sqrt{2}$$

$$\langle 6|D_+|5\rangle = \sqrt{2}$$

$$\langle 5|D_-|6\rangle = \sqrt{2}$$

LINEAR F_2^- SPIN HAMILTONIAN MATRIX

$$
\begin{array}{c|cccccccc}
 & |1\rangle & |2\rangle & |3\rangle & |4\rangle & |5\rangle & |6\rangle & |7\rangle & |8\rangle \\
\langle 1| & F+\frac{1}{2}K & 0 & X^-\sqrt{2} & 0 & Y & 0 & 0 & 0 \\
\langle 2| & 0 & F-\frac{1}{2}K & X^+\sqrt{2} & -Y & 0 & 0 & 0 & 0 \\
\langle 3| & X^-\sqrt{2} & X^+\sqrt{2} & -F & 0 & 0 & 0 & 0 & 0 \\
\langle 4| & 0 & -Y & 0 & -F\frac{1}{2}K & 0 & X^-\sqrt{2} & 0 & 0 \\
\langle 5| & Y & 0 & 0 & 0 & -F-\frac{1}{2}K & X^+\sqrt{2} & 0 & 0 \\
\langle 6| & 0 & 0 & 0 & X^-\sqrt{2} & X^+\sqrt{2} & F & 0 & 0 \\
\langle 7| & 0 & 0 & 0 & 0 & 0 & 0 & F & 0 \\
\langle 8| & 0 & 0 & 0 & 0 & 0 & 0 & 0 & -F
\end{array}
$$

LINEAR F_2^- SPIN HAMILTONIAN MATRIX, $\theta = 90°$

$$
\begin{array}{c|cccccccc}
 & |1\rangle & |2\rangle & |3\rangle & |4\rangle & |5\rangle & |6\rangle & |7\rangle & |8\rangle \\
\hline
\langle 1| & F+\frac{1}{2}K & 0 & \frac{A_\parallel - A_\perp}{\sqrt{8}} & 0 & 0 & 0 & 0 & 0 \\
\langle 2| & 0 & F-\frac{1}{2}K & \frac{A_\parallel + A_\perp}{\sqrt{8}} & 0 & 0 & 0 & 0 & 0 \\
\langle 3| & \frac{A_\parallel - A_\perp}{\sqrt{8}} & \frac{A_\parallel + A_\perp}{\sqrt{8}} & -F & 0 & 0 & 0 & 0 & 0 \\
\langle 4| & 0 & 0 & 0 & -F+\frac{1}{2}K & 0 & \frac{A_\parallel - A_\perp}{\sqrt{8}} & 0 & 0 \\
\langle 5| & 0 & 0 & 0 & 0 & -F-\frac{1}{2}K & \frac{A_\parallel + A_\perp}{\sqrt{8}} & 0 & 0 \\
\langle 6| & 0 & 0 & 0 & \frac{A_\parallel - A_\perp}{\sqrt{8}} & \frac{A_\parallel + A_\perp}{\sqrt{8}} & F & 0 & 0 \\
\langle 7| & 0 & 0 & 0 & 0 & 0 & 0 & F & 0 \\
\langle 8| & 0 & 0 & 0 & 0 & 0 & 0 & 0 & -F
\end{array}
$$

LINEAR F_2^- SPIN HAMILTONIAN MATRIX, $\theta = 0°$

$$\begin{array}{c|cccccccc}
 & |1\rangle & |2\rangle & |3\rangle & |4\rangle & |5\rangle & |6\rangle & |7\rangle & |8\rangle \\
\hline
\langle 1| & F+\frac{1}{2}K & 0 & 0 & 0 & 0 & 0 & 0 & 0 \\
\langle 2| & 0 & F-\frac{1}{2}K & \frac{A_\perp}{2} & 0 & 0 & 0 & 0 & 0 \\
\langle 3| & 0 & \frac{A_\perp}{2} & -F & 0 & 0 & 0 & 0 & 0 \\
\langle 4| & 0 & 0 & 0 & -F+\frac{1}{2}K & 0 & 0 & 0 & 0 \\
\langle 5| & 0 & 0 & 0 & 0 & -F-\frac{1}{2}K & \frac{A_\perp}{2} & 0 & 0 \\
\langle 6| & 0 & 0 & 0 & 0 & \frac{A_\perp}{2} & F & 0 & 0 \\
\langle 7| & 0 & 0 & 0 & 0 & 0 & 0 & F & 0 \\
\langle 8| & 0 & 0 & 0 & 0 & 0 & 0 & 0 & -F
\end{array}$$

```
C
C
C     PROGRAM TO SOLVE THE F2- PROBLEM. FROM A SET OF INITIAL VALUES OF
C     A PARALLEL AND PERPENDICULAR, AND G PARALLEL AND PERPENDICULAR, IT
C     VARIES A PERPENDICULAR UNTIL A MATCH WITH EXPERIMENTALLY DETERMINED
C     LINE POSITIONS IS FOUND.
C     N = NUMBER OF NUCLEI
C     NVAR = NUMBER OF VARIABLES TO BE VARIED IN ORDER TO MINIMIZE.
C     NH = NUMBER OF EXPERIMENTAL LINES
C     NMAX = MAXIMUM NUMBER OF ITERATIONS.
C     DELMIN = MINIMUM VALUE OF THE VARIATION PARAMETER.
C     FREQ = FREQUENCY OF THE SPECTROMETER.
C     APAR = PARALLEL COMPONENT OF THE A-TENSOR
C     APER= PERPENDICULAR COMPONENT OF THE A-TENSOR
C
C
      IMPLICIT REAL*8 (A-H,O-Z)
      COMMON VEC(50,50),EIG(50 ),APAR(2),APER(2),H( 50 ),GPER,GPAR,GO,DELT,
     1THETA,PHI,GN,NH,NVAR,NN,IFLAG
      COMMON/B/XTRA
      DIMENSION TITLE(20),BASE(2,25),DELTA(25),DIFF(50)
      EXTERNAL FCN
    1 READ(5,3)(TITLE(I),I=1,20)
    3 FORMAT(20A4)
      READ(5,5)N,NVAR,NH,NMAX,DELMIN,FREQ
    5 FORMAT(4I5,2F10.5)
      READ(5,10)(APAR(K),APER(K),K=1,N)
   10 FORMAT(2F10.5)
      READ(5,12)GPAR,GPER,XTRA
   12 FORMAT(3F10.5)
      READ(5,15)(H(K),K=1,NH)
   15 FORMAT(8F10.5)
      READ(5,20)(DELTA(I),I=1,NVAR)
   20 FORMAT(8F10.5)
      HTEMP1=H(1)
      HTEMP2=H(2)
      BASE(1,1)=APER(1)
      BASE(1,2)=APER(2)
      IFLAG=0
      THETA=90.0
      THETA=THETA/57.295791
      PHI=0.0
      GN=2.628
      GO=2.0023
      NN=8
      DELT=356.8316*FREQ
      CALL PATSCH(FCN,BASE,NVAR,NCYCLE,NMAX,DELTA,DELMIN,FCNMIN)
      IFLAG=1
      APER(1)=BASE(1,1)
      APER(2)=BASE(1,2)
   76 WRITE(6,94)(TITLE(I),I=1,20)
   94 FORMAT(1H1,20A4,///)
      WRITE(6,2006)(K,APAR(K),K,APER(K),K=1,N)
 2006 FORMAT(//,10X,'A PARALLEL FOR NUCLEUS',I3,' =',3X,E20.10,5X,'A PER
     1PENDICULAR FOR NUCLEUS',I3,' =',3X,E20.10,//)
      WRITE(6,85)GPAR,GPER,FCNMIN,NCYCLE
   85 FORMAT(//,5X,'G PARALLEL =',E20.10,10X,'G PERPENDICULAR =',E20.10,
     */,5X,'FCMIN=',E20.10,5X,'NCYCLE=',I10,/)
```

```
      WRITE(6,100) DELT,XTRA
  100 FORMAT(10X,' THE RESONANCE FIELD = ',E20.10,10X,' XTRA = ',E20.10,
     1//)
      DO 1000 I=1,NVAR
      DO 1000 ITEMP=1,5
      IF(I.EQ.1)H(1)=HTEMP1
      IF(I.EQ.2)H(1)=HTEMP2
      CALL CALMAT(TCOMP,ITEMP)
      IF(I.EQ.1)GO TO 75
      IF(I.EQ.2) GO TO 90
   75 H(ITEMP+1)=H(ITEMP)-1.0D0
      GO TO 1000
   90 H(ITEMP+1)=H(ITEMP)+1.0D0
 1000 CONTINUE
      THETA=0.0
      READ(5,30)(H(K),K=1,3)
   30 FORMAT(3F10.5)
      IFLAG=3
      WRITE(6,40)
   40 FORMAT(1H1,10X,' PARALLEL LINES',///)
      DO 35 ITEMP=1,3
      CALL CALMAT(TCOMP,ITEMP)
   35 CONTINUE
      GO TO 1
      STOP
      END
      FUNCTION FCN(BPLUSD,KI,BITT)
C
C
C     FUNCTION TO BE MINIZED
C
C
      IMPLICIT REAL*8 (A-H,O-Z)
      COMMON VEC(50,50),EIG(50),APAR(2),APER(2),H(50),GPER,GPAR,GO,DELT,
     1THETA,PHI,GN,NH,NVAR,NN,IFLAG
      COMMON/B/XTRA
      DIMENSION BPLUSD(25)
      APER(1)=BPLUSD(1)
      APER(2)=BPLUSD(2)
      FCN=0.0
      DO 10 ITEMP=1,NVAR
      CALL CALMAT(TCOMP,ITEMP)
      TEMP=(DELT-TCOMP)/DELT
   10 FCN=FCN+TEMP*TEMP
      RETURN
      END
      SUBROUTINE CALMAT(TCOMP,ITEMP)
C
C
C     CALCULATION OF MATRIX ELEMENTS FOR THE F2- CASE. IDENTICAL NUCLEI.
C
C
      IMPLICIT REAL*8 (A-H,O-Z)
      COMMON VEC(50,50),EIG(50),APAR(2),APER(2),H(200),GPER,GPAR,GO,DELT
     1,THETA,PHI,GN,NH,NVAR,NN,IFLAG
      COMMON/B/XTRA,G
      DIMENSION DIFF(50),ELEM(50,50)
      IF(IFLAG.GE.1) GO TO 1
      IF(ITEMP.LE.2)THETA=90.0
      IF(ITEMP.GE.3)THETA=0.0
      THETA=THETA/57.295791
    1 G=DSQRT((GPAR*DCOS(THETA))**2+(GPER*DSIN(THETA))**2)
      A=(APER(1)+APER(2))/2.0
      B=(APAR(1)+APAR(2))/2.0
      DO 25 I=1,NN
      DO 25 J=1,NN
   25 ELEM(I,J)=0.0
      AK=(DSQRT((B*GPAR*DCOS(THETA))**2+(A*GPER*DSIN(THETA))**2))/G
      Y=(A**2-B**2)*GPAR*GPER*DCOS(THETA)*DSIN(THETA)/(AK*G)
      XPLUS=A*B/AK+A
      XMIN=A*B/AK-A
      F=0.5*G*H(ITEMP)/GO
      ELEM(1,1)=F+0.5*AK
      ELEM(2,2)=F-0.5*AK
      ELEM(3,3)=-F
      ELEM(4,4)=-F+0.5*AK
      ELEM(5,5)=-F-0.5*AK
      ELEM(6,6)=F
      ELEM(7,7)=F
      ELEM(8,8)=-F
      ELEM(1,5)=0.5*Y
      ELEM(1,3)=XMIN/DSQRT(8.0D0)
      ELEM(2,3)=XPLUS/DSQRT(8.0D0)
      ELEM(2,4)=-0.5*Y
      ELEM(4,6)=XMIN/DSQRT(8.0D0)
      ELEM(5,6)=XPLUS/DSQRT(8.0D0)
      DO 30 I=1,NN
      DO 30 J=1,NN
   30 ELEM(J,I)=ELEM(I,J)
      IF(IFLAG.EQ.0) GO TO 35
      WRITE(6,75) H(ITEMP)
      WRITE(6,2005)((ELEM(I,J),J=1,NN),I=1,NN)
   35 CALL EIGN(NN,ELEM,EIG,VEC,IND)
      CALL CDIFF(DIFF)
      IF(IFLAG.EQ.0)GO TO 31
      WRITE(6,90)(EIG(I),I=1,NN)
      WRITE(6,95)((VEC(I,J),J=1,NN),I=1,NN)
   75 FORMAT(//,10X,' H = ',E20.10,//)
 2005 FORMAT(//,8(8E16.10,/))
   90 FORMAT(//,10X,'THE EIGENVALUES ARE',//,8(20X,E20.10,/))
   95 FORMAT(//,10X,'THE EIGENVECTORS ARE:',//,8(20X,E20.10,/),//)
   31 IF(IFLAG.EQ.3) RETURN
      IF(ITEMP.EQ.1) TCOMP=DIFF(12)
      IF(ITEMP.EQ.2) TCOMP=DIFF(16)
      SUBROUTINE CDIFF(DIFF)
C
C
C     THIS SUBROUTINE CALCULATES THE DIFFERENCE BETWEEN EIGENVALUES
C
C
      IMPLICIT REAL*8 (A-H,O-Z)
      COMMON VEC(50,50),EIG(50),APAR(2),APER(2),H(200),GPER,GPAR,GO,DELT
     1,THETA,PHI,GN,NH,NVAR,NN,IFLAG
      DIMENSION DIFF(50)
      K=0
      INN=NN-1
      DO 15 I=1,INN
      IM=I+1
      DO 15 J=IM,NN
      K=K+1
      DIFF(K)=EIG(I)-EIG(J)
      IF(IFLAG.EQ.0) GO TO 15
      WRITE(6,20)I,J,DIFF(K)
   20 FORMAT(10X,'THE DIFFERENCE BETWEEN EIGENVALUE',I3,'AND EIGENVALUE'
     1,I3,'  IS',E20.10)
   15 CONTINUE
      RETURN
      END
```

```
IF(ITEMP.EQ.3) TCOMP=DIFF(7)
IF(ITEMP.EQ.4) TCOMP=DIFF(19)
RETURN
END
```

```
      SUBROUTINE PATSCH (FCN,BASE,NVAR,NCYCLE,NMAX,DELTA,DELMIN,FCNMIN) PATSC001
C                                                                       PATSC002
C PATSCH FINDS A MINIMUM IN A FUNCTION, FCN, OF NVAR VARIABLES CONTAINEDPATSC003
C                                                                       PATSC004
C IN THE VECTOR BASE(1,*) BY THE PATTERN SEARCH TECHNIQUE  (SEE D.J.    PATSC005
C                                                                       PATSC006
C WILDE, OPTIMUM SEEKING METHODS, PRENTICE-HALL, 1964, P. 145).  THE    PATSC007
C                                                                       PATSC008
C NOTATION HERE FOLLOWS THAT OF WILDE FAIRLY CLOSELY.  THE INPUT        PATSC009
C                                                                       PATSC010
C PARAMETERS ARE:                                                       PATSC011
C                                                                       PATSC012
C FCN  --  ENTRY NAME OF THE FUNCTION TO BE MINIMIZED.  IT HAS THREE    PATSC013
C                                                                       PATSC014
C          ARGUMENTS:  THE FIRST IS A VECTOR CONTAINING THE VALUES OF   PATSC015
C                                                                       PATSC016
C          THE VARIABLES, THE SECOND IS A CONSTANT INDICATING WHICH OF  PATSC017
C                                                                       PATSC018
C          THE VARIABLES WAS CHANGED IMMEDIATELY PRIOR TO THE CALL AND  PATSC019
C                                                                       PATSC020
C          THE THIRD IS A LOGICAL*4 CONSTANT.  IT IS .TRUE. IF ONLY ONE PATSC021
C                                                                       PATSC022
C          VARIABLE HAS BEEN CHANGED SINCE THE LAST CALL TO FCN, AND IS PATSC023
C                                                                       PATSC024
C          .FALSE. IF MORE THAN ONE VARIABLE HAS BEEN CHANGED.          PATSC025
C                                                                       PATSC026
C BASE(1,*)  --  VECTOR CONTAINING THE INITIAL VALUES OF THE VARIABLES  PATSC027
C                                                                       PATSC028
C                IN FCN                                                 PATSC029
```

```
C                                                                       PATSC030
C BASE(2,*)  --  WORK AREA                                              PATSC031
C                                                                       PATSC032
C NVAR  --  THE NUMBER OF VARIABLES IN FCN                              PATSC033
C                                                                       PATSC034
C DELTA(*)  --  VECTOR CONTAINING THE INITIAL VALUES OF THE INCREMENTS  PATSC035
C                                                                       PATSC036
C               TO BE APPLIED TO THE VARIABLES IN BASE(1,*)             PATSC037
C                                                                       PATSC038
C DELMIN  --  THE MINIMUM ALLOWED VALUE OF DELTA(1)                     PATSC039
C                                                                       PATSC040
C NMAX  --  THE MAXIMUM ALLOWED NUMBER OF ITERATIONS                    PATSC041
C                                                                       PATSC042
C THE OUTPUT PARAMETERS ARE:                                            PATSC043
C                                                                       PATSC044
C BASE(1,*)  --  THE OPTIMUM VALUES OF THE VARIABLES IN FCN             PATSC045
C                                                                       PATSC046
C FCNMIN  --  THE MINIMUM VALUE OF FCN FOR THE OPTIMUM VALUES OF THE    PATSC047
C                                                                       PATSC048
C             VARIABLES                                                 PATSC049
C                                                                       PATSC050
C NCYCLE  --  THE NUMBER OF ITERATIONS PERFORMED                        PATSC051
C                                                                       PATSC052
C RETURN MAY OCCUR IN ONE OF TWO WAYS, WHICHEVER OCCURS FIRST:          PATSC053
C                                                                       PATSC054
C 1.  NCYCLE EXCEEDS NMAX.  THIS ALLOWS THE PROGRAMMER TO CONTROL THE   PATSC055
C                                                                       PATSC056
C     TIME ALLOTTED FOR OPTIMIZATION SINCE EACH ITERATION REQUIRES NVAR PATSC057
C                                                                       PATSC058
```

```
C     EVALUATIONS OF FCN.                                               PATSC059
C                                                                       PATSC060
C 2.  DELTA(I) BECOMES LESS THAN DELMIN.  THIS ALLOWS THE CONTROL OF    PATSC061
C                                                                       PATSC062
C     ACCURACY.                                                         PATSC063
C                                                                       PATSC064
C     THIS PROGRAM WAS WRITTEN BY DR. N.H.F. BEEBE, QUANTUM THEORY PROJECT
C     UNIVERSITY OF FLORIDA, GAINESVILLE, FLA.
C
C
C
      REAL*8 FCN,F,T(25),BASE(2,25),DELTA(25),DELMIN,FCNMIN,FOFT,FOFTPD,PATSC065
     $FOFTMD,BEST(25)                                                   PATSC066
      INTEGER*4 BESTN,COMPAR(25),CSUM,COUNT                             PATSC067
      EXTERNAL FCN                                                      PATSC068
      COMMON /PATCOM/ COUNT,IVAR                                        PATSC069
      IVAR = NVAR                                                       PATSC070
C                                                                       PATSC071
C ESTABLISH FIRST TEMPORARY HEAD                                        PATSC072
C                                                                       PATSC073
      DO 1 I = 1,NVAR                                                   PATSC074
      BEST(I) = BASE(1,I)                                               PATSC075
      T(I) = BASE(1,I)                                                  PATSC076
    1 BASE(2,I) = BASE(1,I)                                             PATSC077
      COUNT = 0                                                         PATSC078
      NCYCLE = 0                                                        PATSC079
      BESTN = 0                                                         PATSC080
      FOFT = 0.D0                                                       PATSC081
      FOFTPD = 0.D0                                                     PATSC082
      FOFTMD = 0.D0                                                     PATSC083
      FCNMIN = 1.D75                                                    PATSC084
C                                                                       PATSC085
C BEGIN CALCULATION OF NEW TEMPORARY HEADS, T                            PATSC086
C                                                                       PATSC087
   27 DO 2 K = 1,NVAR                                                   PATSC088
    4 IF ((BESTN.LT.(NCYCLE - 3)) .OR. (K.GT.1)) GO TO 5                PATSC089
    6 FOFT = F(T,0.D0,K,FCN)                                            PATSC090
    5 FOFTPD = F(T,DELTA(K),K,FCN)                                      PATSC091
      IF (FOFTPD - FOFT) 7,8,8                                          PATSC092
C                                                                       PATSC093
C ESTABLISH THE K-TH TEMPORARY HEAD                                     PATSC094
C                                                                       PATSC095
    7 T(K) = T(K) + DELTA(K)                                            PATSC096
      FOFT = FOFTPD                                                     PATSC097
      IF (FOFTPD - FCNMIN) 9,2,2                                        PATSC098
    9 DO 11 I = 1,NVAR                                                  PATSC099
   11 BEST(I) = T(I)                                                    PATSC100
      FCNMIN = FOFTPD                                                   PATSC101
      BESTN = NCYCLE                                                    PATSC102
      GO TO 2                                                           PATSC103
    8 FOFTMD = F(T,-DELTA(K),K,FCN)                                     PATSC104
      IF (FOFTMD - FOFT) 13,14,14                                       PATSC105
C                                                                       PATSC106
C ESTABLISH THE K-TH TEMPORARY HEAD                                     PATSC107
C                                                                       PATSC108
   13 T(K) = T(K) - DELTA(K)                                            PATSC109
      FOFT = FOFTMD                                                     PATSC110
      IF (FOFTMD - FCNMIN) 15,16,16                                     PATSC111
   15 DO 17 I = 1,NVAR                                                  PATSC112
   17 BEST(I) = T(I)                                                    PATSC113
      FCNMIN = FOFTMD                                                   PATSC114
      BESTN = NCYCLE                                                    PATSC115
C                                                                       PATSC116
C IF FOFTMD < FOFT OR FOFTPD, THEN THIS WILL PROBABLY BE THE CASE IN THEPATSC117
C                                                                       PATSC118
C NEXT ITERATION, IN WHICH CASE IT WILL BE MORE PROFITABLE THEN TO STEP PATSC119
C                                                                       PATSC120
C IN THE DIRECTION OF -DELTA(K).  THE SIGN OF DELTA(K) IS THEREFORE     PATSC121
C                                                                       PATSC122
C CHANGED.                                                              PATSC123
C                                                                       PATSC124
   16 DELTA(K) = -DELTA(K)                                              PATSC125
      GO TO 2                                                           PATSC126
   14 IF (FOFT - FCNMIN) 18,2,2                                         PATSC127
   18 DO 19 I = 1,NVAR                                                  PATSC128
   19 BEST(I) = T(I)                                                    PATSC129
      FCNMIN = FOFT                                                     PATSC130
      BESTN = NCYCLE                                                    PATSC131
    2 CONTINUE                                                          PATSC132
C                                                                       PATSC133
C ESTABLISH THE NEW BASE POINT AND THE NEW INITIAL TEMPORARY HEAD       PATSC134
C                                                                       PATSC135
      DO 20 I = 1,NVAR                                                  PATSC136
      BASE(2,I) = T(I)                                                  PATSC137
   20 T(I) = 2.D0*BASE(2,I) - BASE(1,I)                                 PATSC138
      NCYCLE = NCYCLE + 1                                               PATSC139
      IF (NCYCLE - NMAX) 28,28,25                                       PATSC140
```

```
C
C IF FCNMIN IS OBTAINED AT A BASE POINT THE SEARCH WILL CONVERGE, BUT
C
C IF IT IS OBTAINED AT THE LAST TEMPORARY HEAD, THE SEARCH MAY STEP AWAY
C
C FROM THE MIMIMUM.  TO PREVENT THIS, THE SEARCH RETURNS TO THE BEST
C
C POINT, BEST, AND REDUCES DELTA IF IT HAS GONE MORE THAN THREE STEPS
C
C AWAY.
C
   28 IF (BESTN - NCYCLE + 3) 21,22,22
   21 FOFT = FCNMIN
      DO 23 I = 1,NVAR
   23 DELTA(I) = 0.5D0*DELTA(I)
      IF (DABS(DELMIN) - DABS(DELTA(1))) 24,24,25
   24 DO 26 I = 1,NVAR
      BASE(1,I) = BEST(I)
   26 T(I) = BEST(I)
      GO TO 27
   22 DO 32 I = 1,NVAR
      COMPAR(I) = 0
      IF (DABS(BASE(1,I) - BASE(2,I)).LE.1.D-15*DABS(BASE(1,I))) COMPAR(
     $I) = 1
   32 CONTINUE
      CSUM = 0
      DO 34 I = 1,NVAR
      BASE(1,I) = BASE(2,I)
   34 CSUM = CSUM + COMPAR(I)
```

```
      IF (CSUM - NVAR) 27,35,27                                         PATSC170
C                                                                       PATSC171
C THE PATTERN IS DESTROYED AND THE MINIMUM HAS BEEN REACHED OR A        PATSC172
C                                                                       PATSC173
C RESOLUTION VALLEY HAS BEEN CROSSED.  THE STEPSIZE MUST BE REDUCED AND PATSC174
C                                                                       PATSC175
C A NEW TEMPORARY HEAD CALCULATED.                                      PATSC176
C                                                                       PATSC177
   35 DO 37 I = 1,NVAR                                                  PATSC178
   37 DELTA(I) = 0.5D0*DELTA(I)                                         PATSC179
C                                                                       PATSC180
C CHECK THE SIZE OF DELTA                                               PATSC181
C                                                                       PATSC182
   29 IF (DABS(DELMIN) - DABS(DELTA(1))) 27,25,25                       PATSC183
   25 DO 39 I = 1,NVAR                                                  PATSC184
   39 BASE(1,I) = BEST(I)                                               PATSC185
      RETURN                                                            PATSC186
      END                                                               PATSC187
      REAL FUNCTION F*8 (B,DELTA,I,FCN)                                 PATSC192
      REAL*8 B(25),PREVB(25),BPLUSD(25),DELTA,FCN                       PATSC193
      LOGICAL*4 BITT                                                    PATSC194
      INTEGER*4 COMPAR(25),COUNT,CSUM                                   PATSC195
      COMMON /PATCOM/ COUNT,NVAR                                        PATSC196
      EXTERNAL FCN                                                      PATSC197
      IF (COUNT) 3,1,3                                                  PATSC198
    1 DO 2 J = 1,NVAR                                                   PATSC199
    2 PREVB(J) = 0.D0                                                   PATSC200
    3 DO 4 J = 1,NVAR                                                   PATSC201
    4 BPLUSD(J) = B(J)                                                  PATSC202
      BPLUSD(I) = B(I) + DELTA                                          PATSC203
      CSUM = 0                                                          PATSC204
      DO 5 J = 1,NVAR                                                   PATSC205
      COMPAR(J) = 0                                                     PATSC206
    5 IF (DABS(PREVB(J) - B(J)).GT.1.D-15*DABS(B(J))) COMPAR(J) = 1     PATSC207
      DO 6 J = 1,NVAR                                                   PATSC208
    6 CSUM = CSUM + COMPAR(J)                                           PATSC209
      IF (CSUM - 1) 7,7,8                                               PATSC210
    7 BITT = .TRUE.                                                     PATSC211
      GO TO 9                                                           PATSC212
    8 BITT = .FALSE.                                                    PATSC213
    9 IF (COUNT.EQ.0) BITT = .FALSE.                                    PATSC214
      COUNT = COUNT + 1                                                 PATSC215
      DO 10 J = 1,NVAR                                                  PATSC216
   10 PREVB(J) = B(J)                                                   PATSC217
      F = FCN(BPLUSD,I,BITT)                                            PATSC218
      RETURN                                                            PATSC219
      END                                                               PATSC220
      SUBROUTINE EIGN(NN,A,EIG,VEC,IND)                                 EIGN0010
C         NN= SIZE OF MATRIX                                            EIGN0020
C         A = MATRIX (ONLY LOWER TRIANGLE IS USED + THIS IS DESTROYED)  EIGN0030
C         EIG = RETURNED EIGENVALUES IN ALGEBRAIC DESCENDING ORDER      EIGN0040
C         VEC = RETURNED EIGENVECTORS IN COLUMNS                        EIGN0050
C         IND = ERROR RETURN INDICATOR                                  EIGN0060
C                0 FOR NORMAL RETURN                                    EIGN0070
C                1 SUM OF EIGENVALUES NOT EQUAL TO TRACE                EIGN0080
C                2 SUM OF EIGENVALUES SQUARED NOT EQUAL TO NORM         EIGN0090
C                3 BOTH OF THESE ERRORS                                 EIGN0100
      IMPLICIT REAL*8 (A-H,O-Z)
      DIMENSION A(50,50),GAMMA(50),BETA(50),BETASQ(50),EIG(50)          EIGN0110
      DIMENSION W(49),VEC(50,50)                                        EIGN0120
C     THE FOLLOWING DIMENSIONED VARIABLES ARE EQUIVALENCED              EIGN0130
      DIMENSION P(49),Q(49)                                             EIGN0140
      EQUIVALENCE (P(1),BETA(1)),(Q(1),BETA(1))                         EIGN0150
      DIMENSION IPOSV(50),IVPOS(50),IORD(50)                            EIGN0160
      EQUIVALENCE (IPOSV(1),GAMMA(1)),(IVPOS(1),BETA(1)),               EIGN0170
     1(IORD(1),BETASQ(1))                                               EIGN0180
      N=NN                                                              EIGN0190
C     RESET ERROR RETURN INDICATOR                                      EIGN0200
      IND=0                                                             EIGN0210
      IF(N .EQ. 0) GO TO 560                                            EIGN0220
      N1=N-1                                                            EIGN0230
      N2=N-2                                                            EIGN0240
C     COMPUTE THE TRACE AND EUCLIDIAN NORM OF THE INPUT MATRIX          EIGN0250
C     LATER CHECK AGAINST SUM AND SUM OF SQUARES OF EIGENVALUES         EIGN0260
      ENORM=0.                                                          EIGN0270
      TRACE=0.                                                          EIGN0280
      DO 110 J=1,N                                                      EIGN0290
      DO 100 I=J,N                                                      EIGN0300
  100 ENORM=ENORM+A(I,J)**2                                             EIGN0310
      TRACE=TRACE+A(J,J)                                                EIGN0320
  110 ENORM=ENORM-.5*A(J,J)**2                                          EIGN0330
      ENORM=ENORM+ENORM                                                 EIGN0340
      GAMMA(1)=A(1,1)                                                   EIGN0350
      IF(N2) 280,270,120                                                EIGN0360
  120 DO 260 NR=1,N2                                                    EIGN0370
      B=A(NR+1,NR)                                                      EIGN0380
      S=0.                                                              EIGN0390
      DO 130 I=NR,N2                                                    EIGN0400
  130 S=S+A(I+2,NR)**2                                                  EIGN0410
C     PREPARE FOR POSSIBLE BYPASS OF TRANSFORMATION                     EIGN0420
      A(NR+1,NR)=0.                                                     EIGN0430
      IF(S) 250,250,140                                                 EIGN0440
  140 S=S+B*B                                                           EIGN0450
      SGN=+1.                                                           EIGN0460
      IF(B) 150,160,160                                                 EIGN0470
  150 SGN=-1.                                                           EIGN0480
  160 SQRTS=DSQRT(S)                                                    EIGN0490
      D=SGN/(SQRTS+SQRTS)                                               EIGN0500
      TEMP=DSQRT(0.5+B*D)                                               EIGN0510
      W(NR)=TEMP                                                        EIGN0520
      A(NR+1,NR)=TEMP                                                   EIGN0530
      D=D/TEMP                                                          EIGN0540
      B=-SGN*SQRTS                                                      EIGN0550
C     D IS FACTOR OF PROPORTIONALITY. NOW COMPUTE AND SAVE W VECTOR.    EIGN0560
C     EXTRA SINGLY SUBSCRIPTED W VECTOR USED FOR SPEED.                 EIGN0570
```

```
      DO 170 I=NR,N2                                                    EIGN0580
      TEMP=D*A(I+2,NR)                                                  EIGN0590
      W(I+1)=TEMP                                                       EIGN0600
  170 A(I+2,NR)=TEMP                                                    EIGN0610
C     PREMULTIPLY VECTOR W BY MATRIX A TO OBTAIN P VECTOR.              EIGN0620
C     SIMULTANEOUSLY ACCUMULATE DOT PRODUCT WP,(THE SCALAR K)           EIGN0630
      WTAW=0.                                                           EIGN0640
      DO 220 I=NR,N1                                                    EIGN0650
      SUM=0.                                                            EIGN0660
      DO 180 J=NR,I                                                     EIGN0670
  180 SUM=SUM+A(I+1,J+1)*W(J)                                           EIGN0680
      I1=I+1                                                            EIGN0690
      IF(N1-I1) 210,190,190                                             EIGN0700
  190 DO 200 J=I1,N1                                                    EIGN0710
  200 SUM=SUM+A(J+1,I+1)*W(J)                                           EIGN0720
  210 P(I)=SUM                                                          EIGN0730
  220 WTAW=WTAW+SUM*W(I)                                                EIGN0740
C     P VECTOR AND SCALAR K NOW STORED. NEXT COMPUTE Q VECTOR           EIGN0750
      DO 230 I=NR,N1                                                    EIGN0760
  230 Q(I)=P(I)-WTAW*W(I)                                               EIGN0770
C     NOW FORM PAP MATRIX, REQUIRED PART                                EIGN0780
      DO 240 J=NR,N1                                                    EIGN0790
      QJ=Q(J)                                                           EIGN0800
      WJ=W(J)                                                           EIGN0810
      DO 240 I=J,N1                                                     EIGN0820
  240 A(I+1,J+1)=A(I+1,J+1)-2.*(W(I)*QJ+WJ*Q(I))                        EIGN0830
  250 BETA(NR)=B                                                        EIGN0840
      BETASQ(NR)=B*B                                                    EIGN0850
  260 GAMMA(NR+1)=A(NR+1,NR+1)                                          EIGN0860
  270 B=A(N,N-1)                                                  EIGN0870
      BETA(N-1)=B                                                 EIGN0880
      BETASQ(N-1)=B*B                                             EIGN0890
      GAMMA(N)=A(N,N)                                             EIGN0900
  280 BETASQ(N)=0.                                                EIGN0910
C     ADJOIN AN IDENTITY MATRIX TO BE POSTMULTIPLIED BY ROTATIONS.  EIGN0920
      DO 300 I=1,N                                                EIGN0930
      DO 290 J=1,N                                                EIGN0940
  290 VEC(I,J)=0.                                                 EIGN0950
  300 VEC(I,I)=1.                                                 EIGN0960
      M=N                                                         EIGN0970
      SUM=0.                                                      EIGN0980
      NPAS=1                                                      EIGN0990
      GO TO 400                                                   EIGN1000
  310 SUM=SUM+SHIFT                                               EIGN1010
      COSA=1.                                                     EIGN1020
      G=GAMMA(1)-SHIFT                                            EIGN1030
      PP=G                                                        EIGN1040
      PPBS=PP*PP+BETASQ(1)                                        EIGN1050
      PPBR=DSQRT(PPBS)                                            EIGN1060
      DO 370 J=1,M                                                EIGN1070
      COSAP=COSA                                                  EIGN1080
      IF(PPBS .NE. 0.) GO TO 320                                  EIGN1090
      SINA=0.                                                     EIGN1100
      SINA2=0.                                                    EIGN1110
      COSA=1.                                                     EIGN1120
      GO TO 350                                                   EIGN1130
  320 SINA=BETA(J)/PPBR                                           EIGN1140
      SINA2=BETASQ(J)/PPBS                                        EIGN1150
      COSA=PP/PPBR                                                      EIGN1160
C     POSTMULTIPLY IDENTITY BY P-TRANSPOSE MATRIX                       EIGN1170
      NT=J+NPAS                                                         EIGN1180
      IF(NT .GE. N) NT=N                                                EIGN1190
  330 DO 340 I=1,NT                                                     EIGN1200
      TEMP=COSA*VEC(I,J)+SINA*VEC(I,J+1)                                EIGN1210
      VEC(I,J+1)=-SINA*VEC(I,J)+COSA*VEC(I,J+1)                         EIGN1220
  340 VEC(I,J)=TEMP                                                     EIGN1230
  350 DIA=GAMMA(J+1)-SHIFT                                              EIGN1240
      U=SINA2*(G+DIA)                                                   EIGN1250
      GAMMA(J)=G+U                                                      EIGN1260
      G=DIA-U                                                           EIGN1270
      PP=DIA*COSA-SINA*COSAP*BETA(J)                                    EIGN1280
      IF(J .NE. M) GO TO 360                                            EIGN1290
      BETA(J)=SINA*PP                                                   EIGN1300
      BETASQ(J)=SINA2*PP*PP                                             EIGN1310
      GO TO 380                                                         EIGN1320
  360 PPBS=PP*PP+BETASQ(J+1)                                            EIGN1330
      PPBR=DSQRT(PPBS)                                                  EIGN1340
      BETA(J)=SINA*PPBR                                                 EIGN1350
  370 BETASQ(J)=SINA2*PPBS                                              EIGN1360
  380 GAMMA(M+1)=G                                                      EIGN1370
C     TEST FOR CONVERGENCE OF LAST DIAGONAL ELEMENT                     EIGN1380
      NPAS=NPAS+1                                                       EIGN1390
      IF(BETASQ(M) .GT. 1.E-21) GO TO 410                               EIGN1400
  390 EIG(M+1)=GAMMA(M+1)+SUM                                           EIGN1410
  400 BETA(M)=0.                                                        EIGN1420
      BETASQ(M)=0.                                                      EIGN1430
      M=M-1                                                             EIGN1440
      IF(M .EQ. 0) GO TO 430                                            EIGN1450
      IF(BETASQ(M) .LE. 1.E-21) GO TO 390                               EIGN1460
C     TAKE ROOT OF CORNER 2 BY 2 NEAREST TO LOWER DIAGONAL IN VALUE     EIGN1470
C     AS ESTIMATE OF EIGENVALUE TO USE FOR SHIFT                        EIGN1480
  410 A2=GAMMA(M+1)                                                     EIGN1490
      R2=.5*A2                                                          EIGN1500
      R1=.5*GAMMA(M)                                                    EIGN1510
      R12=R1+R2                                                         EIGN1520
      DIF=R1-R2                                                         EIGN1530
      TEMP=DSQRT(DIF*DIF+BETASQ(M))                                     EIGN1540
      R1=R12+TEMP                                                       EIGN1550
      R2=R12-TEMP                                                       EIGN1560
      DIF=DABS(A2-R1)-DABS(A2-R2)                                       EIGN1570
      IF(DIF .LT. 0.) GO TO 420                                         EIGN1580
      SHIFT=R2                                                          EIGN1590
      GO TO 310                                                         EIGN1600
  420 SHIFT=R1                                                          EIGN1610
      GO TO 310                                                         EIGN1620
  430 EIG(1)=GAMMA(1)+SUM                                               EIGN1630
C     INITIALIZE AUXILIARY TABLES REQUIRED FOR REARRANGING THE VECTORS  EIGN1640
      DO 440 J=1,N                                                      EIGN1650
      IPOSV(J)=J                                                        EIGN1660
      IVPOS(J)=J                                                        EIGN1670
  440 IORD(J)=J                                                         EIGN1680
C     USE A TRANSPOSITION SORT TO ORDER THE EIGENVALUES                 EIGN1690
      M=N                                                               EIGN1700
      GO TO 470                                                         EIGN1710
  450 DO 460 J=1,M                                                      EIGN1720
      IF(EIG(J) .GE. EIG(J+1)) GO TO 460                                EIGN1730
      TEMP=EIG(J)                                                       EIGN1740
      EIG(J)=EIG(J+1)                                                   EIGN1750
      EIG(J+1)=TEMP                                                     EIGN1760
      ITEMP=IORD(J)                                                     EIGN1770
      IORD(J)=IORD(J+1)                                                 EIGN1780
      IORD(J+1)=ITEMP                                                   EIGN1790
  460 CONTINUE                                                          EIGN1800
  470 M=M-1                                                             EIGN1810
      IF(M .NE. 0) GO TO 450                                            EIGN1820
      IF(N1 .EQ. 0) GO TO 500                                           EIGN1830
      DO 490 L=1,N1                                                     EIGN1840
      NV=IORD(L)                                                        EIGN1850
      NP=IPOSV(NV)                                                      EIGN1860
      IF(NP .EQ. L) GO TO 490                                           EIGN1870
      LV=IVPOS(L)                                                       EIGN1880
      IVPOS(NP)=LV                                                      EIGN1890
      IPOSV(LV)=NP                                                      EIGN1900
      DO 480 I=1,N                                                      EIGN1910
      TEMP=VEC(I,L)                                                     EIGN1920
      VEC(I,L)=VEC(I,NP)                                                EIGN1930
  480 VEC(I,NP)=TEMP                                                    EIGN1940
  490 CONTINUE                                                          EIGN1950
  500 ESUM=0.                                                           EIGN1960
      ESSQ=0.                                                           EIGN1970
C     BACK TRANSFORM THE VECTORS OF THE TRIPLE DIAGONAL MATRIX          EIGN1980
      DO 550 NRR=1,N                                                    EIGN1990
      K=N1                                                              EIGN2000
  510 K=K-1                                                             EIGN2010
      IF(K .LE. 0) GO TO 540                                            EIGN2020
      SUM=0.                                                            EIGN2030
      DO 520 I=K,N1                                                     EIGN2040
  520 SUM=SUM+VEC(I+1,NRR)*A(I+1,K)                                     EIGN2050
      SUM=SUM+SUM                                                       EIGN2060
      DO 530 I=K,N1                                                     EIGN2070
  530 VEC(I+1,NRR)=VEC(I+1,NRR)-SUM*A(I+1,K)                            EIGN2080
      GO TO 510                                                         EIGN2090
  540 ESUM=ESUM+EIG(NPR)                                                EIGN2100
  550 ESSQ=ESSQ+EIG(NPR)**2                                             EIGN2110
      TEMP=DABS(128.*TRACE)                                             EIGN2120
      IF((DABS(TRACE-ESUM)+TEMP)-TEMP .NE. 0.) IND=IND+1                EIGN2130
      TEMP=256.*ENORM                                                   EIGN2140
      IF((DABS(ENORM-ESSQ)+TEMP)-TEMP .NE. 0.) IND=IND+2                EIGN2150
  560 RETURN                                                            EIGN2160
```

BIOGRAPHICAL SKETCH

Joaquin Victor Martinez de Pinillos was born March 10, 1941 at Habana, Cuba and is the son of Dr. and Mrs. Joaquin J. Martinez de Pinillos. He attended Baldor School in Habana where he received the degree of "Bachiller en Ciencias" in August 1959. He entered the University of Habana in September 1959 as a candidate for the degree of Doctor in Chemical Physics. He left the University of Habana in 1961. In this same year he came to the United States where he entered Miami-Dade Junior College in 1963 and later the University of Miami where he received the degree of Bachelor of Science with a major in Chemistry in August 1966. He attended Bowling Green State University in Ohio under a grant from the National Science Foundation and received the degree of Master of Arts with a major in Chemistry in August 1968. From September 1970 until August 1974, he worked as a graduate assistant at the University of Florida.

He is married to the former Carmen T. Cornejo and has two sons.

I certify that I have read this study and that in my opinion it conforms to acceptable standards of scholarly presentation and is fully adequate, in scope and quality, as a dissertation for the degree of Doctor of Philosophy.

William Weltner Jr.

William Weltner, Jr., Chairman
Professor of Chemistry

I certify that I have read this study and that in my opinion it conforms to acceptable standards of scholarly presentation and is fully adequate, in scope and quality, as a dissertation for the degree of Doctor of Philosophy.

Willis B. Person

Willis B. Person
Professor of Chemistry

I certify that I have read this study and that in my opinion it conforms to acceptable standards of scholarly presentation and is fully adequate, in scope and quality, as a dissertation for the degree of Doctor of Philosophy.

Gardiner H. Myers

Gardiner H. Myers
Associate Professor of Chemistry

I certify that I have read this study and that in my opinion it conforms to acceptable standards of scholarly presentation and is fully adequate, in scope and quality, as a dissertation for the degree of Doctor of Philosophy.

Z. R. Pop-Stojanić

Zoran R. Pop Stojanovic
Professor of Mathematics

I certify that I have read this study and that in my opinion it conforms to acceptable standards of scholarly presentation and is fully adequate, in scope and quality, as a dissertation for the degree of Doctor of Philosophy.

David A. Micha
Associate Professor of Physics

This dissertation was submitted to the Graduate Faculty of the Department of Chemistry in the College of Arts and Sciences and to the Graduate Council, and was accepted as partial fulfillment of the requirements for the degree of Doctor of Philosophy.

August, 1974

Dean, Graduate School